Master's thesis

2019

Marte Ryen Dalsnes

NTNU
Norwegian University of
Science and Technology
Faculty of Natural Sciences
Department of Biotechnology and Food Science

Marte Ryen Dalsnes

Enzymatic protein hydrolysis of residual raw materials from poultry

A study of proteases' selectivity toward collagen and myofibrillar proteins

May 2019

NTNU
Norwegian University of
Science and Technology

NTNU
Norwegian University of
Science and Technology

NTNU
Norwegian University of
Science and Technology

Enzymatic protein hydrolysis of residual raw materials from poultry

A study of proteases' selectivity toward collagen and myofibrillar proteins

Marte Ryen Dalsnes

Food Technology
Submission date: May 2019
Supervisor: Eva Falch, IBT
Co-supervisor: Nils Kristian Afseth, Nofima
Diana Lindberg, Nofima

Norwegian University of Science and Technology
Department of Biotechnology and Food Science

Preface

This master thesis concludes my MSc in Food Technology at the Department of Biotechnology and Food Science at the Norwegian University of Science and Technology (NTNU). The assignment was conducted during the spring of 2019 in collaboration with the Department of Raw Materials and Process Optimization at Nofima AS, Ås. The master thesis was a part of the research project *Notably* (Novel cascade technology for optimal utilization of animal and marine by-products), headed by Nofima.

First, I would like to thank my supervisors at Nofima, Nils Kristian Afseth and Diana Lindberg, for excellent guidance, advices, and support during my work with my thesis. Thank you for letting me a part of the Notably project and for believing in me. I would also like to thank my supervisor at NTNU, Eva Falch, for contributing with a third point of view on the assignment and for helping me improve my writing. In addition, I would extend my gratitude to Kenneth Aase Kristoffersen for teaching me size exclusion chromatography, and Katinka Dankel for helping out with analyzes.

I am also very grateful for my brilliant and very much helpful lab partners in crime, Linn Maria Hunnes and Julia Döring, making the long hours at lab a pure pleasure. At last, I would like to thank the rest of the friendly department at Nofima who directly or indirectly have contributed with their valuable help.

Trondheim, 15th of May 2019

Marte R Dalsnes

Marte Ryen Dalsnes

Abstract

Residual raw materials from the poultry industry have a complex composition of nutrients which are not completely utilized in the current enzymatic protein hydrolysis (EPH) industry. The main aim of this master thesis was to study several proteases' activities towards hydrolysis of residual raw materials from poultry to search for proteases with high selectivity towards collagen and/or myofibrillar proteins.

Measurements of the proteases' activities towards the nonspecific protease substrate Azo-Casein was conducted to obtain normalized activities for all proteases. A small-scale EPH methodology was developed and evaluated, aiming to screen the proteases' digestion of four different poultry residual raw materials: Achilles tendons of turkey, chicken leg bone, chicken meat, and mechanically deboned chicken residue (MDCR). Based on the ratio of digested Achilles tendons and chicken meat, the two proteases Bromelain and Endocut-02 were chosen for further studies. These proteases were tested in a small-scale hydrolysis with duplicates and time points, and in a upscaled hydrolysis to study the methods' and proteases' reproducibility and scalability of hydrolysis. In these experiments, an artificial MDCR consisting of one-third of tendons, meat and bones was also included. All obtained hydrolysates were analyzed by Fourier-transform infrared spectroscopy (FTIR) and size exclusion chromatography (SEC). FTIR was used to study the degradation of peptide bonds during hydrolysis and the formation of terminal amino (NH_3^+) and carboxyl (COO^-) groups, while SEC was conducted for characterization of the hydrolysates' peptide composition.

Hydrolysis in both small-scale and upscale showed that Bromelain had the highest digestion of Achilles tendons (24.4 and 39.9 %) and chicken meat (36.7 and 42.8 %), while Endocut-02 had a greater digestion of the more complex residual raw materials as MDCR (24.8 and 44.6 %) and artificial MDCR (10.2 and 20.0 %). However, Bromelain had a higher digestion than Endocut-02 of the artificial MDCR in the upscaled hydrolysis (30.6 %). An increase in yield was observed with upscaling of hydrolysis, while the molecular weight distributions were quite similar in hydrolysates obtained from the same raw material in both small-scale and upscale. The obtained knowledge could be of importance for further development of the future multistep processing of residual raw materials of poultry, possibly leading to complete utilization of the raw material and value creation for the industry.

Sammendrag

Restråstoff fra fjørfeindustrien har en kompleks sammensetning av næringsstoffer som ikke blir fullstendig utnyttet i dagens enzymatiske proteinhydrolyseprosesser. Hovedmålet med denne masteroppgaven var å studere aktiviteten til ulike proteaser ved hydrolyse av restråstoff fra fjørfe for å undersøke ulike proteasers selektivitet for kollagen og myofibrillære proteiner.

For å oppnå en normalisert aktivitet av alle proteaser ble aktiviteten målt opp imot det uspesifikke substratet Azo-Casein. Det ble utviklet en metode for enzymatisk proteinhydrolyse i liten skala for å screene de ulike proteasenes nedbrytning av fire forskjellige restråstoff fra fjørfe: Akilles sener fra kalkun, lårbein av kylling, kyllingkjøtt og restene etter mekanisk utbeining av kylling, også kalt kyllingskrog. Basert på forholdet mellom nedbrutt mengde av Akilles sener og kyllingkjøtt ble de to proteasene Bromelain og Endocut-02 valgt ut for videre vurdering. Disse proteasene ble igjen testet i liten skala, men denne gangen med duplikater og tidsuttak, samt i en oppskalert versjon av hydrolysen for å studere om metodene og proteasene ga reproduserbare resultater med mulighet for oppskalering. Her ble det i tillegg laget en egen versjon av kyllingskroget med kontrollert sammensetning bestående av en tredjedel av sener, kjøtt og bein fra kylling. Hydrolysatene ble analysert med Fourier-transform infrared spectroscopy (FTIR) og size exclusion chromatography (SEC). FTIR ble brukt for å studere degraderingen av peptidbindinger under hydrolysen og dannelsen av terminale amino (NH_3^+) og karboksyl (COO^-) grupper, mens SEC ble gjennomført for å karakterisere sammensetningen av peptider i hydrolysatene.

Hydrolyse i både liten og oppskalert skala viste at Bromelain hadde den største nedbrytningen av Akilles sener (24.4 and 39.9 %) og kyllingkjøtt (36.7 and 42.8 %), mens Endocut-02 hadde en større nedbrytning av de mer komplekse restråstoffene som kyllingskrog (24.8 and 44.6 %) og den egenkomponerte versjonen av kyllingskrog (10.2 and 20.0 %). Bromelain hadde derimot større nedbrytning enn Endocut-02 av sistnevnte råstoff i den oppskalerte hydrolysen (30.6 %). En økning i utbytte ble observert ved oppskalering av hydrolysen, mens distribusjonen av molekylvekt var omtrent lik i hydrolysat produsert fra samme restråstoff i både liten og oppskalert skala. Denne kunnskapen kan være nyttig for videre utvikling av den fremtidige flertrinnsprosessen av restråstoff fra fjørfe som forhåpentligvis kan føre til fullstendig utnyttelse av råstoffet samt økt verdiskapning for industrien.

Table of Contents

List of Figures

List of Tables

Abbreviations

ABP	Animal by-product
Da	Dalton
DH	Degree of hydrolysis
EMSC	Extended multiplicative scatter correction
EPH	Enzymatic protein hydrolysis
EY	Enzymatic yield
FTIR	Fourier-transform infrared spectroscopy
MDCR	Mechanically deboned chicken residue
MDPR	Mechanically deboned poultry residue
MMPs	Mammalian matrix metalloproteinases
MWD	Molecular weight distribution
PCA	Principal component analysis
SEC	Size exclusion chromatography

1. Introduction

By 2050 it is estimated that the world's population has reached 9 billion (FAO, 2009). An increase in population combined with an increased standard of living in developing countries are assumed to create a demand for more animal based protein (Boland *et al.*, 2013). To achieve this, it is important to utilize the resources we already have to their fullest potential. The industrial processing of fish and animal products generate huge amounts of protein-rich residual raw materials, approximately 40-60 % of the total weight depending on the species. This residual raw material has great potential for higher-value applications in food and feed (Aspevik *et al.*, 2018). Residual raw materials of poultry have a complex composition of nutrients which have a great potential for value creation for the industry. At the same time, the residues can be a good source of protein and fat for the growing world population. Today, the industry runs enzymatic protein hydrolysis (EPH) using an enzyme to enable separation of a fat product, a protein hydrolysate and a residue rich in collagen and minerals (Böcker *et al.*, 2017; Wubshet *et al.*, 2017; Aspevik *et al.*, 2018; Wubshet *et al.*, 2018). The traditional EPH leaves behind several valuable components in the residue, and a possibility is to use specific enzymes that can release connective tissue proteins and myofibril proteins in separate steps in the same process. The extracted protein hydrolysates are often used as feed ingredients, however the interest to point these products against human consumption are growing. Earlier, complete utilization of the residuals has been difficult and there is a need to improve the biotechnological processes to be able to free the components which is found in complex materials, e.g. mechanically deboned poultry residue (MDPR). In the *Notably* project, the goal of the multistep processing is to produce separate products with the highest yield and quality, which hopefully could lead to better utilization of the raw material and increased value creation for the food industry.

1.1 The main aim and sub goals

The aim of this master thesis was to study the enzymatic activity of a range of proteases towards hydrolysis of residual raw materials from poultry, with main focus on their activities towards collagen and myofibrillar proteins.

Sub goals:

- Study the proteases' activities towards the nonspecific protease substrate Azo-Casein to obtain normalized activities for all proteases.
- Study the proteases' activities towards different residual raw materials from poultry in small-scale.
- Choose the two proteases with highest selectivity towards residual raw materials rich in collagen and myofibrillar proteins, respectively.
- Study reproducibility and scalability of hydrolysis reactions using the selected proteases.

2. Theory

2.1 Proteins

Proteins are macromolecules consisting of one or several polypeptide chains, where each chain is made up of amino acids linked together by peptide bonds formed between the α-amino and α-carboxylic acid groups of two adjacent amino acids (Walsh, 2014; Li-Chan and Lacroix, 2018). Amino acids are made up of a carbon atom (α-carbon) carrying an amino group ($-NH_2$), a carboxyl group (-COOH), and a side chain (R-group) unique to each amino acid. The unique sequence of amino acids decides the properties and complex structure of proteins. Hydrogen bonds connect the carboxyl oxygen of one amino acid to another amino acid, forming an α-helix. Side chains in the helical structure are able to form bonds in form of covalent linkages between different regions of the polypeptide chain which can stabilize the structure. Temperature and pH can disturb these linkages and lead to denaturation of the protein (Coultate, 2009). Proteins are the building blocks of several materials, e.g. bones, hair, skin, and cartilage, in addition to enzymes. These are very different materials, but their common denominator is that they are all made of amino acids and proteins. The difference lays in the specific R-group of each amino acids which results in diverse properties of the protein (Hart *et al.*, 2012).

Proteins can be classified as fibrous or globular proteins. Fibrous proteins are the structural materials of animals and can be further divided into collagen, elastin and keratin. These proteins have helical structures and a large fraction of the R-groups are non-polar, making the proteins insoluble in water. The helical structure is being held together by disulfide cross-links, which makes the fibrous protein highly rigid. Globular proteins have amino acids with polar or ionic side chains, making it soluble in water. An example of globular proteins are enzymes (Hart *et al.*, 2012).

2.2 Enzymes

Enzymes are proteins with catalytic properties that have an active site containing specific amino acids, allowing the enzymes to be highly specific in the recognition and binding of specific substrates, and catalyzing them to unique products (Scanlon, Henrich and Whitaker, 2018). The enzymes are sensitive to reaction conditions, e.g. pH, buffer composition, temperature, and substrate concentration (Shyu, Tzen and Jeang, 2006). One of the qualities of enzymes are their ability to enhance the rate of a reaction without being considerably consumed during the process, in addition to work precisely and being highly selectively while operating under mild conditions (Dwevedi and Kayastha, 2011). However, they could also have several limitations, such as being unstable, soluble, inhibited by substrate, and poorly selective on non-natural substrates (Dwevedi and Kayastha, 2011). Enzymes can be inhibited by the peptides formed during the reaction as well as by autohydrolysis and thermal unfolding (Margot, Flaschel and Renken, 1997).

Proteases, also known as proteolytic enzymes, cleave the peptide chains of the protein at the expense of a water molecule, thus belonging to the class of enzymes know as hydrolases. The hydrolyzed peptide bond results in C-terminal carboxylate (COO^-) and N-terminal amino (NH_3^+) groups at the specific site of cleavage. This particular shortening of the peptide chain can affects the secondary structure (Böcker *et al.*, 2017). Protases can be classified into groups based on the position of the hydrolyzed peptide bond, or the molecular mechanism used during hydrolysis. Endopeptidases and exopeptidases are the description of the proteases' cleavage site of the peptide chain. Endopeptidases, e.g. Trypsin, Pepsin, Papain, Bromelain, and Alcalase, hydrolyzes peptide bonds within the protein sequence, while exopeptidases, e.g. Flavourzyme, break peptide bonds at the N- or C-terminus, often no more than three residues from the terminus (Aryee, Agyei and Udenigwe, 2018). When digesting insoluble proteins, the protease acts on the easily accessible peptide chains on the surface of the substrate and as the reaction progress, the structure opens up and more of the substrate will become accessible for proteolysis

(Wubshet *et al.*, 2019a). To get an more optimal hydrolysis, a cocktail of several protease can be used, where proteases with broad specificity can cleave more peptide bonds and expose new or several sites for the more specific proteases (Aryee, Agyei and Udenigwe, 2018). Khiari, Ndagijimana and Betti (2014) found that a cocktail of Alcalase, Flavourzyme and Trypsin worked better than the proteases alone on turkey by-products. According to Cheng *et al.* (2008), the use of Alcalase rather than Pepsin and Trypsin on chicken bone gave the highest peptide content and degree of hydrolysis (DH). Pepsin is reported to not cleave the Gly-X-Y repeats of collagen (Hong *et al.*, 2017). The combined effect of Alcalase and Flavourzyme is also studied, where it was found that the combination of two proteases with endopeptidase and exopeptidase activity could have greater effect than one alone. Starting the hydrolysis with an endopeptidase could increase the number of N-terminal sites available for the exopeptidase. In addition, using the proteases sequentially and not simultaneous could create a higher output, due to the proteases different pH and temperature optimums (Nchienzia, Morawicki and Gadang, 2010).

When it comes to mechanism of action and residues found in the active site, proteases can be divided into six groups; serine, cysteine, aspartic, glutamic, and threonine proteases, in addition to metalloproteases (Walsh, 2014). Without the match in the active site, the proteases are not able to carry out the specific reaction. Denaturation of the proteins can affect this particular match, and the proteolytic activity is often better in proteins that have not been denatured (Nchienzia, Morawicki and Gadang, 2010). Serine proteases are usually endopeptidases and have the presence of an essential serine residue at their active site. This is the most common class of proteases with a widely distribution in nature, and the bacterial subtilisin and trypsin are subgroups of great industrial significance (Di Cera, 2009; Walsh, 2014). The occurrence of aspartic proteases is less abundant than the serine proteases, and the aspartic proteases have an essential aspartic acid residue at their catalytic site. Proteases in this group are mainly produced in the stomach, by lysosomes, or fungi, and the best known proteases are pepsin, chymosin, and cathepsins (Tang and Wong, 1987). Cysteine proteases are also widely distributed in nature and have a cysteine and histidine residue at the active site. The proteases papain and bromelain are the best known in this group. Glutamic proteases are fungal proteases and consist of a glutamic acid residue and a glutamine residue, which together hydrolyze the peptide bond. Threonine proteases contain a threonine residue at the active site, and the best known of this group are the proteasomes. Metalloproteases require a metal ion to sustain biological activity, and collagenases are an example of proteases in this group (Walsh, 2014).

2.3 Enzymatic protein hydrolysis (EPH)

Enzymatic protein hydrolysis (EPH) is a mild processing method where proteins are cleaved by proteases into smaller peptides and free amino acids (Nchienzia, Morawicki and Gadang, 2010; Tavano, 2013). Use of commercial proteases has been considered as the best option for production of food-grade protein hydrolysates since EPH is a highly specific and reproducible method. This can lead to a production of products with higher market value (Aspevik *et al.*, 2018). The prices of the commercial proteases can vary depending on the difficulty of the isolation (Dwevedi and Kayastha, 2011). The EPH is dependent on type and state (native or denatured protein) of substrate, duration of hydrolysis, pH, and temperature, in addition to the type, specificity, and concentration of protease (Lasekan, Abu Bakar and Hashim, 2013). Bitter taste and off-flavors can occur if the hydrolysis is excessive and uncontrolled, reducing the consumer acceptability of the product (Aryee, Agyei and Udenigwe, 2018). However, using an protease of endopeptidase activity could produce a bitter hydrolysate, therefore a possibility is to use an protease with both endo- and exopeptidase activity (Fonkwe and Singh, 1996).

Protein hydrolysates are one of the complex products from the EPH, containing a mixture of different peptides and free amino acids. The hydrolysate can be characterized by using the degree of hydrolysis (DH), which describe the extent of enzymatic peptide cleavage of the protein substrate. It is calculated as a percentage ratio between the number of cleaved peptide bonds and the total number of peptide bonds in the substrate (Manninen, 2009; Pasupuleti, Holmes and Demain, 2010; Lasekan, Abu Bakar and Hashim, 2013).

The enzymatic hydrolysis reaction begins as a rapid linear phase followed by a decline in reaction rate, which is a consequence of substrate digestion (Figure 1). Reaching the theoretical maximum degradation of substrate can be difficult due to several factors, such as a decrease in the available peptide bonds, protease inhibition by substrate or protease deactivation where the protease can lose activity during the reaction due to autolysis, inhibition, aggregation, or denaturation (Moreno and Cuadrado, 1993; Wubshet *et al.*, 2019a).

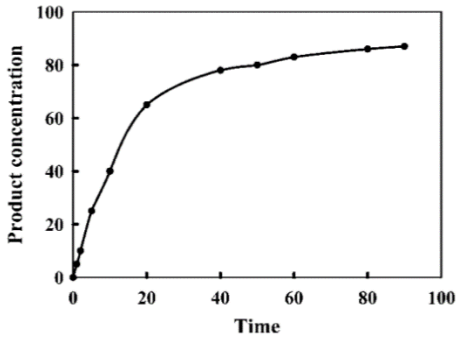

Figure 1. Plot of progress curve during the enzymatic reaction showing the correlations between product concentration and hydrolysis time (Shyu, Tzen and Jeang, 2006).

When producing protein hydrolysates with desired functional properties to use as functional components, the molecular weight of the hydrolyzed protein is one of the most important factors. The peptide composition depend on the specificity of the protease as well as the process conditions (Rossi *et al.*, 2009). The protein hydrolysate can consist of small and/or larger peptides, and the different products have diverse areas of utilization. The small peptides with characteristic amino acid composition and defined molecular weight are e.g. highly desired in human nutrition formulas (Clemente, 2000). The solubility of the hydrolysate increases with increased DH, where small peptides from myofibrillar proteins have more polar residues and the ability to form hydrogen bonds with water, resulting in increased solubility (Gbogouri *et al.*, 2004). However, hydrolysates of larger or hydrophobic peptides have better emulsifying properties (Mutilangi, Panyam and Kilara, 1996).

The advantage of EPH is the mild processing conditions including temperature and pH, since acid and alkaline hydrolysis can destroy some of the essential amino acids. In addition, use of proteases are more specific which enables control of the DH and tailored products. It is possible to use a single protease or multiple proteases in several enzymatic steps. The choice of protease depends on the substrate and the desired end-product. The process simply requires small amounts of protease that easily can be inactivated after hydrolysis. There are many proteases to choose from, making it possible to pick the proteases that is best suited for the substrate and desired product (Pasupuleti and Braun, 2010). Extraction of both collagenous and non-collagenous proteins are possible with the use of proteolysis (Fonkwe and Singh, 1996). In addition, EPH could be a replacement for the conversion of biological waste from the food industry which often are cooked at high pressure, including high energy inputs. Use of proteases for waste conversion is more flexible than traditionally rendering processes and could generate several convertible waste products, e.g. enzymatic digestion of poultry feathers (Walsh, 2014).

2.4 Muscle proteins

Muscle proteins represent about 18-22 % of the lean meat from e.g. poultry and pork. The proteins can be divided into three groups based on their solubility characteristics: myofibrillar (soluble in salt solutions), sarcoplasmic (water soluble), and connective tissue proteins (soluble in acid or alkaline solutions), where they make up approximately 10 %, 9 %, and 3 %, respectively (Toldrá and Reig, 2006; Barbut, 2015a; Xiong, 2018).

Myofibrillar proteins are long, fibrous proteins which are responsible for continuity and strength of the muscle fiber, in addition to contraction and relaxation of the muscle, water holding capacity and protein functionality. The most prominent constituents in the myofibrillar protein are myosin and actin which form the structural backbone of the protein. Sarcoplasmic proteins are globular proteins which function as proteases and cofactors in energy metabolism, in addition to the pigmentation proteins as myoglobin and hemoglobin. Connective tissue, also known as stromal proteins, are fibrous and strong proteins that can be found in tendons, ligaments, skin, cartilage, and bone (Alvarado and Owens, 2005; Toldrá and Reig, 2006).

An important characteristic of proteins is foamability, where they act as surfactants and form a flexible film around air bubbles. The foamability is dependent upon the rate of protein denaturation, revealing the quality of the protein. Proteins with good foamability rapidly unfold and create foam during processing (Chan, Omana and Betti, 2011).

2.5 Collagen

The major structural element found in connective tissue is collagen. Collagen consists of cross-linked tropocollagen molecules which form a characteristic right-handed and 300 nm long triple helix of three left-handed polypeptide chains (Figure 2A) (Gross, 1961; Gelse, Pöschl and Aigner, 2003). The polypeptide chains of collagen are composed of repeating triplets of glycine and two amino acids (Gly-X-Y), where X and Y often are the imide residues proline and hydroxyproline, respectively (Figure 2B) (Zhang *et al.*, 2015). Approximately one-third of the amino acid residues are glycine, while proline and hydroxyproline account for 20-25 % (Coultate, 2009). The composition of amino acids varies depending on the source of collagen, where the Gly-Pro-Hyp triplet is interspersing about every dozen amide residues in the polypeptide chain (Prystupa and Donald, 1996).

Glycine is positioned in the center of the triple helix while the other amino acids fill the outer positions which allows a close packaging along the central axis of the collagen molecule. The stability of the triple helix is caused by interchain hydrogen bonds and inter- and intramolecular cross-links (Harrington, 1996), where the hydrogen bonds links nitrogen in glycine and oxygen in proline (Charvolin and Sadoc, 2012). The stability of the triple helix and the formation of intramolecular hydrogen bonds are depending on the content of hydroxyproline (Ferreira *et al.*, 2012). The N- and C-terminal regions, called telopeptides, contain 15-26 amino acid residues and do not form a triple helical structure due to their content of lysine and hydroxylysine residues, and aldehyde derivates (Gómez-Guillén *et al.*, 2011). The collagen molecule consists of a large fraction of nonpolar R groups, which together with the cross-links gives fibrous proteins with rigid, insoluble structures (Hart *et al.*, 2012).

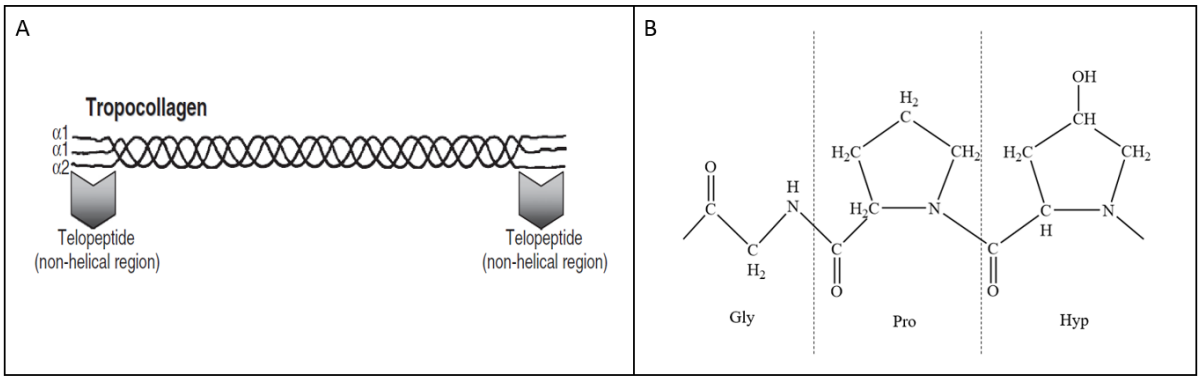

Figure 2. (A) Structure of a cross-linked tropocollagen molecule (Benjakul, Klomklao and Simpson, 2009). (B) Molecule structure of the repeating Gly-Pro-Hyp structure of collagen.

The collagen molecules are arranged in collagen fibrils which constitute a fibril and then a collagen fiber (Figure 3A). The collagen fibrils are stabilized by di- and trivalent cross-links that link two and three different collagen molecules, respectively. The cross-links form a covalent bond between side chains of the residues of two tropocollagen molecules (Figure 3B) (Depalle *et al.*, 2015). The fibril's strength and toughness is caused by the cross-links, in addition to the characterized 67 nm axial periodicity (Bosman and Stamenkovic, 2003). The solubility and digestibility of collagen are determined by the amount and type of covalent linkages (Xiong, 2018). The heat-unstable divalent cross-links are usually present in younger animals, converting to more heat-stable trivalent cross-links during maturation (Depalle *et al.*, 2015).

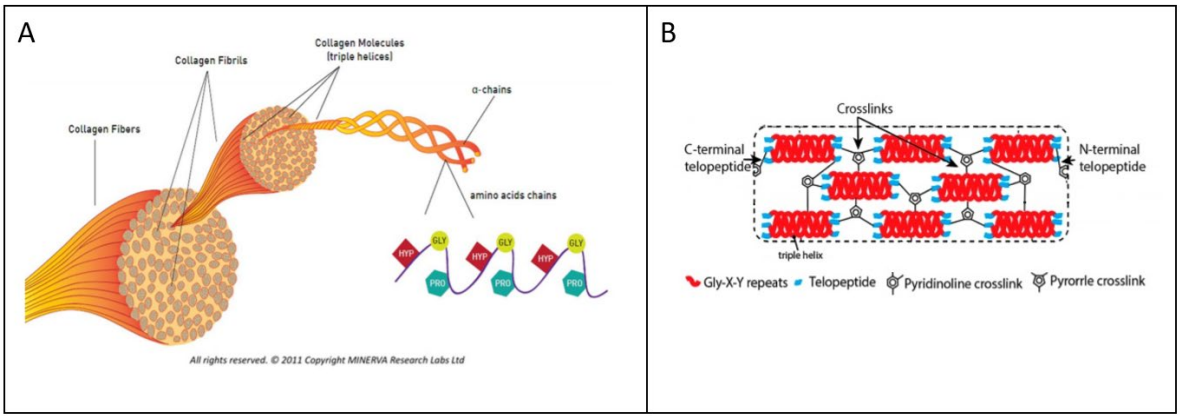

Figure 3. (A) Hierarchical structure of a collagen fiber, showing the collagen fibrils, collagen molecules and α-chains containing chains of amino acids (from Sibilla et al. (2015) with permission). (B) Structure of collagen showing cross-links which are mostly located in the telopeptides (figure edited from Hong et al. (2017)).

The collagens are sorted into 28 groups due to their variation of size, function and tissue distribution (Shoulders and Raines, 2009; Ricard-Blum, 2011). However, only collagen types I, II, III, V, and XI form fibrils, where type I, II, and III are the most commonly occurring collagens (Table 1) (Bateman, Lamande and Ramshaw, 1996). Collagen is arranged in fibrils in tendons, cartilage, skin, and bones, which are tissues that have to resist shear, tensile, or pressure forces. Collagen type I can be found in all fibrous tissues except cartilage, which consists of type II and XI collagen (Bosman and Stamenkovic, 2003).

Table 1. Types of fibril-forming collagens with molecular form and tissue distribution (Bateman, Lamande and Ramshaw, 1996; Gelse, Pöschl and Aigner, 2003; Shoulders and Raines, 2009; Sibilla et al., 2015).

Collagen type	Molecular form	Tissue distribution
I	$[\alpha1(I)]_2\alpha2(I)$	Bone, dermis, tendon, ligaments
II	$[\alpha1(II)]_3$	Cartilage
III	$[\alpha1(III)]_3$	Skin, blood vessels, dermis, intestine
V	α1(V),α2(V),α3(V)	Bone
XI	α1(XI)α2(XI)α3(XI)	Cartilage

The collagen types I, II, V and XI are reported found in poultry residuals where type I and V contribute to the structural backbone of bone while type II and XI contribute to the fibrillar matrix of articular cartilage (Gelse, Pöschl and Aigner, 2003). Collagen type III is distributed widely in many tissues that also contain collagen type I (Bateman, Lamande and Ramshaw, 1996).

2.5.1 Degradation of collagen

Collagen can be degraded from fibers to fibrils and eventually end up as peptides and amino acids (Figure 4). As previously mentioned, collagen is soluble in acid or alkaline solutions, but they can also be solubilized by slow, moist cooking (Xiong, 2018). Otherwise, degradation of collagen requires special proteinases coming from bacteria or mammals. Proteases that can degrade collagen are regarded as collagenases, also known as collagenolytic proteases, including mammalian matrix metalloproteinases (MMPs), mammalian cysteine proteases and some bacterial proteases. The bacterial collagenolytic proteases are e.g. *Clostridium* collagenases and *Vibrio* collagenases (Zhang *et al.*, 2015). MMPs are zinc-dependent endopeptidases which can cleave the fibril-forming collagens type I, II and III (Ricard-Blum, 2011). Collagen molecules are more resistant to proteinases and proteolysis when they are wounded up in a triple helix, cross-linked and arranged in insoluble fibers due to physical obstacles (Garnero *et al.*, 1998; Chung *et al.*, 2004; Hong *et al.*, 2017). The C-terminal telopeptide must be proteolyzed before collagenases can gain access to the cleavage site. Only selected parts of the triple helix will be accessible from the surface of the fibril (Perumal, Antipova and Orgel, 2008). Collagenases cleave helical regions of the collagen molecule in fibrillar form. Other mammalian proteases (e.g. Pepsin, Trypsin, Chymotrypsin and Papain) can degrade gelatin and the nonhelical regions of the collagen molecule (Harrington, 1996). Collagenases bind and locally unwind the triple helix before hydrolyzing the peptide bonds with unique specificity (Chung *et al.*, 2004; Watanabe, 2004). Collagenases cleave the peptide bond between Y-Gly in the repeating Gly-X-Y sequence three quarters away from the N-terminus (Chung *et al.*, 2004; Zhang *et al.*, 2015). The trivalent cross-links are linked between two telopeptides and the helix of another collagen molecule, and proteinases are not able to cleave these links. Hong *et al.* (2017) found that removal of collagen telopeptides could break the connection between trivalent cross-links and the two nearby collagen molecules. This could result in an unorganized arrangement of collagen molecules and an increased solubility.

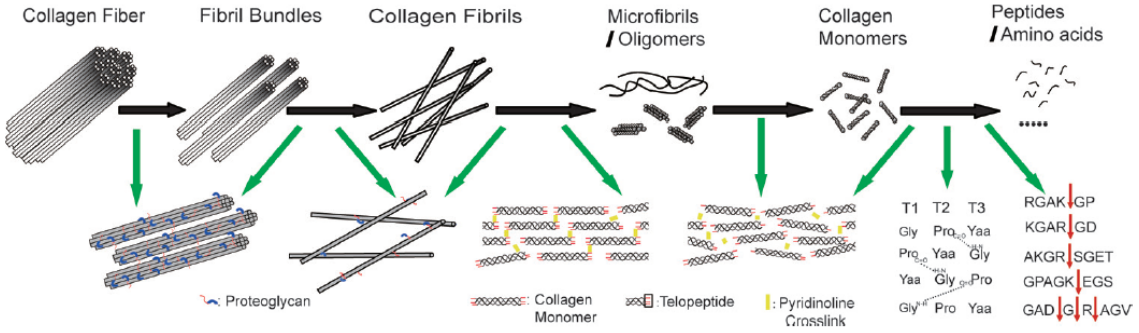

Figure 4. Stepwise degradation of collagen from fibers to peptides and amino acids (Zhang et al., 2015).

When exposed to heat, collagen will go through a structural denaturation and solubilization (Powell, Hunt and Dikeman, 2000). The hydrogen bonds that maintain the structure are weakened and the fibers can shorten as the polypeptide chains adopt a more compact helical structure, which happen already at 40 °C (Coultate, 2009; Provost *et al.*, 2016). Around 65 °C, the cross-links and triple helix will begin to break down. This leads to a loss of the three-dimensional structure, resulting in a solubilization of the collagen, which cause a gelatinization when it cools and the hydrogen bonds are re-established. An increase in time and temperature could lead to more collagen converting into gelatin (Powell, Hunt and Dikeman, 2000; Coultate, 2009; Barbut, 2015a). Denatured collagen is more easily degraded by proteases, but the degradation of native collagen is very slow (Lantto *et al.*, 2009).

Before enzymatic hydrolysis can take place, the mixture needs to be heated to unwound the triple helix of collagen to separate the chains. The mixture is then cooled down, making the denatured mass of tangled chains soaking up all the surrounding water and forming gelatin. Collagen insoluble in water is resistant to most proteases and special collagenases are required for enzymatic hydrolysis. However, gelatin which is a product of denatured collagen is susceptible to most proteases (Vasileva-Tonkova, Nustorova and Gushterova, 2007).

2.5.2 Gelatin

As previously mentioned, gelatin is formed by heat-denaturation of native, insoluble collagen. During denaturation of collagen, the hydrogen bonds disperse causing the collagen triple helix to unravel due to hydrolyzation of the intramolecular, intermolecular and main-chain peptide bonds. The collagen fibrils will disassemble which results in a viscous solution of gelatin (Tarté, 2009). The re-established hydrogen bonding in the gel after cool down is the predominant stabilizing force, making the gelatin gel thermo reversible and melting at body temperature

(Xiong, 2018). Based on the possible extraction temperatures and pH of gelatin, the melting point of gelatin from poultry can vary between 36-40 °C (Kim *et al.*, 2012; Choe and Kim, 2017). Formation of gel is mainly determined by the structure, molecule size and temperature of the system (Gómez-Guillén *et al.*, 2011). Through denaturation and hydrolysis, collagen can be converted into two different types of gelatin. Type A gelatin is derived from young collagen, e.g. skin from pigs and chickens, and is suitable for a broad range of food applications. Gelatin extracted from mature collagen sources, e.g. bones and cartilage, is called Type B gelatin and is more limited for usage in food (Xiong, 2018). Type A and B gelatin can be obtained under acid and alkaline pre-treatment conditions, respectively (Gómez-Guillén *et al.*, 2011).

Gelatin consists of multiple collagen peptides, where the collagen peptides or hydrolysate are soluble in water and has a better bioavailability than gelatin in the human body (Czech, 2016). Gelatin contains eight essential amino acids and therefore an important source of protein (Czech, 2016). The properties of gelatin are dependent on the species specific amino acid composition, the molecular weight distribution and the preservation of the raw material (Gómez-Guillén *et al.*, 2002; Xiong, 2018).

2.5.3 Usage of collagen and gelatin

Traditionally, collagen and gelatin have been extracted from bovine and porcine (Cao and Xu, 2008). After the outbreak of bovine spongiform encephalopathy (BSE), also known as mad cow disease, and banning of collagen from pig in some regions for religious reasons, a need of new sources appeared, e.g. from marine species or poultry. Research for alternative sources and new functionalities for collagen and gelatin has experienced a grown interest the last decade due to an increased desire for economical valorization of industrial by-products from the meat and fish industry, in addition to achieve an environmentally friendly management of industrial wastes. It is also an on-going search for innovative processing conditions as well as potential novel applications (Gómez-Guillén *et al.*, 2011).

Collagen can be used as ingredient in food products for water-holding, product yield, as a clarification agent, emulsifier, and whipping agent. Another market is the pharmaceutical where it can be used as tissue engineering material, microencapsulation or tablet coating (Cao and Xu, 2008). Gelatin has a wide area of utilization and is used in products as emulsifiers, stabilizers, foaming and binding agents, and is an alternative in the growing trends to replace synthetic agents with more natural products (Gómez-Guillén *et al.*, 2011; Czech, 2016; Xiong, 2018). The surface properties of collagen and gelatin are based on the presence of charged groups in

the protein side chains, and hydrophilic or hydrophobic amino acids on certain parts of the collagen sequence (Gómez-Guillén *et al.*, 2011).

Proteases can be used to produce hydrolysates and peptides from collagen and gelatin (Gómez-Guillén *et al.*, 2011; Lasekan, Abu Bakar and Hashim, 2013). Hydrolyzed collagen is produced from collagen naturally found in bones, skin and connective tissue of animals, and consists of small peptides with low molecular weight (0,3-8,0 kDa) (Sibilla *et al.*, 2015). The average molecular weight of hydrolysates can indicate the functional properties of the product (Deeslie and Cheryan, 1992). The low molecular weight can make the hydrolyzed collagen easily digested, absorbed and distributed in the human body (Sibilla *et al.*, 2015). Collagen peptides with low molecule weight and characteristic amino acid composition are desirable in nutrition and food science due to both functional and nutritional purposes (Lin and Li, 2006; Khiari, Ndagijimana and Betti, 2014). The hydrolysates and peptides could have properties and functionalities that benefit the end consumer, e.g. as bioactive peptides (Gómez-Guillén *et al.*, 2011). Collagen and gelatin hydrolysates are presumed to have antihypertensive properties due to their unique composition of amino acids (Kim and Mendis, 2006).

2.6 Residual raw materials from poultry

In 2018, approximately 98 165 tons of poultry was slaughtered in Norway (SSB, 2019), and the percentage amount of residual raw materials produced from chicken and turkey are 51 % and 45 %, respectively (Lindberg *et al.*, 2016). Residual raw materials, also known as plus-products, are defined as that is left after removing the primary main product using a raw material (Olafsen *et al.*, 2014). This can further be divided into co-products, which has food-grade quality and can be used for human consumption, or by-product which are not fit for human consumption due to commercial, safety or regulatory reasons (Roupas *et al.*, 2007; Aspevik *et al.*, 2018). However, several scientific publications use the term by-products as residual raw materials that can be processed for human use (Stevens *et al.*, 2018; Bruno *et al.*, 2019). The Commission of the European Communities Regulation (EC) No. 1069/2009 defines animal by-products (ABPs) as materials of animal origin that are not intended for human consumption due to a potential source of risks to public and animal health, and to protect the safety of the food and feed chain (European Union, 2009). The utilization of by-products is strictly regulated and no ABPs can be used for human consumption, only by-products that end up in category 3 can be used for feed. ABPs are divided into three categories based on the risk involved. Category 1 is a high-risk category and comprises e.g. sick animals, zoo and circus animals, and carcasses from experiments. These ABPs are not suited for ether food or feed and goes straight to disposal.

Category 2 is also of high risk and includes dead-in-shell poultry, carcasses of dead livestock, and animals killed for disease control purpose. By-products from this category can be used as e.g. landfill after sterilization. Category 3 is of low risk and comprises carcasses and part of animals which are fit for human consumption according to the Community legislation, but are not intended for human consumption for commercial reasons. Examples of by-products in this category are domestic catering waste, heads of poultry, feathers, and blood. These by-products can be used for animal feed and organic fertilizers (European Union, 2009; Aspevik *et al.*, 2018).

Processing of ABPs should only be carried out in approved establishments or plants. It is important to separate by-products from the food chain to prevent cross-contamination, and when a product has become an ABP it should not re-enter the food chain. In addition, processing of residual raw materials also require general hygiene requirements to be classified as suitable for human consumption (European Union, 2009). Good quality of the raw material is important for further processing, and there is advantageous that the slaughterhouse is close by or even connected to the processing facility for residual materials, ensuring fresh residual raw materials (Aspevik *et al.*, 2018). To minimize microbial growth of the residuals, effective chilling during and after processing is required (Barbut, 2015b).

The many definitions and designations for leftovers from poultry production could create misunderstandings. To clarify, the general term residual raw materials will be further used in this thesis, in this coherence meaning animal-based products that can be processed for human consumption.

2.6.1 Mechanically deboned poultry residue (MDPR)

In the industry, mechanical deboning is a processing technology used for optimal recovery of meat mince from carcasses that have been through a standard filleting process. The carcasses are grinded to form a meat and bone slurry which is further separated by pressure (Wubshet *et al.*, 2019b).

Mechanically deboned poultry residue (MDPR) consists of bones, cartilage, tendons and remains of tissue from poultry, which contains considerable amounts of insoluble and difficult to decompose structural proteins like collagen (Brandelli, Sala and Kalil, 2015). The residue is a good source of protein, consisting of approximately 24 % (w/w) crude protein of which 35-40 % is collagen (Kijowski and Niewiarowicz, 1985; Cheng *et al.*, 2008). Mechanically

deboned poultry residue has high chemical complexity due to the abundance of connective tissue and bones (Lasekan, Abu Bakar and Hashim, 2013), making it a raw material of high composition variation. Hydrolysis of residual raw materials from the poultry industry with a high amounts of connective tissue and bones has shown lower protein yield due to poor extraction of connective tissue proteins (Wubshet *et al.*, 2017; Wubshet *et al.*, 2018).

2.6.2 Connective tissue in poultry residues

The strong and rigid structure of connective tissue is caused by the content of many cross-linked collagen fibrils (Gómez-Guillén *et al.*, 2011). Cross-links are most abundant in connective tissue in which the greatest strength is required, such as bones, cartilage, and the Achilles tendon (Coultate, 2009). Approximately 90 % of the protein content in poultry leg bone is collagen (Gelse, Pöschl and Aigner, 2003; Lasekan, Abu Bakar and Hashim, 2013; Brandelli, Sala and Kalil, 2015). The bones of poultry are unique due to their great strength and relatively lightness. In addition to connective tissue, bones consist of an organic matrix and inorganic salts, such as calcium salts. The organic matrix contains collagen fibers and a ground substance that consists of proteins and sugar complexes (Barbut, 2015a). Bone and cartilage have a preponderance in collagen type I and III (Xiong, 2018). The properties of cartilage can vary due to differing in amount of collagen fibers and extracellular material. Examples of different properties of cartilage are hyaline cartilage which is found on the surface of joints and bones, and fibrocartilage which is found in tendons and joint ligaments (Barbut, 2015a). In bone, the collagen fibrils are organized like the struts and girders of a bridge where the mineralization of bone follows the detailed fine structure of the fibrils. The thin collagen fibers of cartilage that coats the inner surface of joints must have considerable elasticity and smoothness. In tendons, the collagen fibers are arranged in long parallel bundles (Gross, 1961).

2.7 Analytical methods

2.7.1 The Azo-Casein assay for protease activity

The Azo-Casein assay is a well-used method to measure protease activity. The original protocol is from Charney and Tomarelli (1947), but today a newer, faster, and more sensitive method from Megazyme is mostly used. The red-orange Azo-Casein is a sulphanilamide dyed casein substrate, and the substrate from Megazyme is carefully dyed to produce a substrate with 5-times the sensitivity of similar products (Megazyme, 2007). Measuring protease activity is often based on following the rate of substrate disappearance or the rate of product formation (Wubshet *et al.*, 2019a). The Megazyme method is based on the formation of colored components when proteolytic proteases digest the sample. If the whole substrate is digested, the solution would achieve the maximum color intensity since the bonds between the proteins and chromophoric groups are broken and the hydrolyzed groups go into solution with the termination regent trichloroacetic acid (TCA) (Coelho *et al.*, 2016). When adding TCA, the non-hydrolyzed substrate is precipitated from the solution, and after centrifugation the function of the proteolytic activity can be determined by the intensity of the color in the solution (Charney and Tomarelli, 1947).

2.7.2 Fourier-Transform Infrared Spectroscopy (FTIR)

Fourier-transform infrared spectroscopy (FTIR) is a fast and non-destructive method that can be used to analyze structural or chemical changes in a sample. The method is also suitable for monitoring enzymatic protein hydrolysis since it is found to be in agreement with the breakdown of the amide backbone and formation of amino and carboxyl terminals (Böcker *et al.*, 2017). The FTIR spectrum reflects the degradation of amide bonds during a hydrolysis process and the concurrent formation of terminal amino groups (NH_3^+) and carboxyl (COO^-) groups (Wubshet *et al.*, 2017). The repeating units in the protein and peptide chains are based on nine distinctive IR absorption bands, where amide I and II are the most prominent (Barth, 2007). There are amide groups providing these absorption bands and FTIR is a suitable tool to assess protein secondary structure (Böcker *et al.*, 2017). The effect of the protease and heating treatments on the triple helix structure of collagen can be investigated by the changes in collagen secondary structure using FTIR (Hong *et al.*, 2017). Derivates can be used to reduce scatter effects for continuous spectra. Using the 2nd derivate of the raw data, the shape of the original spectrum changes with peaks appearing at similar locations, uncovering underlying bands (Næs *et al.*, 2002).

Polar groups like C=O, N-H, and O-H give rise to strong IR bands. The amide I band lies near 1650 cm^{-1} and arises mainly from the C=O stretching vibration (Table 2). It is influenced by the secondary structure of the protein backbone and is sensitive to changes in the peptide chain conformation (Prystupa and Donald, 1996; Böcker, 2007). Differences between raw materials are mainly due to the complexity of the amide I band. The amide II band lies around 1550 cm^{-1} and is a mixture of in-plane N-H bending and C-N stretching (Wubshet *et al.*, 2017). The region between 1200-800 cm^{-1} is referred to as the fingerprint region, where similar molecules can give different absorptions patterns (Stuart, 1997; Böcker *et al.*, 2017). Proteins start to lose their secondary structure when converted into smaller peptide fragments. This can be seen as decreasing bands at 1655 and 1548 cm^{-1}, which is characteristic for α-helices bands. The band at 1516 cm^{-1} are attributed to the $-NH_3^+$ group of the N-terminal (Böcker *et al.*, 2017). The bands around 1585 cm^{-1} and 1406 cm^{-1} are originating from asymmetric and symmetric stretching of carboxyl groups (COO^-), respectively (Wubshet *et al.*, 2017).

Table 2. The 2nd derivative bands between 1700 and 800 cm^{-1} on FTIR analyses of residual raw material from poultry. The values are based on and modified from the paper of Böcker et al. (2017).

Annotation	**Band positions (cm^{-1})**
C=O amide I: turns	1687-1664
C=O amide I: α-helix	1655-1645
COO^- (asymmetric stretch)	1593-1583
Amide II: α-helix	1550-1546
$-NH_3^+$ (scissor)	1516-1515
COO^- (symmetric stretch)	1406-1396
Fingerprint region	1200-800

When processing the FTIR spectra, extended multiplicative scatter correction (EMSC) are used to remove physical effects like particle size and surface blaze from the spectra, which do not carry any chemical or physical information (Maleki *et al.*, 2007). EMSC is used when the scatter effect is the dominating source of variability (Næs *et al.*, 2002).

2.7.3 Size Exclusion Chromatography (SEC)

Size exclusion chromatography (SEC) is a liquid column chromatographic technique that is used to measure average molecular weight and distribution of molecular weight to a polymer (Mori and Barth, 1999). Therefore, this method can be used to analyze the molecular weight of the protein fractions (Wubshet *et al.*, 2018). The method is favored for routine and validated analyses due to its speed and reproducibility (Hong, Koza and Bouvier, 2012). The analyzed sample is dissolved in a solvent (mobile phase) and injected into a column of porous particles with defined pore size. As the sample passes through the column, molecules that are too large to enter the pores will be washed out first, whereas the smaller molecules that can diffuse into the pores will be washed out eventually (Figure 5) (Mori and Barth, 1999; Striegel *et al.*, 2009). It is to mention, that the separation is based on the Stokes radii, and the different shapes of proteins, e.g. globular, fibrous, or flexible chains, could cause the Stokes radii to not be in exactly correlation with the molecular weight (Hong, Koza and Bouvier, 2012).

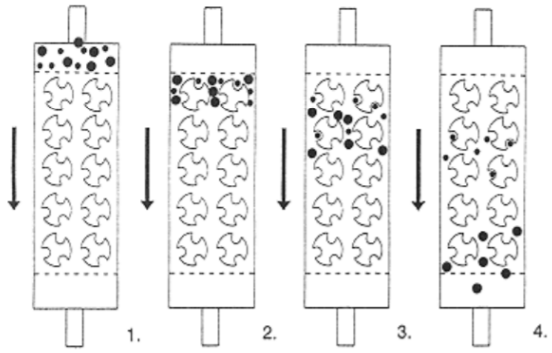

Figure 5. SEC separation of two macromolecular sizes: (1) sample mixture before entering the column packing; (2) sample mixture upon the head of the column; (3) size separation begins; (4) complete resolution (Malawer, 1995).

UV absorption is often used for detection, and near UV (~ 280 nm) or longer wavelengths give great response for the aromatic amino acids, e.g. tryptophan, and is commonly used for measurement of proteins (Aitken and Learmonth, 2009). Far UV or low wavelengths (214 or 220 nm) provide higher sensitivity, where the amide peptide bonds have a strong absorbance (Hong, Koza and Bouvier, 2012). Using a calibration curve based on proteins and peptides of known molecular weight, the molecular weight distribution (MWD) of the sample can be estimated (Hong, Koza and Bouvier, 2012; Aluko, 2018).

2.7.4 Principal Component Analysis (PCA)

Principal component analysis (PCA) is a multivariate analytical method based on latent variables (Perisic *et al.*, 2011). PCA can be used to find the underlying structure in a data set (Böcker, 2007), such as outlier identification, identification of trends and groups, and exploration of similarities. Using PCA, the essential data structures are enlarged while the irrelevant noise is ignored. The central axis is called the first principal component (PC-1), lying along the direction of maximum variance in the dataset (Figure 6). PC-2 represent the second most variance of the dataset, PC-3 the third, and so on.

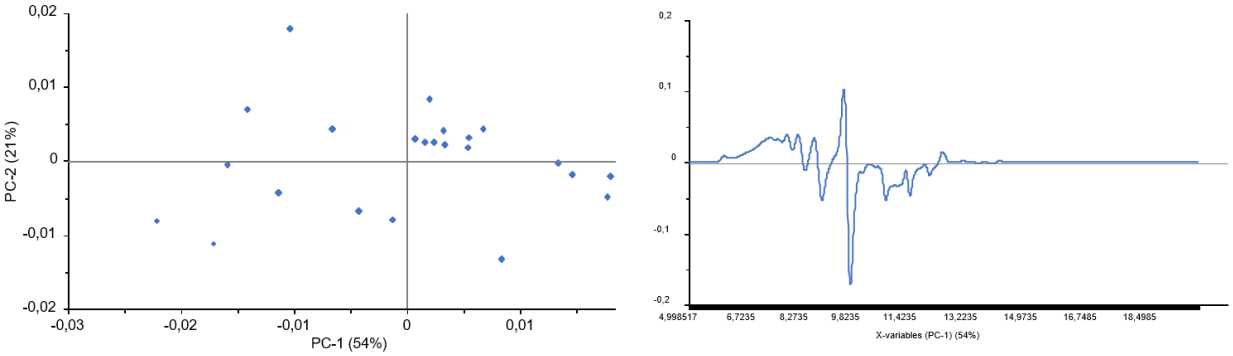

Figure 6. An example of a PCA score plot (left) and the corresponding loading of PC-1 (right).

The score plot of the PCA consists of two pair of score vectors plotted against each other, and the most commonly plot is the score vector of PC-1 (x-axis) against PC-2 (y-axis). This explains the largest and second largest variations in the data set. Loadings give information about the relationship between the variables and the principal component. The loadings show how much each variable contributes to each principal component. The corresponding score and loading plots are complementary and give most information when studied together (Esbensen, Schönkopf and Midtgaard, 1994).

3. Materials and Methods

3.1 Experimental outline

The experimental outline of materials and methods in this master thesis is presented in Figure 7.

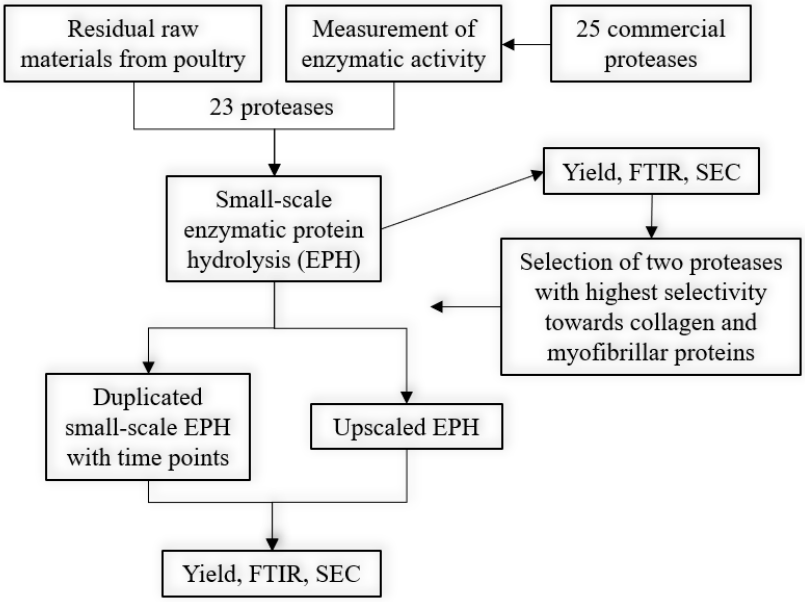

Figure 7. Experimental setup of materials and methods.

The enzymatic activity of 25 different commercial proteases were measured to obtain normalized activities. Experimental method development was a major part of this master thesis, and designs of a small-scaled and upscaled enzymatic protein hydrolysis (EPH) were developed. The small-scale EPH was first conducted with 23 selected proteases on four different residual raw materials of poultry to screen their selectivity towards collagen and myofibrillar proteins. The raw materials were Achilles tendons from turkey, leg bone and meat from chicken, and mechanically deboned chicken residue (MDCR). Based on the results from the first small-scale EPH, the two proteases with highest selectivity towards collagen and myofibrillar proteins were chosen. These two proteases were again tested in the small-scale EPH, this time with duplicates and three time points. The two proteases were also tested in a upscaled version of the EPH to study the scalability. All hydrolysates from the EPHs were analyzed using Fourier-transform infrared spectroscopy (FTIR) and size exclusion chromatography (SEC).

3.2 Measurement of proteolytic activity

For estimation of protease activity, the Megazyme Assay of endo-protease using Azo-Casein was used with some adjustments (Megazyme, 2007). A total of 25 different commercial proteases were measured, and the utilized proteases were Alcalase 2.4L[1], Bromelain[2], Corolase 2TS[3], Corolase 7090[3], ENDOCUT-01[4], Endocut-02[4], ENDOCUT-03[4], Flavourzyme[1], FoodPro 30L[5], FoodPro 51 FP[5], FoodPro PNL[5], MaxiPro NPU[6], Neutrase[1], PROMOD 144GL-100TU[7], PROMOD P950L[7], Protamex[1], TAIL-10[4], Tail-189[4], Tail-190[4], Tail-191[4], Tail-192[4], Tail-193[4], Tail-194[4], Tail-197[4], and VERON L[3].

Selection of buffer depended on the utilized protease, where the thiol-proteases (Bromelain, PROMOD 144L-100TU, PROMOD P950L and VERON L) needed buffer B for extraction and dilution. All the other proteases employed buffer A.

- Buffer A (Sodium phosphate, 0.1 M, pH 7.0): 89.09 g of di-sodium hydrogen phosphate dihydrate ($Na_2HPO_4 \bullet 2H_2O$, Merck, Germany) was dissolved in 400 ml of distilled water and the pH was adjusted to 7.0 with 5 M HCl. The volume was then adjusted to 500 ml. To achieve a 0.1 M solution, 50 mL buffer was diluted in 450 ml distilled water.
- Buffer B (Sodium phosphate, 0.1 M, pH 7.0), with cysteine and EDTA: 1.78 g of di-sodium hydrogen phosphate dihydrate ($Na_2HPO_4 \bullet 2H_2O$, Merck, Germany) was dissolved in 75 ml distilled water, and 0.53 g L-cysteine hydrochloride monohydrate ($C_3H_7NO_2S \bullet HCl \bullet H_2O$, C-7880, Sigma-Aldrich, Germany) and 1.12 g EDTA ($C_{10}H_{14}N_2Na_2O_8 \bullet 2H_2O$, Calbiochem, Germany) were added and dissolved. The pH was adjusted to 7.0 with 1 M sodium hydroxide, and the volume was adjusted to 100 ml

The casein substrate was prepared mixing 0.5 g of Azo-Casein in a 50 ml tube with 1 ml of ethanol. The solution was stirred on a vortex mixer to remove all lumps, then treated with 24 ml of sodium phosphate buffer (0.1 M, pH 7.0; buffer A). The suspension was again well stirred until the substrate was completely dissolved. Powered proteases (0.02 g) was suspended in 1000 µl of buffer A or B, while liquid proteases (20 µl) was suspended in 980 µl buffer, to get a dilution of 1:50. The preparations were further diluted to achieve a concentration within the linear area at the spectrophotometer. In addition, blank samples of the protease solution and substrate were prepared.

[1] Novozymes ApS (Denmark)
[2] Ultra Bio-logics (Canada)
[3] AB Proteases GmbH (Germany)
[4] Tailorzyme ApS (Denmark)
[5] DuPont-Danisco (USA)
[6] DSM (The Netherlands)
[7] Biocatalysts LtD (UK)

Eppendorf tubes with protease solution (250 µl) and substrate (200 µl) were placed in a thermomixer (42 °C, 500 rpm, Eppendorf, Germany) for pre-equilibration. After 20 minutes, 200 µl of the protease solution was added to the corresponding tube with substrate. The solution was stirred on a vortex mixer and incubated at 42 °C for 10 minutes. The reaction was terminated by adding 1.2 ml of 5 % (w/v) trichloroacetic acid (TCA, Cl_3CCOOH, Sigma-Aldrich, Germany) with vigorous stirring for 3 seconds on a vortex mixer, making non-hydrolyzed Azo-Casein to precipitate. Reaction blanks were prepared by adding TCA to the substrate solution immediately before the protease preparation was added. The tubes were cooled down to room temperature for 5 minutes before centrifuged at 5000 rpm for 10 minutes in a microcentrifuge (VWR Microstar 17R). The absorbance of the supernatant solutions was read against the reaction blank at 440 nm in cuvettes using a spectrophotometer (Pharmacia Ultrospec 3000).

3.3 Experimental method development

3.3.1 Calculation of protease concentrations

In the beginning of the experimental method development, a protease concentration of 1 % w/w was used. However, to equalize the differences in activity of the proteases, the results from the measurements of proteolytic activity were used to get a more optimized concentration of each protease. Based on this screening, 23 different proteases, both proteases and collagenases, were chosen and an individually concentration for each protease was calculated. Using the linear regression function in GraphPad Prism 8 (GraphPad Software, California, USA), an individually linear function ($y = ax + b$) for each protease was created based on results from the spectroscopy measurements, and based on this equation an x-value was calculated when $y = 1$. The dilution fold was calculated dividing each x-value by y. The mean of the dilution fold of both the liquid and powder proteases were 3707 and 4630, respectively, the deviation for each protease was calculated based on the mean. Finally, the individually concentration for each protease was calculated based on the addition of 20 µl or mg of protease in the screening of activity.

3.3.2 Preparation of raw materials

Achilles tendons and mechanically deboned chicken residue (MDCR), both frozen, were collected from a slaughterhouse (Nortura, Hærland, Norway). Chicken thighs (frozen) and chicken filet (fresh) were bought from a local grocery store in Ås, Norway.

Since tendons from chicken were more difficult to collect, it was decided that Achilles tendons from turkey could be used with the regard of a possible difference in structure and composition. Meat remaining on the Achilles tendons after slaughtering was removed using a knife before the tendons were cut in 5 mm pieces. The chicken filet was homogenized using a blender (BL-1200, Wilfa, Norway) for 5 seconds. The MDCR was already preprocessed and grounded at Nofima. The chicken thighs were cleared of meat, and the joint was cut over resulting in two separate bones from each chicken thigh. Several methods of crushing the bones were investigated. All the different methods included freezing in a -40 °C freezer before the bones were treated with liquid N_2 and crushed. The first attempt involved crushing using an iron mortar which worked to a certain degree. However, the use of this equipment could cause transfer of iron ions into the raw material and possibly affect the activity of certain proteases. A mortar of porcelain was used to avoid this problem, but the smooth surface resulted in difficulties since the bones slipped away from the pestle. Crushing with a vise was also tried, resulting in both small and big pieces of bones. Finally, crushing bones using a blender was tried, and this method seemed most representative to the grounding method of the MDCR in the industry. However, this method leaved some big parts of bones that did not get crushed.

3.3.3 Test of equipment and methods of separation

To find a suitable tube size and buffer volume for the small-scale hydrolysis, tubes of 8, 10 and 14 ml were tested. In the 8 ml tube it was room for 6 ml buffer, while the 10 ml and 14 ml tubes roomed 8.5 ml and 12 ml, respectively. Based on these tests it was concluded that the 10 ml tubes had the most appropriate volume for this experiment considering optimal movement and stirring of the sample. In each tube there was room for 8.5 ml of buffer independent of type of raw material, leaving a small air pocket for improved mixing.

To be able to run many tubes at the same time, a self-composed setup of an end-over-end mixer (Cell culture roller drum, Bellco Biotechology, USA) was developed (Figure 8). The tubes were fastened on the side and front of the wheel using rubber bands and paper clips.

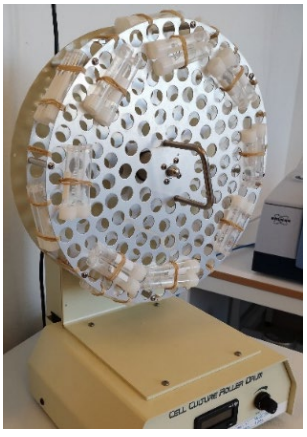

Figure 8. Setup of the end-over-end mixer.

After proteolysis, the sample consists of three different phases, i.e. a water-soluble phase, a fat-rich phase, and a residue. Calculations of yield was based on the residue, thus wanting a good separation of the three phases to obtain a pure residue. Separation of these three phases

using centrifugation was tested. When centrifuging the samples at 4 °C, a clear gelatin layer mixed with the sediment layer was formed in the samples of tendons. However, it appeared to be difficult to extract this gelatin layer. When re-heated, some of the liquid gelatin would still be trapped in the residue when trying to extract it. Another approach was tried, centrifuging the samples at 40 °C trying to get a combined water/gelatin phase that could be poured into a new tube immediately after centrifugation. The hypothesis was that a following centrifugation at 4 °C would separate the water/gelatin phase into two separate layers. However, this did not work out as expected. The alternative of filtration of the sample was tried, appearing to work better than centrifugation since it was easier to get a "gelatin-free" residue. In addition, foaming appeared to be a prominent problem for the samples of tendons and chicken meat when filtrating using a small funnel. The foam could be decreased using warm water to heat the funnel before filtration. Several paper filters were tried where several torn apart, except the Whatman 597 paper filter which was thicker and more appropriate for filtration of these raw materials.

3.3.4 Small-scale enzymatic protein hydrolysis

After a thorough method development phase, a final procedure for the small-scale enzymatic protein hydrolysis could be established, in addition a general protocol was developed (Appendix A). All raw materials were prepared before starting the experiment, weighing 2 g (between 2.000 – 2.050 g) of raw material into a 10 ml tube (79x16mm, Sarstedt, Germany). The weights of the sample and the empty tube were noted, and the tubes were marked with type of raw material. All samples were stored in a -40 °C freezer before use.

On the experiment day, eight tubes of each raw material were taken out of the freezer and defrosted in a cold water bath. The tubes were marked according to protease and duration of hydrolysis, in addition of name and date. During the experiment, background samples of each raw material without addition of protease were included. To be able to work under controlled conditions, a weak buffer solution was used. Using a serological pipette, 7.5 ml of 0.01 M sodium phosphate buffer was added in each tube (Figure 9). The samples were pre-heated for 10 minutes in a water bath at 45 °C to achieve a sample temperature of 40 °C.

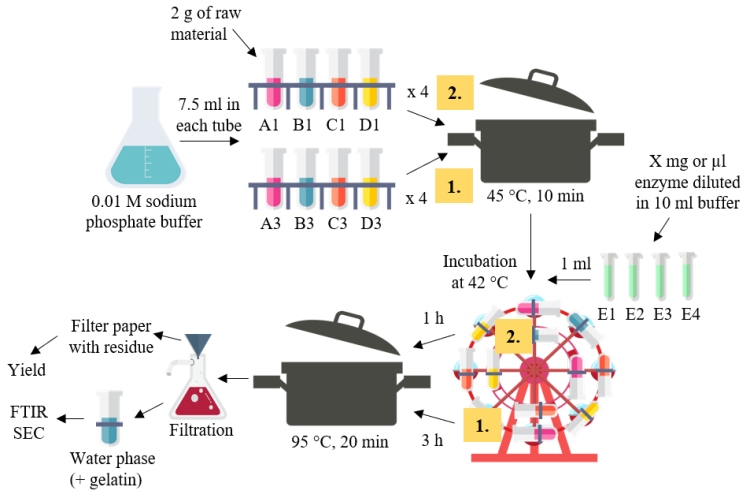

Figure 9. Flow chart of the small-scaled enzymatic protein hydrolysis on Achilles tendons (A), chicken bones (B), chicken meat (C), and MDCR (D) for 1 and 3 hours. Four protease solutions (E1-E4) were used each round.

As described in chapter 3.3.1, an individually amount of each protease needed was found and four solutions with different proteases were made. A certain amount of protease was diluted in 10 ml buffer and 1 ml from this solution was added in each corresponding tube after pre-heating. After addition of protease, the tubes were placed in the end-over-end mixer which was placed in a heating cabinet (TS8136, Termaks, Norway) for incubation at 42 °C. The 3-hours samples were put on the outside of the wheel while it was standing on the bench for easier access to the rubber bands. When the 3-hours samples were ready and put for incubation, the 1-hour samples were prepared.

When the hydrolysis was finished, samples were taken out from the cabinet and placed in a water bath at 95 °C for 20 minutes to inactivate the proteases. The lids were opened to avoid excess pressure in the tubes. After inactivation, the samples were vacuum filtrated using a Büchner flask with a glass funnel and a 597 Whatman filter paper. A 50 ml tube was put into the flask to collect the filtrated liquid phase. The filter paper and funnel were pre-heated with hot water before filtration. After filtration, the filter papers including residuals were dried until completely dry in the heating cabinet at 50 °C, in addition to the empty tubes after filtration in case of remaining samples. The dried filters and tubes were weighted for calculation of yield and enzymatic reactions.

Since the samples of tendons usually formed a gel after cooling down, the samples that formed gel or were viscous were diluted 1:4. Samples for FTIR and SEC analyses were prepared using a 5 ml syringe and needle (0.8x55 mm) to extract the liquid phase and then filtrate the sample

through a 0.45 µl Millipore filter. The liquid phase was filtrated into Eppendorf tubes and vials for analysis with FTIR and SEC.

3.3.5 Small-scale enzymatic protein hydrolysis with duplicates and time points

Based on the results from the first small-scale hydrolysis, the two proteases with the highest specificity towards collagen and myofibrillar proteins were chosen. This selection was based on the ratio of tendons/meat (A/C) that was digested by proteases. Data from FTIR and SEC were also used in the decision to see if some of the proteases were standing out from the rest.

The small-scale hydrolysis as described in chapter 3.3.4 was again conducted with these two proteases, this time with duplicates, and a timeline with three time points (15, 30 and 60 minutes). The utilized raw materials were Achilles tendons, mechanically deboned chicken residue (MDCR), and artificial MDCR made of one-third of tendons, chicken bones, and chicken meat. The new approach followed the same protocol as the first small-scale hydrolysis (Appendix A). However, microwave inactivation was conducted to quickly start the inactivation (Figure 10). The samples were immediately put on ice before microwaved, transferring each sample into a bigger tube (15 ml) to avoid boiling over. Special lids with a drilled hole was used while microwaving for 4-5 seconds until the sample started boiling, before put in a water bath at 95 °C for 15 minutes.

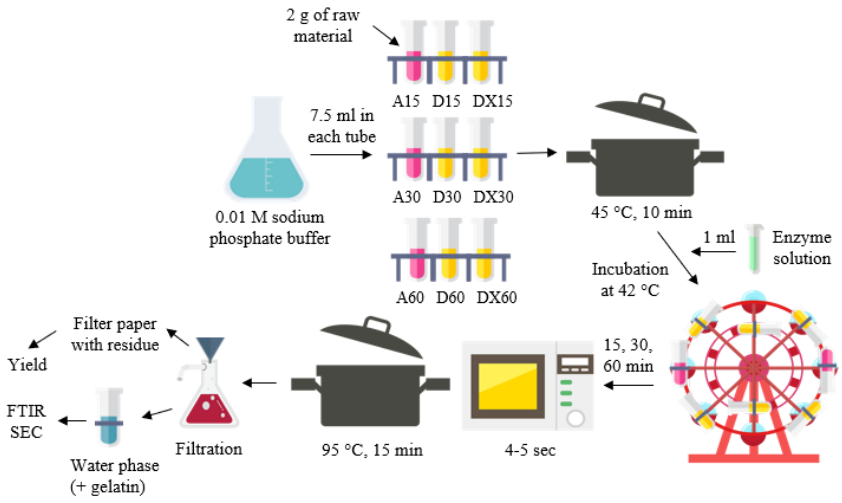

Figure 10. Flow chart of the small-scale enzymatic protein hydrolysis with duplicates of Achilles tendons (A), MDCR (D), and an artificial MDCR (DX) with the time points of 15, 30, and 60 minutes.

3.3.6 Upscaled enzymatic protein hydrolysis

A upscaled version of the small-scale enzymatic protein hydrolysis was developed. The selected proteases from chapter 3.3.5 were also used in this experiment. The utilized raw materials were Achilles tendons, chicken leg bone, chicken meat, and MDCR, in addition to an artificial MDCR composed of 1/3 of the first three raw materials. Of each raw material, a duplicate of 40 g was weighed into a 500 ml screw cap bottle and mixed with 150 ml of 0.01 M sodium phosphate buffer (Figure 11). Protease solutions of 20 ml was prepared based on previous calculated protease concentrations. Several heating methods were tried, e.g. magnet stirrer in water bath, beaker with water on a magnet stirrer, and wrapping of a pre-heated bottle in aluminum foil standing on a magnet stirrer. The last alternative was concluded as the most convenient method due to speed and stability of heating.

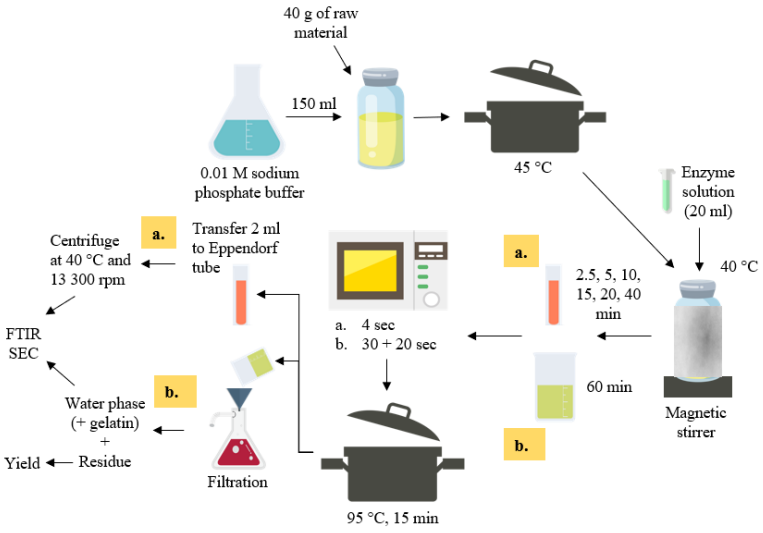

Figure 11. Flow chart of the upscaled enzymatic protein hydrolysis for 1 hour including sampling after 2.5, 5, 10, 15, 20, and 40 minutes.

The hydrolysis was running for 1 hour in total, with sampling (2 ml) after 2.5, 5, 10, 15, 20 and 40 minutes. The stirrer was stopped for 5-10 seconds before extraction of samples to avoid residue in the sample. Samples were taken out in a 15 ml tube, inactivated in both microwave for 4 seconds and 15 minutes in a 95 °C water bath, before poured into a 2 ml Eppendorf tube and centrifuged at 40 °C and 13 300 rpm. After 60 minutes the hydrolysis was complete, and the remaining sample was inactivated in microwave for 30 + 20 seconds before 15 minutes in 95 °C water bath. The 60 minutes sample was vacuum filtrated using a Büchner flask and a flat funnel, and liquid phases from all samples were filtrated through a 0.45 µl Millipore filter into Eppendorf tubes and vials for analysis with FTIR and SEC. The final protocol with more details can be found in Appendix B.

3.4 Fourier-Transform Infrared Spectroscopy (FTIR)

To get an indication of the ability for each protease to break down the residual raw materials, FTIR analyses were conducted. From each sample, five replicates with 7 µl of the liquid phase were pipetted onto a 96-well microplate and dried at room temperature (Figure 12). The plate was analyzed in a High Throughput Screening eXTension (HTS-XT) connected to a Tensor 27 spectrometer (Bruker Optics, Germany) and the OPUS/LAB software. The data obtained from the analysis was further analyzed using the computer software *The Unscrambler* (Camo Analytics, Norway). The raw data were preprocessed using the Savitzky-Golay algorithm to create a second derivate with 13 smoothing points and a polynomial degree of two. For normalization of the spectra, extended multiplicative scatter correction (EMSC) was used followed by creating an average of the parallels of each sample. Then, a Principal Component Analysis (PCA) was made within the spectral region from 1800-400 cm^{-1}.

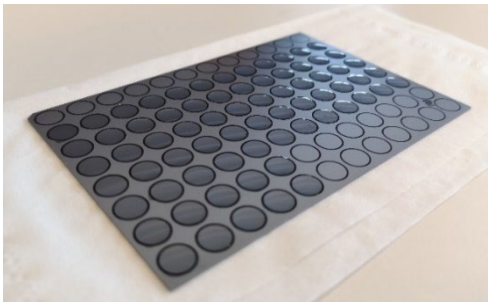

Figure 12. 96-well microplate with applied samples before drying.

3.5 Size Exclusion Chromatography (SEC)

To study the average molecular weights of peptides and free amino acids dissociated in the hydrolyses, SEC analyses were conducted based on the protocol from Wubshet *et al.* (2017). Chromatographic separation of filtrated hydrolysates was performed on an UltiMate 3000 HPLC series instrument (Thermo Scientific, USA) consisting of a RS variable wavelength detector, an autosampler and a pump. For separation, an injection volume of 10 µl was sent through a BioSep-SEC-s2000 column (5 µl, 145 Å, 300 x 7.8 mm, Phenomenex) at 20 °C. The mobile phase consisted of a mixture of 30 % acetonitrile (ACN) (v/v) and MilliQ water with 0.05 % trifluoroacetic acid (TFA). For cleaning of the column, a 0.1 M NaH_2PO_4 solution was used. The UV wavelength area was 214-254 nm. The chromatographic runs were controlled in Chromeleon 7.2 Chromatography Software (Thermo Scientific, USA). Calculations of average molecular weight (M_w) were performed using PSS winGPC UniChrom V 8.00 (Polymer Standards Service, Mainz, Germany), and a UV trace at 214 nm. The obtained data were normalized due to the differing amount of proteins in the column. Normalization made it possible to compare the fractions of different size. Using a pre-made calibration column of polynomial third degree, a mass distribution curve was created from the range of 5 to 20 minutes. This curve was then divided into sections based on peptide sizes.

4. Results and Discussion

The main focus for discussion will be the results from the hydrolyses on Achilles tendons and chicken meat, since they were the purest components of collagens and myofibrillar proteins of the utilized residual raw materials. Chicken bones was in general difficult for the proteases to digest, thus the Achilles tendons was a more accessible substrate for connective tissue. The mechanically deboned chicken residue (MDCR) was a mixture of all the mentioned components, and was used to study the proteases' digestion of a substrate rich in both collagen and myofibrillar proteins.

4.1 Proteolytic activity

The proteases' activities towards the nonspecific protease substrate Azo-Casein were measured to obtain normalized activities for all proteases. Each protease was measured twice for adjustments and customizing of the dilution series. An example of a dilution series and obtained absorbance can be seen in Table 3. The linear range of the spectrophotometer was 1.5-0.10 OD, and the dilutions were prepared trying to match this interval. The first 1:50 dilution for each protease were not measured since it often was far above the interval range.

Table 3. Example of dilution series and absorbance of the liquid protease TAIL-10.

Protease	Measurement	Dilution	Concentration (µl/µl)	Absorbance (OD, 440 nm)
TAIL-10	First	1:10	0.001	>3.0
		1:5	0.0002	2.0
		1:4	0.00005	0.64
	Second	1:50	0.0002	1.9
		1:4	0.00005	0.61
		1:2	0.000025	0.29

The concentrations were calculated by dividing the amount of protease (µl or mg) on the total volume of 1000 µl, then dividing by 10 or 5 if a 1:10 or 1:5 dilution, respectively. Further, these values were divided by two based on the concentration in the Megazyme assay (50 % substrate and 50 % protease solution). However, some of the powder proteases were not divided by two, which lead to the use of double concentrations of these proteases in the following experiments. It is to mention that Bromelain and Protamex were calculated the same way as the liquid proteases even though they were powders due to a misinterpretation. The errors of the powder proteases should be kept in mind while further reading. The results from the measurements were used to find an equation for y using linear regression (see Appendix C, Table C.1 for an example of TAIL-10) which was used to create plots of all protease concentrations against

absorbance (Appendix C, Figure C.1). All the 25 proteases showed varying extent of activity against Azo-Casein. However, there were big differences in activity where the liquid proteases differenced with a factor of 28 times and the powder proteases with a factor of 11 (Table 4). MaxiPro NPU and Neutrase were excluded from further trials due to a low proteolytic activity and the need of high concentrations of 199 and 157 µl, respectively.

Table 4. Calculations of protease concentrations based on the results from the screening of the proteolytic activity (powder proteases).*

Protease	*Activity*	*a*	*b*	*x when y = 1 (10^{-3})*	*Dilution fold*	*Deviation from the arithmetic mean*	*Amount of protease (µl or mg/1000 µl)*
Alcalase 2.4L	Endo, Exo	4771	-0.12	0.23	4272	0.87	17.4
*Bromelain**	Endo	9183	0.14	0.094	10683	0.35	6.9
Bromelain (new batch)*	Endo	9173	0.10	0.098	10198	0.36	7.3
Corolase 2TS	Endo	890.5	0.0040	1.1	894	4.1	82.9
Corolase 7090	Endo	1515	-0.021	0.67	1483	2.5	50.0
ENDOCUT-01	Endo	957.2	-0.0044	1.0	953	3.9	77.8
Endocut-02	Endo	7998	0.25	0.093	10698	0.35	6.9
ENDOCUT-03	Endo	6697	0.10	0.13	7474	0.50	9.9
Flavourzyme	Exo	1580	-0.030	0.65	1534	2.4	48.3
FoodPro 30L	Endo	6491	0.10	0.14	7244	0.51	10.2
*FoodPro 51 FP**	Endo, Exo	1196	0.099	0.75	1327	2.8	55.9
FoodPro PNL	Endo	1531	-0.055	0.69	1451	2.6	51.1
MaxiPro NPU	Endo	3838	-0.031	2.7	372	10	199.1
Neutrase	Endo	489.9	-0.037	2.1	472	7.8	156.9
PROMOD 144GL-100TU	Endo	1187	-0.043	0.88	1138	3.3	65.1
PROMOD P950L	Endo	4674	0.057	0.20	4956	0.75	15.0
*Protamex**	Endo	1728	-0.061	0.61	1629	2.3	45.5
TAIL-10	Endo	9260	0.12	0.095	10572	0.35	7.0
*Tail-189**	Collagenase	11057	0.14	0.078	12806	0.36	7.2
*Tail-190**	Collagenase	2472	0.022	0.40	2527	1.8	36.6
*Tail-191**	Collagenase	4267	-0.093	0.26	3904	1.2	23.7
*Tail-192**	Collagenase	4443	0.15	0.19	5215	0.89	17.8
*Tail-193**	Collagenase	4034	0.21	0.19	5128	0.90	18.1
*Tail-194**	Collagenase	1006	0.098	0.90	1116	4.2	83.0
Tail-197	Collagenase	1894	-0.11	0.58	1714	2.7	54.0
VERON L	Endo	4050	-0.13	0.28	3570	1.0	20.8

It must be taken in consideration that the proteases' activities were tested towards casein, not collagen and myofibrillar proteins. Unfortunately, there are no acknowledged assay kits available for testing of protease activity towards these proteins. The assay using Azo-Casein was conducted due to being a well-known method for measuring protease activity (Eason *et al.*, 2007; Franco *et al.*, 2017). Thus, it was assumed that the proteases will have different activities toward the residual raw materials used in the following experiments.

4.2 Small-scale enzymatic protein hydrolysis

The small-scale enzymatic protein hydrolysis was developed based on the desire of testing the proteolytic activity of several proteases towards different residual raw materials without wasting large amounts of neither proteases or raw materials. The analyzed residual raw materials were Achilles tendons, chicken meat, chicken bones, and mechanically deboned chicken residue (MDCR).

4.2.1 Yield of the small-scale hydrolysis

The yield of the hydrolysis was based on the remaining residue and not the peptide content of the hydrolysate, since a high degradation of peptide bonds not necessarily corresponds with a high yield. Calculations of yield were conducted to study the degree of decomposed raw material. The water content of each raw material was found by drying at 50 °C until completely dried (Table 5). To demonstrate that a background reaction will occur when exposing the raw material to buffer solution and heat, a background sample of each raw material without a protease were included in the experiment. The background reaction (%) was the fraction of the raw material that will dissolve into the liquid phase when exposed to buffer solution and heating treatment. This fraction was calculated by dividing the dried weight of the background sample on the dried weight of the raw material (Appendix D).

Table 5. Water content (%) and background reactions (%) in the different raw materials based on background samples from the small-scale hydrolysis run for 1 and 3 hours.

Raw material	Water content (%)	Background reaction 1 hour (%)	Background reaction 3 hours (%)
Achilles tendons	59.9	21.5	22.4
Chicken meat	75.0	18.4	18.5
Chicken bones	53.6	14.0	24.5
MDCR	60.0	3.9	18.8
Artificial MDCR	62.8	17.9	-

As seen in Table 5, the background reactions for Achilles tendons and chicken meat were stable between 1 and 3 hours, from 21.5 to 22.4 %, and from 18.4 to 18.5 %, respectively. However, the values for chicken bones and MDCR showed larger variations, from 14.0 to 24.5 %, and from 3.9 to 18.8 %, respectively. This can be explained by the variation of sample, since bones and MDCR consisted of both small and large pieces of bones. When having samples of small volumes (2 g), homogeneous and reproducible samples could be difficult to achieve. The difficulties with enzymatic digestion of bones could also explain the differences between 1 and 3 hours, where big and small particles, in addition to cleaved particles with accessible bone marrow etc. (Figure 13), gave different starting points for hydrolysis. The artificial version of MDCR was not used in this experiment, however a background reaction was calculated for later use based on the values for the consisting components, meaning one-third of tendons, meat, and bones. No background reaction for artificial MDCR for 3 hours was calculated.

Figure 13. Dried pieces of chicken bones after hydrolysis with Bromelain.

The lack of parallels was also an explanation for the differences in background reactions, thus a solution easy to attain. However, this method was developed and conducted to find promising proteases which could be further investigated. Repetitions were excluded from this experiment due to first and foremost, time limitations, considering the large number of samples and the fact that it was just a first screening of the proteases' activities towards residual raw materials from poultry. Another possible explanation for the variations could be the presence of endogenous proteases, e.g. cathepsins. Cathepsins are native proteases found in meat and are involved in the postmortem degradation of myofibrillar proteins. In addition, they have shown activity against collagen (Xiong, 2018). It could be possible that endogenous proteases in bones and mechanically deboned residue caused autolysis, which is in accordance to the findings of Lapeña *et al.* (2018) where chicken by-products (heart, liver, and digestive tract) lead to a protein solubilization of around 30 % and 50 % when hydrolyzed for 1 and 2 hours, respectively.

The total yield was calculated as the difference between the dry-weight of the residues before dissolution to the dry-weight of the remaining amount of residue in the proteolyzed samples (Appendix D, Table D.1-D.4). However, in this case it was more interesting to look at the yield after proteolysis, and the term yield will further be based on how much of the raw material that has been digested by protease and dissociated into the liquid phase. This value can be found

when subtracting the background reaction from the total yield. The enzymatic yield of all proteases on Achilles tendons, chicken bones, chicken meat, and MDCR for 1 and 3 hours are shown in Figure 14.

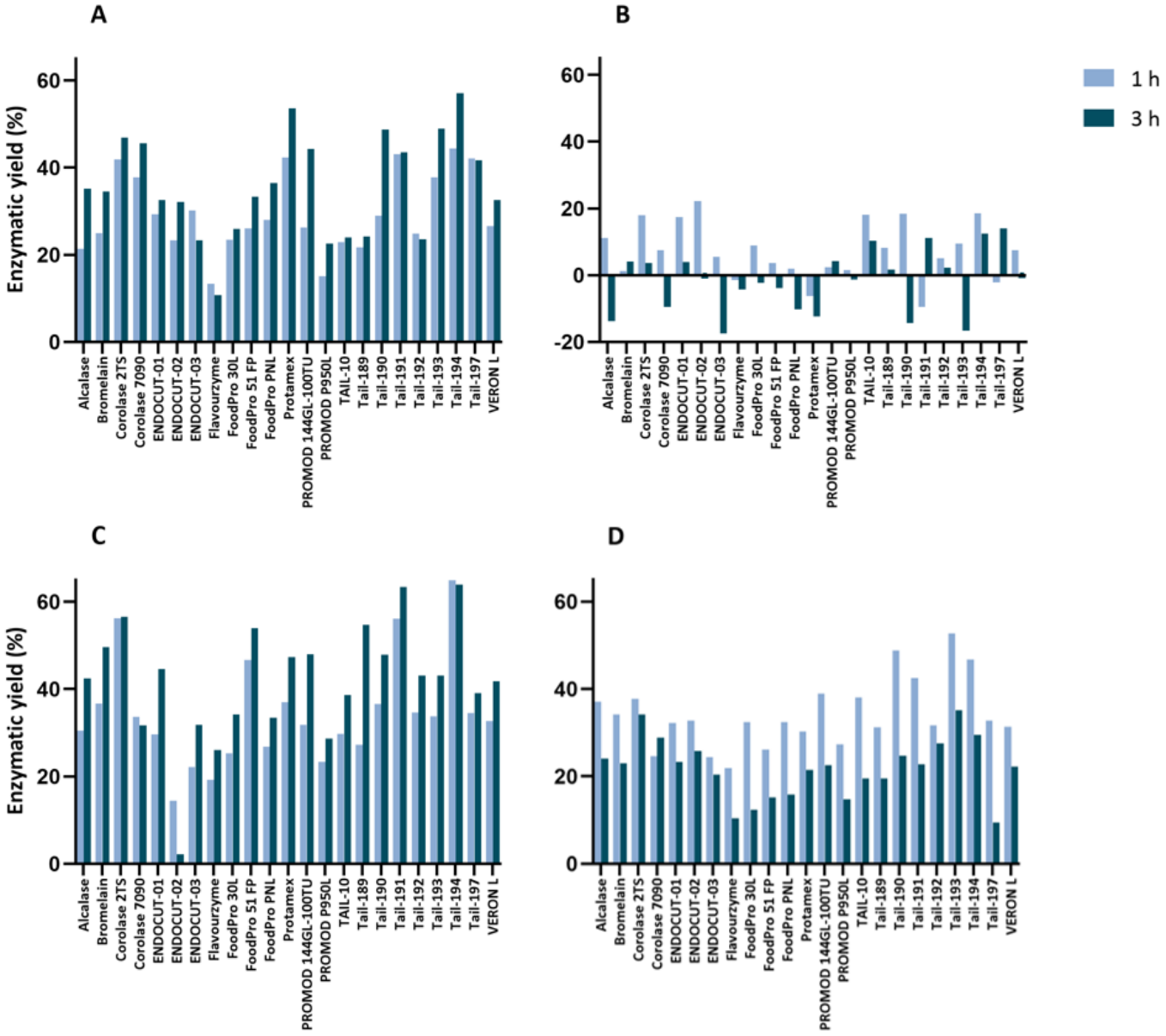

Figure 14. The enzymatic yield of the raw materials Achilles tendons (A), chicken bones (B), chicken meat (C), and MDCR (D), after 1 and 3 hours of small-scale hydrolysis.

As seen in Figure 14, there was a great difference between the proteases' abilities to break down the residual raw materials. The enzymatic yield increased from 1 to 3 hours for Achilles tendons and chicken meat, but decreased for MDCR. Negative values were observed for chicken bones, which could be explained by the background reaction's influence on the yield. After 3 hours,

multiple proteases had negative values for bones, in addition to a decreased value of MDCR which corresponds to the larger background reactions at 3 hours than 1 hour for these raw materials. The durations of hydrolysis were chosen to study if there were any proteases that had activities that needed longer time for optimal utilization. In this case, the availability of substrate and substrate inhibition could matter. However, it is known that most of the dissociation of peptides happen within the first hour of hydrolysis (Nchienzia, Morawicki and Gadang, 2010). Thus, for the rest of the thesis the results from 3 hours are excluded and the main focus will be the 1-hour results.

To compare the enzymatic yield of the four residual raw materials by all proteases, a principal component analysis (PCA) was conducted (Figure 15). The main variation in the dataset, PC-1, showed that 60 % of the variation was due to a high degradation of Achilles tendons, chicken meat and MDCR, and a low degradation of chicken bones. The second variation, PC-2, showed that 23 % of the variation was mainly due to degradation of chicken bones.

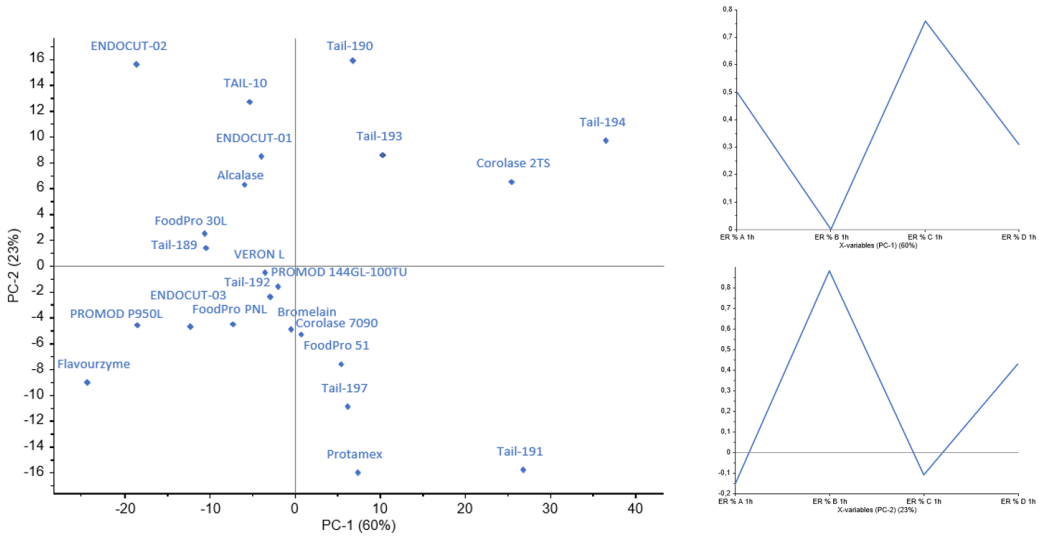

Figure 15. PCA plot of the enzymatic yield (%) for 1 hour for all proteases on Achilles tendons, chicken bones, chicken meat, and MDCR. The loadings to the right show the main variation (PC-1) (top) and the second variation (PC-2) (bottom) when it comes to the enzymatic yield of the different raw materials.

As seen in Figure 15, Tail-194 is the protease pointing out to the right, having the greatest degradation of Achilles tendons, chicken meat, and MDCR. This corresponds to the values of calculated enzymatic yield of 44.4 %, 64.9 %, and 46.7 %, respectively (Appendix D, Table D.1-D.4). On the top left side is Endocut-02 which was the protease with the highest degradation of chicken bones (22.2 %). Thus, the proteases on the top had a high digestion of bones, while the proteases at the bottom had a very low digestion of bones (in this case, negative

values). This corresponded with the enzymatic yield of Protamex and Tail-191 of -6.2 and -9.5 %, respectively.

One of the goals of this thesis was to find the proteases that had the highest selectivity towards collagen and myofibrillar proteins. The ratio between the enzymatic yield of Achilles tendons (A) over chicken meat (C) was used to find a protease that preferred tendons over meat, and vice versa. The highest (1.6) and lowest (0.7) ratios were chosen, appearing to be Endocut-02 and Bromelain, respectively (Appendix D, Table D.3). Endocut-02 did not have the highest yield of tendons, but the lowest yield of meat, thus giving the highest A/C ratio. Several proteases had a ratio of 0.7, where both Bromelain and Tail-192 had a similar yield of meat around 35 %. It is to mention that this was not the highest yield of meat, but these proteases were used with one of the lowest enzyme concentrations. However, Bromelain was used at a lower concentration than Tail-192, more precisely 6.9 mg/1000 µl versus 17.8 mg/1000 µl. Tail-192 was one of the proteases that had an error in the calculation of concentration, and hence was used with double concentration resulting in Bromelain being twice as effective as Tail-192. Endocut-02 did also have the low concentration of 6.9 µl/1000 µl. Even though the same concentrations were used, the proteases were expected to show different activity.

One would expect that the collagenases (Tail-189, Tail-190, Tail-191, Tail-192, Tail-193, and Tail-194) were more specific towards collagen rich materials. They were not standing out even though they were used with a double concentration due to an error in calculation of concentration of the powder enzymes, which were of abundance with collagenases. However, an explanation could be that the experiment was not conducted in their favorable environment. These enzymes were sent by the vendor for testing, thus no preferences for temperature and pH followed with the collagenases.

4.2.2 Characterization of hydrolysates using FTIR and SEC

To obtain insight of the hydrolysates from the small-scale hydrolysis, the hydrolysates were analyzed using FTIR and SEC. FTIR was used to study the degradation of amide bonds during hydrolysis and the formation of terminal amino (NH_3^+) and carboxyl (COO^-) groups, thus being used as a measurement of degradation. SEC was used for characterization of the peptide composition which influences the functional properties and usability of the hydrolysate (Lapeña *et al.*, 2018). This insight was obtained by studying the molecular weight distribution (MWD) of the hydrolyzed protein fractions. The MWD of a hydrolysate can be divided into fractions based on peptide size. Four different fractions (F1-F4) of peptides were created based on their

retention time through the column (Table 6). The fractions were based on the molecular weight of known proteins and peptides.

Table 6. The molecular weight distribution divided into fractions based on peptide size.

Fraction	Number of amino acids	Retention time (min)
F1	> 15	5 – 8.2
F2	7 – 15	8.2 – 9.3
F3	2 – 7	9.3 – 11.9
F4	Free amino acids	11.9 – 20

The early eluting peptides in fraction F1 contained more than 15 amino acids and had a retention time between 5 and 8.2 minutes. Midsize peptides (F2) had a retention time through the column between 8.2 to 9.3 minutes. The smallest peptides (F3) and free amino acids (F4) had a retention time between 9.3 to 20 minutes. These fractions can be used do divide the obtained chromatograms from the SEC analysis (Figure 16).

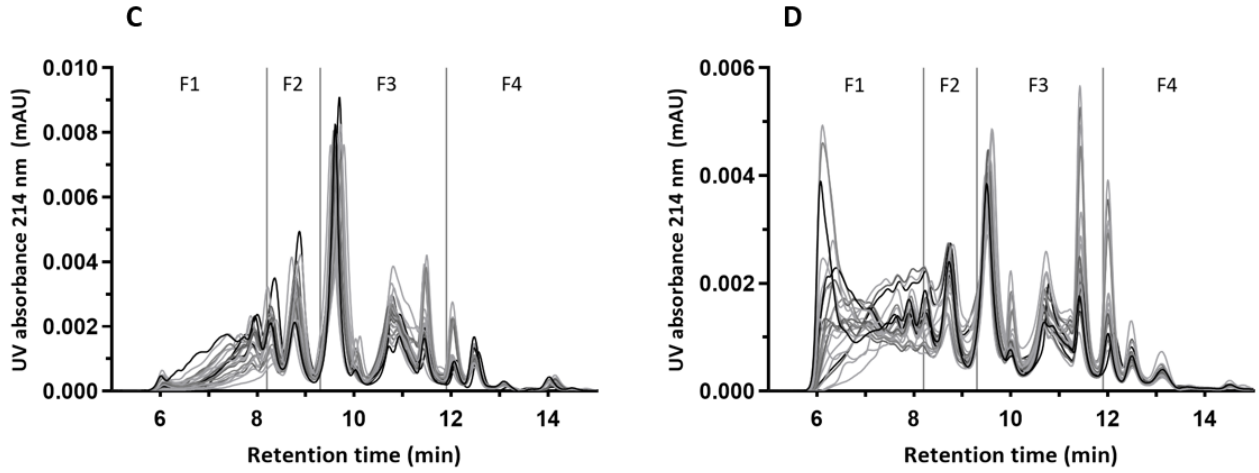

Figure 16. Chromatograms of the non-normalized data from the small-scale hydrolysis on chicken meat (C) and MDCR (D), with 23 different proteases. The fractions F1-F4 show the distribution of peptide size in the protein hydrolysates.

As seen in Figure 16, the different proteases give rise to peaks of distinct intensity. The differences between chicken meat and MDCR are most clearly in the F1 fraction of the chromatogram. Wubshet *et al.* (2017) did also make this observation and explained it by the relatively poor extractability of proteins from MDCR compared to proteins from chicken meat. The chromatogram of bones showed a similar pattern as the MDCR (not illustrated).

In general, SEC columns have a limited separation range dependent on the mobile and stationary phase (Hong, Koza and Bouvier, 2012). The BioSep 2000s column has an exclusion range between 1000 – 300 000 Da (Ahmed and Modrek, 1992). A mobile phase consisting of water and acetonitrile gives good separation of proteins and peptides with a lower molecular weight range when using a BioSep 2000s column (Phenomenex, n.d.). However, this can result in errors in the measured MWD of samples containing larger amounts of molecules outside the exclusion range. The sudden initial increase seen in MDCR chromatograms are likely caused by the separation limitation of the SEC setup. As a result, the calculated average molecule weight would not give a correct picture of the size distribution. Another major factor responsible for the limitation of the SEC measurements is the detection method used. UV detection at 214 nm will result in a systematic underestimation of free amino acids and overestimation of proteins and peptides (Kuipers and Gruppen, 2007). Analyzing the area below the curve could therefore be more relevant when comparting samples derived from different raw materials and proteases.

It should be noted that samples of Achilles tendons were not analyzed by SEC due to the risk of clogging the column. Most of these samples created a gel when cooled down, and even diluted there was a great risk that the column could get damaged. The residual raw materials Achilles tendons and chicken meat are as mentioned earlier, the most interesting materials for this experiment. The sudden and initial peak in the F1 fraction for chicken bones and MDCR, in addition to their poor accessibility and MDCR being a mixture of all the other raw materials, made it more relevant to create a PCA plot of the obtained SEC data from the chicken meat hydrolysates (Figure 17). The PCA plot can be used to find hidden explanations and correlations of the MWD, and the retention time was used as variables. The correlations between the hydrolysates produced from the different proteases are easily visible in the plot, where the proteases that have a similar MWD cluster together.

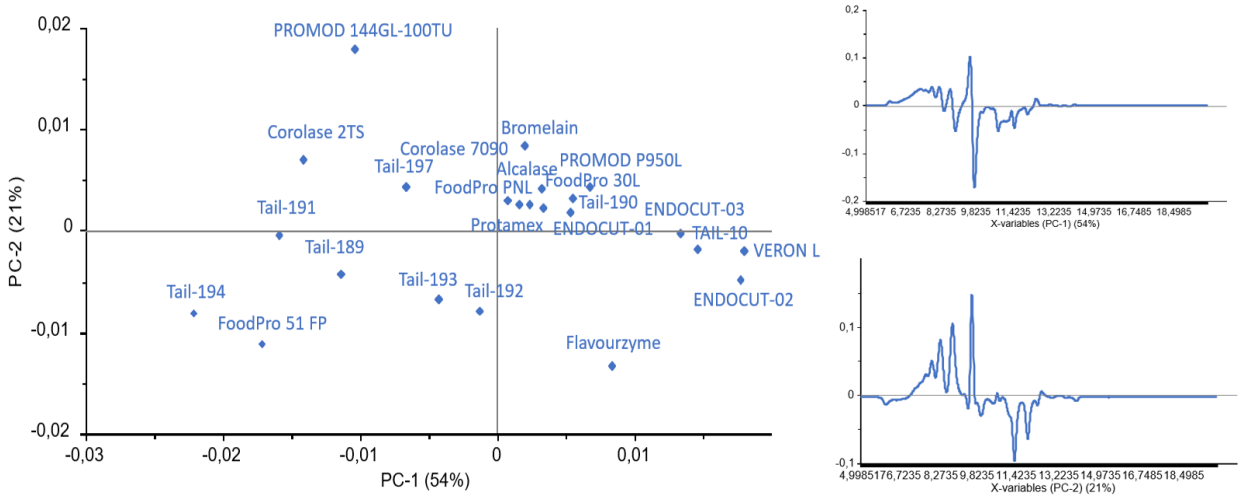

Figure 17. PCA plot of the normalized data from SEC on chicken meat run for 1 hour in the small-scale hydrolysis. To the left, the corresponding loading plots (PC-1 on the top, PC-2 on the bottom).

The PCA plot relieved that PC-1 and PC-2 explained 54 % and 21 % of the variance in the dataset, respectively. The loadings are expressed copies of the chromatograms, where the highest peaks indicated the largest variances. The outcome along PC-1 was an indirect effect of size which can be observed as a shift in the band in the loading of PC-1, probably affected by interactions of protein fragments and peptides (Podzimek, 2011). The PC-1 loading showed that the main variation was in the F3 fraction, where small peptides had a retention time between 9.3 to 11.9 minutes. The proteases farthest to the right, e.g. VERON L and Endocut-02, had the lowest share of small peptides. In contrast, the proteases to the left, e.g. Tail-194 and FoodPro 51 FP, had the highest share of small peptides. The second variance indicated proteases that had a high share of large peptides and a low share of small peptides. This can be represented by the exopeptidase Flavourzyme which cuts the ends of the peptide chain, resulting in big peptides and free amino acids.

To study the proteases' ability to break down the residual raw materials, all of the hydrolysates from the small-scale hydrolysis were analyzed using FTIR. The results from these analyses are presented in Figure 18.

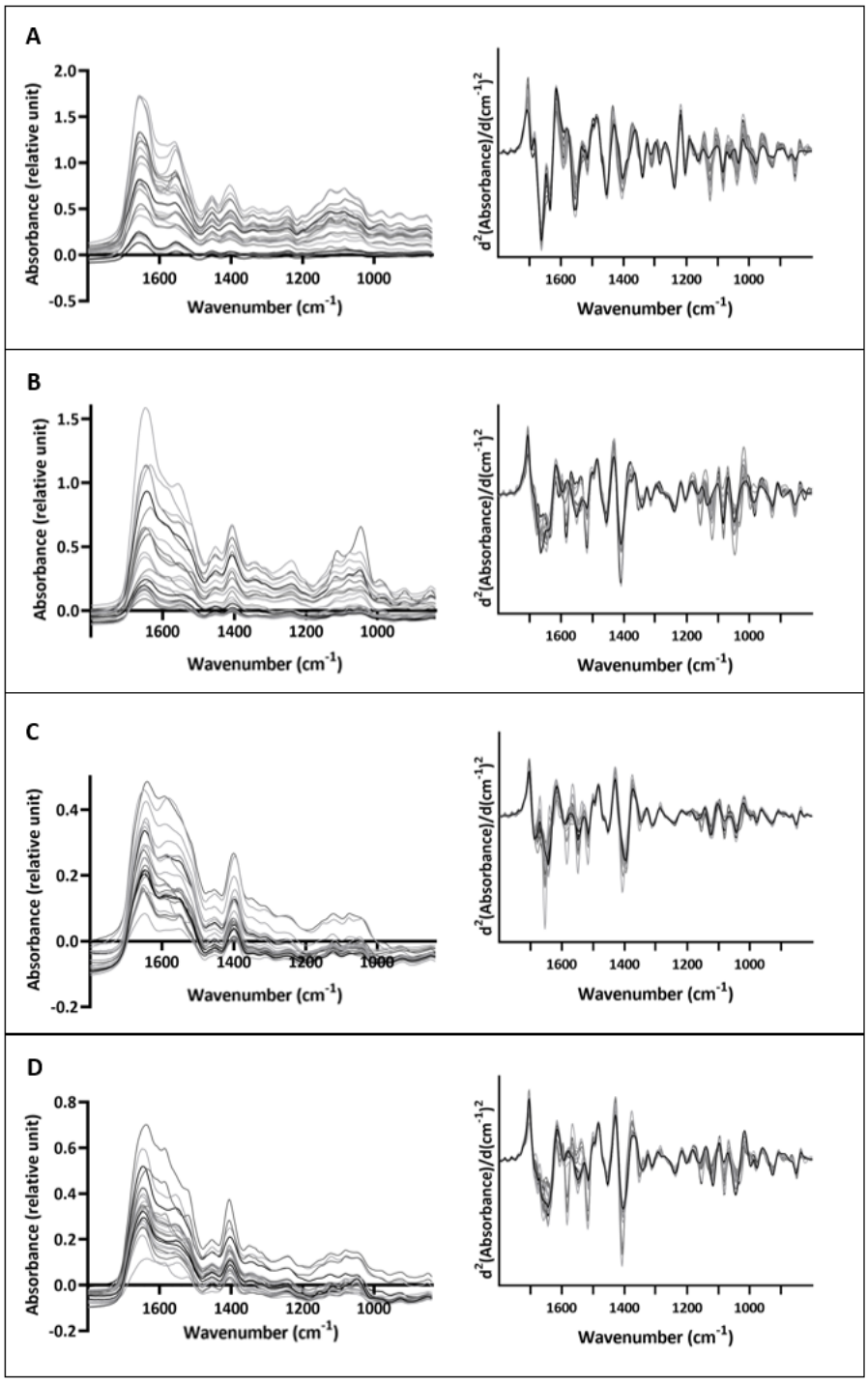

Figure 18. FTIR spectra of Achilles tendons (A), chicken bones (B), chicken meat (C), and MDCR (D), with all proteases run in the small-scale hydrolysis for 1 hour. Raw spectra are shown to the left, while the 2nd derivatives are to the right. The y-axis of the 2nd derivatives are adjusted due to values and cannot be directly used for comparison between the raw materials.

As seen in Figure 18, the spectra of the residual raw materials were quite different, especially in the amide I band at ~1650 cm^{-1}. Achilles tendons showed distinct peaks between 1700-1500 cm^{-1} which could illustrate the content of gelatin in the sample, since Hashim *et al.* (2010) found that increased concentration of gelatin in the analyzed sample showed an increasing in the amide II band in the raw FTIR spectrum. Cao and Xu (2008) found that collagen from chicken cartilage showed high intensity peaks around 1658 cm^{-1}, and that it was connected to intermolecular cross-links. This could be in accordance to the increasing in the band representing the α-helix at the same signal. The differences between raw materials are known to be in the complexity of the amide I band (Wubshet *et al.*, 2017). The organized 2nd derivative spectra of Achilles tendons can be explained by the raw material composition of nearly pure type I collagen (Gelse, Pöschl and Aigner, 2003; Freedman, Gordon and Soslowsky, 2014). In contrast, the more complex residual raw materials such as chicken bones, chicken meat and MDCR had disorganized peaks between the proteases at the amide I region in the 2nd derivative spectra. The spectral fingerprint of the product is possibly connected to the composition and homogeneity of the raw material (Böcker *et al.*, 2017). This can be illustrated in the spectra, where chicken bones had a large variety, while meat had less variety. This could be in correlation to the distribution and homogeneity of the samples, where Achilles tendons and chicken meat were the easiest materials to manage into equal samples. However, the chicken meat contained strands of connective tissue which could be observed in the spectrum as outsiders. The two proteases that stood out in the spectra of chicken meat were ENDOCUT-03 and Flavourzyme, differing the most in the amide I and II regions. These proteases are two of the proteases with the lowest enzymatic yield of chicken meat. In addition, they were the proteases with the highest average molecular weight, including many big peptides and free amino acids (Appendix E, Table E.2).

To study if there were any correlations between the information from the FTIR spectra and enzymatic yield, PCA score plots were created where wavelengths were used as variables. The obtained data from the SEC analysis was also used to discuss these results. In Figure 19, the PCA score plot with the corresponding loading plots derived from chicken meat hydrolysates is shown, where PC-1 and PC-2 explained 41 % and 31 % of the variance, respectively. The loadings are representing the 2nd derivative spectra from FTIR, where the highest peaks indicate at which band the largest variance is occurring. The PC-1 loading showed that the main variance was in the amide I, COO^-, and NH_3^+ bands.

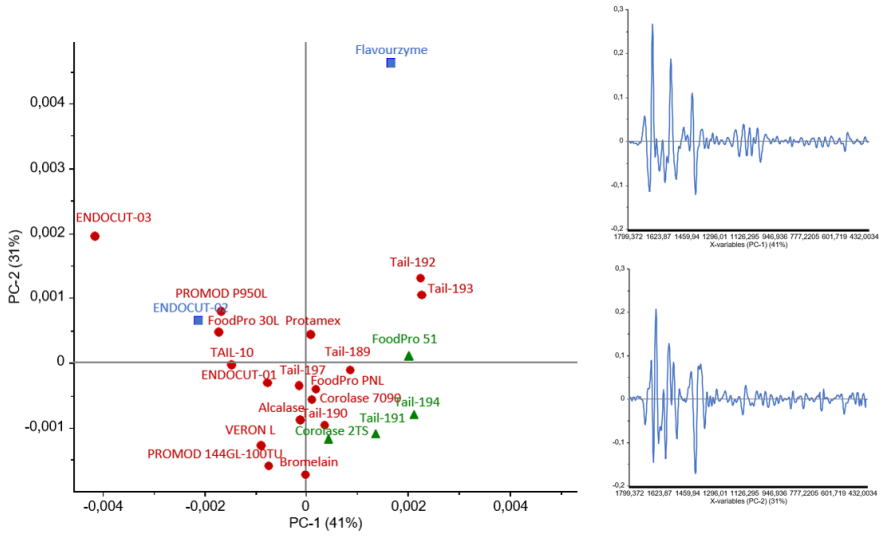

Figure 19. PCA score plot of the correlation between FTIR (1800-400 cm^{-1}) and enzymatic yield (%) of all proteases on chicken meat (■ EY% < 20, ● EY% 20-40, ▲ EY % >40). To the left, the corresponding loading plots (PC-1 on the top, PC-2 on the bottom).

According to the molecular weight distribution, PC-1 showed a tendency of big peptides towards smaller peptides and free amino acids when moving to the right in the plot, while PC-2 showed an increase from a poor amount of free amino acids to an abundant occurrence of small peptides and free amino acids. From the FTIR spectrum, Flavourzyme had the deepest peak at ~1406 cm^{-1}, ~1516 cm^{-1}, and ~1585 cm^{-1}, followed by the other proteases to the right in the plot. ENDOCUT-03 stood out in the 2nd derivative, having a deep peak at the amide I and II bands. The proteases with the lowest yield of chicken meat were Flavourzyme and Endocut-02. However, they did not have the same molecular weight distribution, where Endocut-02 consisted of a large fraction of big peptides, and Flavourzyme of small peptides and free amino acids. The proteases to the right, Tail-192 and Tail-193, did also create hydrolysates with a larger fraction of small peptides and free amino acids. The proteases that had the highest enzymatic yield, Corolase 2TS, FoodPro 51 FP, Tail-191, and Tail-194, created hydrolysates

with a large fraction of small peptides and free amino acids. However, Corolase 2TS and Bromelain were the proteases with the lowest amount of free amino acids. The molecular weight distributions can be found in Appendix E, Table E.2.

In Figure 20, the score plot of Achilles tendons with the corresponding loading plots are shown, where PC-1 and PC-2 explained 53 % and 21 % of the variance, respectively. The loadings are representing the 2nd derivative spectra from FTIR, where the highest peaks indicate at which band the largest variance is occurring. The interpretation of the loadings was challenging, making it difficult to find reasonable explanations for the protease activities in the score plot.

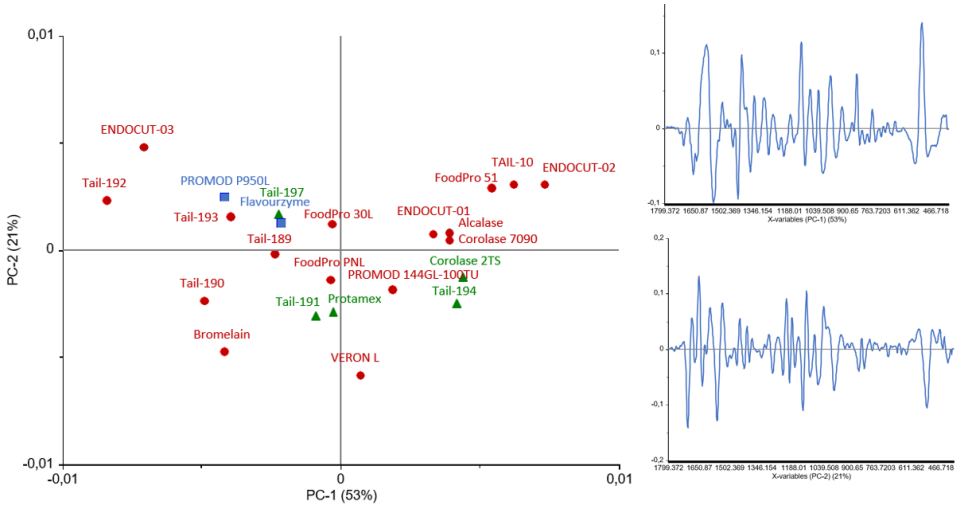

Figure 20. PCA score plot of the correlation between FTIR (1800-400 cm^{-1}) and enzymatic yield (%) of all proteases on Achilles tendons (■ EY% < 20, ● EY% 20-40, ▲ EY % >40). To the left, the corresponding loading plots (PC-1 on the top, PC-2 on the bottom).

The yield and the formation of free amino and carboxyl ends seemed not to correlate. The number of cut ends do not give an accurate information about the yield. Endopeptidases can give a high yield by just a few cuts in the peptide chain since they release large peptides into the liquid phase, while several cuts by an exopeptidase would result in many small peptides and free amino acids, resulting in a low yield. As seen in the PCA plot, the proteases with the highest yield are positioned in the middle. The proteases at each side of the plot had their deepest peaks at different bands, where Tail-192 had the strongest peaks at ~1406 cm^{-1} and ~1516 cm^{-1}, while Endocut-02 was outstanding at ~1550 cm^{-1}. When considering the enzymatic yield, Tail-192 and Endocut-02 nearly had the same yield at 24.9 % and 23.4 %, respectively. The none relation between yield and degree of degradation was highlighted by the exopeptidase Flavourzyme which had a low yield and a relative high degree of formation of amino and carboxyl ends.

Looking at the PCA plot of chicken bones, there are clearly two groupings of proteases (Figure 21). The main variance was explained by 53 %, while PC-2 was explained by 23 % of the variance. The loadings are representing the 2nd derivative spectra from FTIR, where the highest peaks indicate at which band the largest variance is occurring.

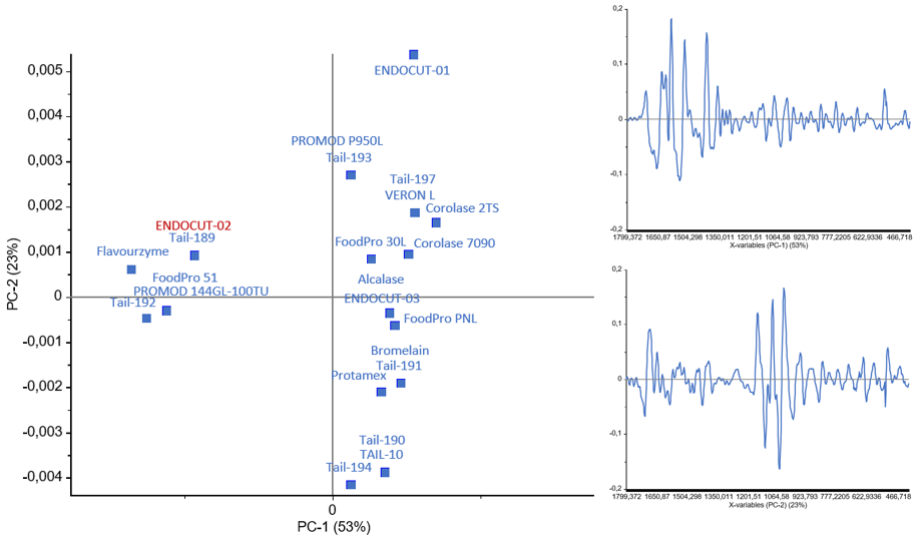

Figure 21. PCA score plot of the correlation between FTIR (1800-400 cm^{-1}) and enzymatic yield (%) of all proteases on chicken bones (■ EY% < 20, ● EY% 20-40). To the left, the corresponding loading plots (PC-1 on the top, PC-2 on the bottom).

When looking at the PC-1 loadings, the main variance was probably in the bands around 1550 cm^{-1}, 1516 cm^{-1}, and 1406 cm^{-1}. This can be confirmed by the FTIR spectra, where the cluster to the left created hydrolysates with a deep peak at ~1406 cm^{-1} and ~1516 cm^{-1}, in addition to have a different pattern in the spectrum than the rest. These proteases created hydrolysates with one of two possibilities: a hydrolysate of many large peptides, or many small peptides. Flavourzyme created many small peptides and free amino acids, and few larger peptides. On the other hand, Endocut-02 created many big peptides and few small peptides. In addition, Endocut-02 was the only protease that had an enzymatic yield larger than 20 %.

The second largest variance (PC-2) appeared to be in the fingerprint region. This was also highlighted in the 2nd derivative spectrum where the different proteases gave a great variance in this region. However, the proteases along PC-2 produced a hydrolysate containing many big peptides and few small peptides at the positive side, and few big peptides and many small peptides at the negative side. The molecular weight distribution can be found in Appendix E, Table E.1.

The PCA plot in Figure 22 shows the correlation between FTIR and enzymatic yield of MDCR, a mixture of connective tissue and myofibrillar proteins, expecting to show tendencies of a combination of the proteases' activities towards tendons, bones, and meat. The main variance (PC-1) and second largest variance (PC-2) explained 71 % and 11 % of the variance, respectively. The loadings are representing the 2nd derivative spectra from FTIR, where the highest peaks indicate at which band the largest variance is occurring. In this PCA plot, three different groupings occurred.

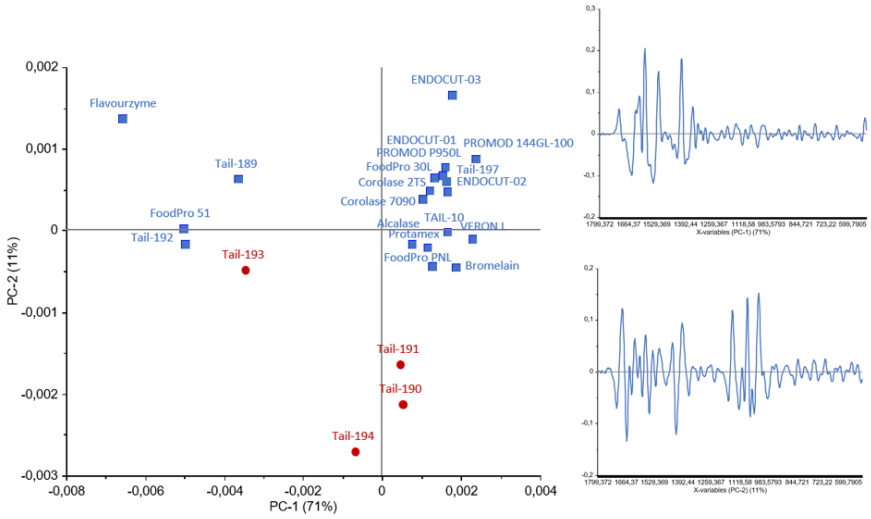

Figure 22. PCA score plot of the correlation between FTIR (1800-400 cm^{-1}) and enzymatic yield (%) of all proteases on MDCR (■ ER% 20-40, ● ER% >40). To the left, the corresponding loading plots (PC-1 on the top, PC-2 on the bottom).

When looking at the molecular weight distribution, the PCA plot of MDCR showed a completely opposite trend than the PCA plot of chicken meat. The group to the left, and the red group at the bottom, had large fractions of small peptides and free amino acids. The group to the left had deepest peaks at 1406 cm^{-1}, 1516 cm^{-1}, and 1585 cm^{-1}. This was also the main variance according to the PC-1 loading. In the 2nd derivative spectrum, this particular group followed another easily visible pattern than the rest of the proteases. The red group at the bottom did not stand out in the FTIR spectrum and followed the same pattern as the group to the left. The big blue group to the right had the deepest peak in in the amide I and II bands, visible as downfacing peaks in the first loading. These proteases created a larger fraction of bigger peptides. According to yield, the groups having an abundance of small peptides had the greatest enzymatic yield. The molecular weight distribution can be found in Appendix E, Table E.3.

The results from the PCA plots in correlation with data obtained from FTIR and SEC regarding the selected proteases will be further discussed thoroughly in the following chapter.

4.2.3 Assessment of the selected proteases

Based on the ratio of Achilles tendons and chicken meat as described in chapter 4.2.1, Endocut-02 and Bromelain were chosen, being the proteases with the highest and lowest ratios of 1.6 and 0.7, respectively. Bromelain provided a yield of 25.0 % and 36.7 % of Achilles tendons and chicken meat, while Endocut-02 created a yield of 23.4 % and 14.5 %, respectively. Endocut-02 also had a yield of 22.2 % and 32.8 % of chicken bones and MDCR, while Bromelain had a yield of 1.3 % and 34.2 % of the same raw materials. This is in accordance to the PCA plot of the enzymatic yield (Figure 15), where Endocut-02 was laying along the positive side of PC-2, and the negative side of PC-1, having a high digestion of chicken bones and a poorer digestion of the other raw materials. Bromelain was placed at the mid of PC-1, digesting a considerable amount of Achilles tendons, chicken meat, and MDCR.

The results from the FTIR analysis of Bromelain and Endocut-02 are shown in Figure 23, where the 2nd derivative spectrum showed a considerable variation between the proteases' digestion of the different raw materials.

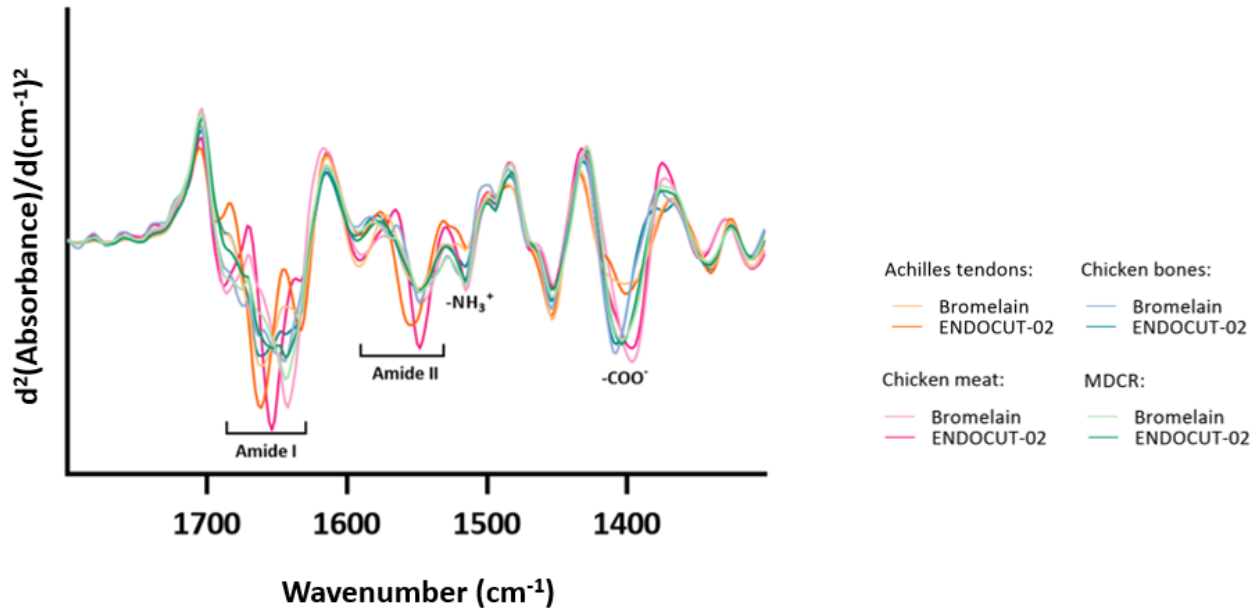

Figure 23. The 2nd derivative spectrum from the FTIR analysis of the chosen proteases, Bromelain and Endocut-02, on Achilles tendons, chicken bones, chicken meat, and MDCR.

As seen in Figure 23, there are large fluctuations in the amide I region. Bromelain was most prominent in the COO^- band for chicken meat and bones, while Endocut-02 had a deeper peak for Achilles tendons and MDCR. In the $-NH_3^+$ band, Bromelain had the deepest peaks for both meat and MDCR. However, these results are only based on the first screening without any replicates, thus further experiments had to be conducted.

Looking at the PCA plots from chapter 4.2.2, Bromelain and Endocut-02 exhibited very different positions in most of the plots, except for MDCR where they stayed in the same cluster of proteases. In the PCA plot derived from the SEC analysis of the hydrolysates obtained from chicken meat (Figure 17), Bromelain was laying along PC-2's positive side which was indicating a high share of larger peptides and a low share of smaller peptides. Endocut-02 was laying along PC-1's positive side, having a low share of small peptides. This could be confirmed by the PCA plot derived from the FTIR results of chicken meat, which showed that Endocut-02 created a hydrolysate with a high share of large peptides, laying along PC-1's negative side. Bromelain was at the negative side of PC-2, which indicated a low share of small peptides and free amino acids. The plot derived from the FTIR results of Achilles tendons showed that Endocut-02 was the protease with the possible highest formation of NH_3^+ and COO^- groups at the negative side of PC-1, while Bromelain was placed on the opposite side of the same principal component indicating a low formation of these terminals. The plot of chicken bones showed that the proteases belonged to two different groups, where Endocut-02 was laying along PC-1's negative side having many big peptides and few small peptides. Bromelain was on the negative side of PC-2, having few big peptides and many smaller peptides. In the PCA plot of MDCR, Endocut-02 and Bromelain belonged to the same cluster which was pointing out in the amide I and II regions of the FTIR spectrum, in addition to have a majority of larger peptides. However, Endocut-02 and Bromelain were on the positive and negative side of PC-2, containing larger share of peptides in fraction F1 and F2, respectively.

The observations from the PCA plots can be confirmed by the molecular weight distribution of chicken meat, chicken bones, and MDCR, where a clear difference in peptide size due to the use of different proteases was observed (Table 7).

*Table 7. Average molecular weight (g/mol), area below the chromatogram (elution volume*detector signal), fractions based on peptide size (A%), and the enzymatic yield (%) of hydrolysates from chicken bones, chicken meat, and MDCR made by Bromelain and Endocut-02 in the first small-scale hydrolysis.*

		M_w (g/mol)	Area (ml*V)	F1 >15 aa (A%)	F2 7-15 aa (A%)	F3 2-7 aa (A%)	F4 free aa (A%)	Yield (%)
Bromelain	Chicken meat	1684	83.0	18.1	25.3	49.5	7.1	36.7
	Chicken bones	3735	33.8	39.2	19.9	31.1	9.9	1.3
	MDCR	2900	75.6	36.0	24.6	32.7	6.7	34.2
Endocut-02	Chicken meat	2953	47.0	31.9	16.9	42.2	9.1	14.5
	Chicken bones	6672	50.1	52.6	14.1	25.4	7.8	22.2
	MDCR	7141	62.6	48.4	14.2	29.9	7.5	32.8

The hydrolysates made from chicken meat by Bromelain and Endocut-02 had an average molecular weight (M_w) of 1684 g/mol and 2953 g/mol. The largest differences were in the F1 and F2 fractions, showing a variance of 18.1 % and 25.3 %, versus 31.9 % and 16.9 %, for Bromelain and Endocut-02, respectively. Hydrolysates made from chicken bones by Bromelain and Endocut-02 had an M_w of 3735 g/mol and 6672 g/mol, where the F1 fraction had the largest variance of 39.2 % versus 52.6 %, respectively. The hydrolysates from MDCR by Bromelain and Endocut-02 had an M_w of 2900 g/mol and 7141 g/mol. The largest differences were in the F1 and F2 fractions, showing a variance of 36.0 % and 24.6 %, versus 48.4 % and 14.2 %, for Bromelain and Endocut-02, respectively. The M_w of background samples from chicken bones, chicken meat, and MDCR were 2084 g/mol, 2541 g/mol, and 5108 g/mol, respectively. They had a very low share of peptides in the F2 fraction and a very high share of free amino acids. The accurate molecular weight distribution of the background samples can be seen in Appendix E, Table E.4.

The results from the first small-scale hydrolysis showed that Endocut-02 had a higher yield than Bromelain when it came to Achilles tendons and chicken bones, while Bromelain was better on chicken meat and MDCR. The exact composition of the MDCR should have been studied to be able to optimize the hydrolysis. In residual raw materials rich in collagen, the proteases will break the cross-links between collagen chains depending on the persistence of the cross-links, which will lead to a variation in molecular weight distribution in the final product (Ahmad *et al.*, 2017). However, the proteases had different outcome according to different peptide sizes, and the best protease for proteolysis of the residual raw material is depending on the desired end-product.

After the first small-scale screening of all proteases on the different residual raw materials, the two proteases Endocut-02 and Bromelain were chosen based on their selectivity towards collagen and myofibrillar proteins, respectively. To study their reproducibility and scalability, a small-scale hydrolysis with duplicates and time points, and a upscaled hydrolysis with duplicates were conducted and these results will be discussed in the following chapters.

4.3 Small-scale hydrolysis with duplicates and time points

The first screening of the proteases was performed without duplicates and analysis at different time points. A new small-scale hydrolysis was therefore conducted with the selected proteases. The time points of 15, 30, and 60 minutes were used to get an indication of how the proteases worked during the hydrolysis. The selected proteases, Bromelain and Endocut-02, were applied on the residual raw materials Achilles tendons, mechanically deboned chicken residue (MDCR), and an artificial MDCR which was created of one-third of Achilles tendons, chicken bones, and chicken meat. The 2nd derivative from the FTIR spectra of the hydrolysates are shown in Figure 24.

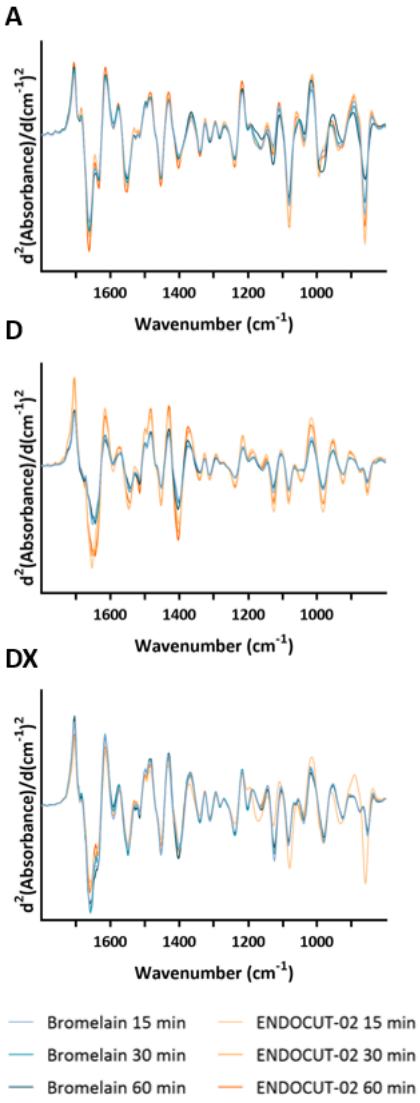

Figure 24. The 2nd derivative of the FTIR spectra from the duplicated small-scale hydrolysis with time points (15, 30 and 60 min), on the raw materials, Achilles tendons (A), MDCR (D), and artificial MDCR (DX). The spectra are an average of the duplicates.

Based on the observations from the FTIR analysis and the duplicates of yield, Endocut-02 was more prominent on Achilles tendons than Bromelain. Endocut-02 had the most distinct peaks at the amide I and II band, and at the 1400 cm^{-1} band. These peaks were all increasing with the duration of hydrolysis. During the hydrolysis process, an increase in the COO^- and $-NH_3^+$ bands and a decrease in the bands representing the α-helix are often observed (Böcker *et al.*, 2017; Wubshet *et al.*, 2017). Bromelain had the highest final yield of 24.4 % of Achilles tendons, however having a high standard deviation of the duplicates. Endocut-02 had a final average yield of 19.2 % with a low standard deviation.

Looking at the spectrum of MDCR, a clear variance between the proteases can be observed where Endocut-02 had the deepest peaks at the amide I and II regions, which were decreasing with the duration of hydrolysis, in addition deep peaks in the NH_3^+ and

COO^- bands which showed an increase with time. During hydrolysis of artificial MDCR, Bromelain was the dominating protease. At the amide I and II regions, the bands of time points were overlapping which made it difficult to observe the decreasing in the bands. An increase in the 1406 cm^{-1} and 1516 cm^{-1} bands was observed for Bromelain.

An interesting observation was the changes in the fingerprint region, where Achilles tendons had larger fluctuations than MDCR. The fluctuation in the artificial MDCR can be explained by the one-third content of tendons in the sample. Since this material also consisted of chicken meat, it can explain why Bromelain had a higher degree of degradation. In contrast, the original MDCR consisted of grounded chicken carcasses, thus having an abundant of pieces of bones and cartilage. This could explain why Endocut-02, the protease that preferred bones and tendons, had a higher digestion of MDCR.

As earlier mentioned, Achilles tendons were not analyzed by SEC due to the risk of clogging the column, thus only the molecular weight distribution of MDCR and artificial MDCR were studied (Table 8).

*Table 8. Average molecular weight (g/mol), area below the chromatogram (elution volume*detector signal), fractions based on peptide size (A%), and the enzymatic yield (%) of hydrolysates from MDCR and artificial MDCR made by Bromelain and Endocut-02 in the small-scale hydrolysis with duplicates and time points. All values are an average of the duplicates for each time point.*

		Time (min)	M_w (g/mol)	Area (ml*V)	F1 >15 aa (A%)	F2 7-15 aa (A%)	F3 2-7 aa (A%)	F4 free aa (A%)	Yield (%)
Bromelain	MDCR	15	4972	36.7	45.5	19.0	27.9	7.6	15.2
		30	4361	53.3	42.3	21.9	29.1	6.7	19.8
		60	3927	48.5	37.8	20.5	33.6	8.1	15.2
	Artificial MDCR	15	8771	66.2	57.8	14.3	23.0	4.9	4.4
		30	9394	73.8	60.8	13.2	21.4	4.7	7.5
		60	8546	76.0	55.7	13.9	25.1	5.3	1.1
Endocut-02	MDCR	15	6557	31.5	47.1	15.0	29.3	8.7	19.7
		30	5948	44.2	45.8	16.7	30.0	7.4	23.6
		60	5235	47.6	41.9	16.9	33.0	8.2	24.8
	Artificial MDCR	15	6017	48.4	42.0	17.2	33.6	7.2	12.5
		30	9890	62.0	57.0	12.7	24.9	5.5	-1.5
		60	9174	71.1	55.4	12.5	26.3	5.8	10.3

The hydrolysates after 60 minutes hydrolysis of MDCR by Bromelain and Endocut-02 had an average molecular weight (M_w) of 3927 g/mol and 5235 g/mol, respectively. Their molecular weight distributions (MWD) were quite similar, where Endocut-02 had a higher share of larger peptides and a larger yield. The duplicates showed a similar MWD, however the yield of Bromelain varied from 9.1 % to 21.3 % for the 60-minute sample (Appendix E, Table E.5). The M_w of the artificial MDCR were 8546 g/mol and 9174 g/mol for Bromelain and Endocut-02, respectively. Both proteases produced hydrolysates with a high share of large peptides, in addition to smaller peptides. The duplicates of the MWD by the two proteases were very similar. It is to mention that one of the duplicates of Endocut-02 on artificial MDCR for 15 minutes was not analyzed by SEC due to being very viscous. Thus, these values are only based on one measurement. However, the yield varied for this raw material as well and there was no increasing in yield with duration of hydrolysis. Endocut-02 had the highest final yield of 10.3 %.

In general, there were no considerable differences between the increasing time points of the hydrolyses. This could be explained by that most of the hydrolysis reaction happens within the first 20 minutes (Shyu, Tzen and Jeang, 2006). If looking at the 60-minute samples, the yield of the duplicates of Achilles tendons and MDCR by Endocut-02 were quite stable, while Bromelain was having a higher variation (Appendix D, Table D.5). These results agree with the findings from the first screening for Endocut-02, but did not concur in the same degree for Bromelain. Regarding artificial MDCR, the duplicates were relatively stable for both proteases.

4.4 Upscaled enzymatic protein hydrolysis

The enzymatic protein hydrolysis using Bromelain and Endocut-02 was also conducted in a larger scale, more precisely, 20 times upscaled compared to the small-scale hydrolysis. The upscaled hydrolysis was conducted to study the approach's scalability. In this experiment, chicken bones and meat were also included. It is to be mentioned that the upscaled hydrolysis initially was conducted with time points of 2.5, 5, 10, 15, 20 and 40 minutes, in addition to the last 60 minutes sample. However, the samplings were not giving sufficient results due to a poorly extraction method. The samplings were extracted from the surface of the mixture to avoid extracting larger particles, leading to a decrease in the final sample's yield. Due to the raw materials poor ability to dissolve into the liquid phase, the samples were determined as useless when looking at the FTIR spectra of these samples. Therefore, only the 60 minutes samples were used for further analysis with FTIR and SEC. The 2nd derivative spectra of the hydrolysates from the upscaled hydrolysis can be seen in Figure 25.

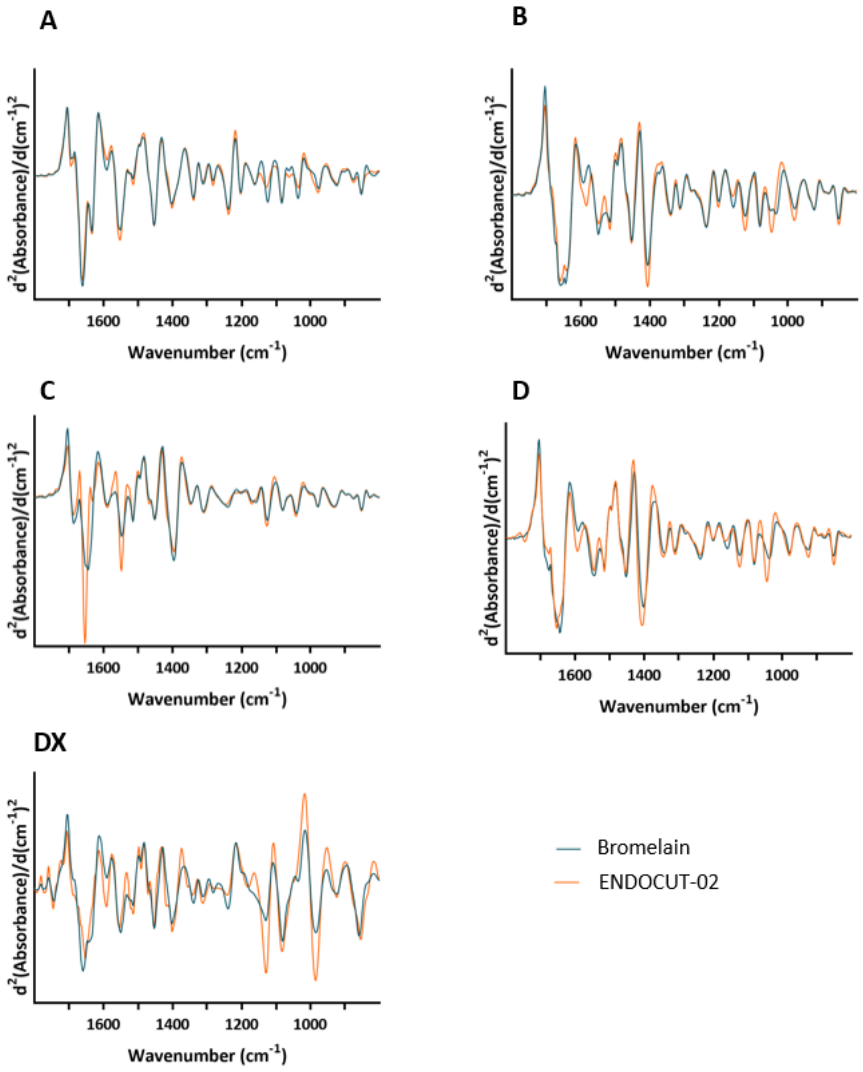

Figure 25. The 2nd derivative FTIR spectra of the upscaled hydrolysis, using Bromelain and Endocut-02 on Achilles tendons (A), chicken bones (B), chicken meat (C), MDCR (D), and artificial MDCR (DX). Only the last sampling at 60 min is illustrated. The spectra are an average of the duplicates.

As seen in Figure 25, Endocut-02 had an overall greater degradation of peptide bonds and formation of free amino and carboxyl terminals. This was the scenario for all residual raw materials in the upscaled hydrolysis, expect for chicken meat where Bromelain was the dominant protease for degradation. However, Endocut-02 had the deepest peaks at the amide I and II regions, which should decrease during hydrolysis. Another interesting observation was the fluctuation in the fingerprint region of the artificial MDCR, which also was prominent in the small-scale hydrolysis.

The molecular weight distribution of the hydrolysates from the upscaled hydrolysis are shown in Table 9. However, the hydrolysate by Endocut-02 of artificial MDCR did not get analyzed by SEC due to being very viscous and nearly impossible to filtrate.

*Table 9. Average molecular weight (g/mol), area below the chromatogram (elution volume*detector signal), fractions based on peptide size (A%), and the enzymatic yield (%) of hydrolysates from chicken bones, chicken meat, MDCR, and artificial MDCR made by Bromelain and Endocut-02 in the upscaled hydrolysis with duplicates. Only the 60 min samples are used. The values are an average of the duplicates.*

		Mw (g/mol)	Area (ml*V)	F1 >15 aa (A%)	F2 7-15 aa (A%)	F3 2-7 aa (A%)	F4 free aa (A%)	Yield (%)
Bromelain	Chicken meat	1866	85.4	19.7	22.1	49.8	8.4	42.9
	Chicken bones	4123	32.0	44.9	17.4	29.0	8.8	-1.8
	MDCR	3955	41.8	41.8	19.1	31.5	7.6	41.8
	Artificial MDCR	6179	53.6	53.6	15.5	25.9	5.0	30.6
Endocut-02	Chicken meat	3154	31.0	31.0	15.8	43.0	10.2	28.1
	Chicken bones	8066	33.2	51.0	12.7	27.2	9.1	1.2
	MDCR	6641	40.6	40.6	14.6	35.4	9.3	44.6
	Artificial MDCR	-	-	-	-	-	-	20.0

The hydrolysates derived from chicken meat had an average molecular weight (M_w) of 1866 g/mol and 3154 g/mol for Bromelain and Endocut-02, where the largest variation was in the F1 fraction with 19.7 % and 31.0 %, respectively. Bromelain had the highest yield of 42.9 % compared to 28.1 %. The M_w of chicken bones were 4123 g/mol and 8066 g/mol when produced by Bromelain and Endocut-02, respectively. The molecular weight distributions (MWD) were quite similar where they had a high share of large peptides, and a very low yield. This can be explained by the poor accessibility of this raw material for the proteases. The M_w of MDCR were 3955 g/mol and 6641 g/mol, where the proteases had a similar distribution of peptide sizes and yield. The M_w of the hydrolysate on artificial MDCR by Bromelain was 6179 g/mol, containing a high share of large peptides. The yield by Bromelain was higher that of Endocut-02, of 30.6 % and 20.0 %, respectively. The duplicates of the yield by Bromelain and Endocut-02 on all residual raw materials had low variations in the upscaled hydrolysis, with the exception of Bromelain on chicken bones (Appendix E, Table E.6). In addition, all duplicates of the MWD had low variations (Appendix D, Table D.6).

4.5 Comparison of the small-scale and upscaled hydrolysis

To compare the results from the small-scale and upscaled hydrolyses, the results of yield, degradation of peptide bonds and of formation of amino (NH_3^+) and carboxyl (COO^-) terminals, and molecular weight distributions (MWD) obtained by Bromelain and Endocut-02 on the different residual raw materials were studied. Higher yields of all residual raw materials were obtained by upscaling of hydrolysis (Figure 26). A high yield can be explained by a large amount of the raw material dissolving into the liquid phase as large peptides. On the other hand, a high degradation and formation of NH_3^+ and COO^- can be caused by a large number of small peptides and free amino acids resulting in a low yield, or many big peptides which results in a higher yield.

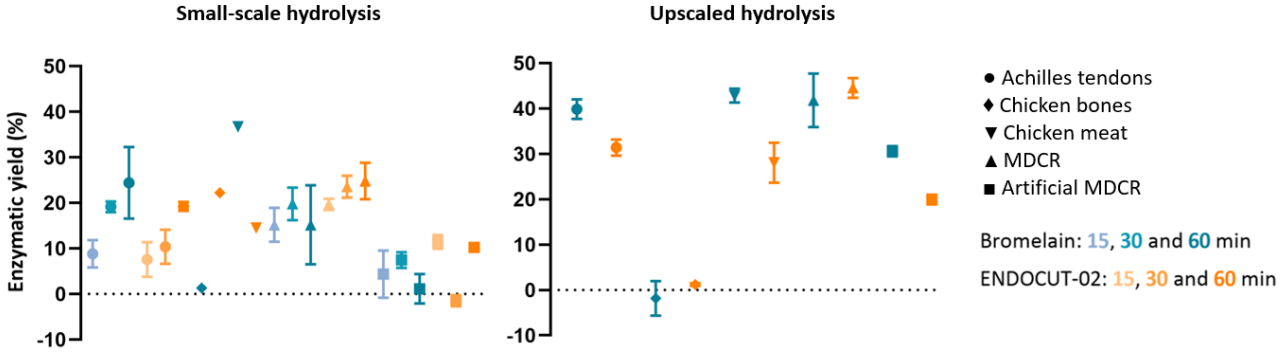

Figure 26. Comparison of the average yields with standard deviations from the small-scale and upscaled hydrolysis with duplicates. Chicken bones and chicken meat in the small-scale hydrolysis were not tested in the small-scale hydrolysis with duplicates and timepoints, thus having no standard deviation.

The time points from the small-scale hydrolysis showed that an increased duration of hydrolysis created a higher yield, with the exception of artificial MDCR. However, the 60 minutes samples of Bromelain on Achilles tendons and MDCR showed a large standard deviation. Bromelain had a higher yield of chicken meat and Achilles tendons in both small and larger scale. However, Endocut-02 showed a higher formation of amino and carboxyl terminals of Achilles tendons, which could indicate that Endocut-02 produced a hydrolysate consisting of many small peptides and free amino acids while the hydrolysate by Bromelain consisted of many large peptides. The solubilization of connective tissue by Bromalin was also supported by Kang and Rice (1970). Endocut-02 had the highest yields of chicken bones and MDCR, in addition to the highest formation of amino and carboxyl terminals of these residual raw materials, thus indicating hydrolysates with many large peptides. However, the artificial MDCR had the

highest yield when hydrolyzed by Endocut-02 in small-scale, and by Bromelain in larger scale. The FTIR analysis showed the opposite results where Endocut-02 had the highest degradation in large scale and Bromelain in the smaller scale. The molecular weight distributions of the hydrolysates produced by these two proteases were quite similar where both consisted of a high share of large peptides, explaining why both proteases showed high yields. It is to mention that chicken bones and chicken meat did not get tested in the small-scale hydrolysis with duplicates. Bones were not included due to the poor digestion by the proteases and meat got excluded by time limitations. This last-minute approach was created when the results from the larger scale did not go as planned, therefore containing some flaws that in hindsight were difficult to logically explain. Thus, the results from the first screening in small-scale of these residual raw materials was used for comparison. A summary of the results of the comparison can be seen in Table 10.

Table 10. Comparison of yield and degradation according to the results from FTIR by Bromelain and Endocut-02 in the different experiments.

Experiment	*Highest yield*	*Highest degradation of peptide bonds and formation of NH_3^+ and COO^-*
First small-scale hydrolysis without duplicates	- Bromelain: Chicken meat - Endocut-02: Chicken bones	- Bromelain: Chicken meat, MDCR - Endocut-02: Achilles tendons, chicken bones
Small-scale hydrolysis with duplicates	- Bromelain: Achilles tendons - Endocut-02: MDCR, artificial MDCR	- Bromelain: Artificial MDCR - Endocut-02: Achilles tendons, MDCR
Upscaled hydrolysis with duplicates	- Bromelain: Achilles tendons, chicken meat, artificial MDCR - Endocut-02: Chicken bones, MDCR	- Bromelain: Chicken meat - Endocut-02: Achilles tendons, chicken bones, MDCR, artificial MDCR

When it comes to the molecular weight distribution (MWD) of the hydrolysates, the values from the small-scale and upscaled hydrolysis in Table 7, 8, and 9 were compared. The hydrolysates by Bromelain on chicken meat showed very similar MWDs between small-scale and upscaled hydrolysis, where the yield increased from 36.7 % to 42.9 %. Endocut-02 also produced hydrolysates with a similar distribution of peptide sizes. However, the small-scale of chicken meat was conducted without replicates, making an uncertainty to the results. The hydrolysates of chicken bones by Bromelain had a quite similar MWD and a low yield. The use of Endocut-02 created larger difference in MWD, where the yield changed from 22.2 % to 1.2 % from small-scale to upscale. This can be explained by the proteases' difficulties of bone

digestion and the problems of even sample distribution. The hydrolysates by Bromelain on MDCR had a similar MWD, but a large variation in yield which increased from 15.2 % in the small-scale to 41.8 % in the upscaled hydrolysis. The duplicates in the small-scale hydrolysis produced yields of 9.1 % and 21.3 %, resulting in a low average of the yield. However, the yield of the small-scale hydrolysis was considerably lower than the upscaled. The hydrolysates by Bromelain on artificial MDCR showed a similar distribution of peptide fractions, but a large variation in average molecular weight. The yield of the small-scale hydrolysis was also very low compared to the upscaled, a yield of 1.1 % compared to 30.6 %, respectively. The very low yield in the small-scale hydrolysis of artificial MDCR can be explained by the uneven distribution of raw material. Since it was difficult to measure 0.67 grams of each material, a mixture was premade before distribution into the tubes. This was also highlighted in the hydrolysate by Endocut-02 where the yield declined from 12.5 % after 15 minutes to -1.5 % after 30 minutes. The hydrolysates of Endocut-02 on artificial MDCR in larger scale was not analyzed by SEC due to its viscosity and formation of gel.

To sum up, Bromelain had the highest digestion of Achilles tendons and chicken meat, while Endocut-02 had a greater digestion of the complex raw materials as MDCR and artificial MDCR. However, Bromelain digested more of the artificial MDCR in the upscaled hydrolysis which can be explained by the selectivity towards tendons and meat, which were two-thirds of the sample. The yield increased when upscaling the hydrolysis which can be explained by the better mixing method in the larger scale. It would be highly interesting to combine these two proteases sequentially in a hydrolysis process with more optimal temperature and pH, due to the high yield of Bromelain on Achilles tendons and chicken meat and the high formation of amino and carboxyl terminals by Endocut-02 on tendons.

4.6 Challenges and improvements of methods

One of the main challenges in the method development was to manage the formation of gelatin in the samples of Achilles tendons. Most of the filtrated liquid phases from tendons formed a gel when room temperate. Only three proteases did not form gel after 1 hour of hydrolysis of tendons, Corolase 2TS, PROMOD 144GL-100TU, and Tail-194, respectively. An explanation can be that these proteases created hydrolysates of small gelatin peptides that did not have the ability to form a gel after cool down. Gel formation could be related to molecular size (Gómez-Guillén *et al.*, 2011), thus an assumption is that these proteases would have a different molecular weight distribution than the rest. Filtration of samples containing tendons was also a challenge, trying to get the released collagen transferred into the liquid phase instead of mixing with the

remaining residue. An error of method could be the risk of foaming in the funnel when filtrating, which was tried avoided using hot water to pre-heat the funnel. However, the hot sample was quickly cooled down when poured through a narrow funnel. This was most prominent by the samples of tendons, due to the production of gelatin which has a great ability to foam (Czech, 2016), in addition to the samples of chicken meat with high concentrations of proteins, which also easily foam.

The disadvantages of the first small-scale screening were the lack of parallels and uneven distribution of samples. Repetitions are needed to receive reliable results, but this method was developed and conducted to be able to find promising proteases which could be further investigated. Repetitions were excluded from this experiment due to the large number of samples and the fact that it was just a first screening of the proteases' activity towards residual raw materials from poultry. Including parallels in this first screening would have taken too much time, thus the use of duplicates was only conducted in the hydrolyses with the selected proteases. Despite the use of duplicates, calculation of significance was difficult with few samples. For some raw materials, even distribution of the material's components in tubes appeared to be a challenge. Crushing of chicken bones resulted in varying size of particles, contributing to an uneven composition of samples since some tubes contained a larger fraction of big particles than small, and vice versa. This could affect the results, especially when parallels were not conducted. Since the experiment took place in small volumes (2 g), small variation of weighing could affect the results.

A source of error with the larger scale was the calculations of background reaction. No background samples of large scale were included in this experiment, thus assuming that the background reaction was the same in small and larger scale. However, this was probably not correct and should have been tested to get more precise results. In addition, the background reaction for the artificial MDCR was calculated based on the values of the components, one-third of tendons, bones and meat, respectively.

Proteases have different optimal temperatures and pH, and to get the optimal utilization of the protease, parameters should have been measured and carefully monitored during the process. Taking Alcalase and Bromelain as an example, they have optimal temperatures and pH at 50-60 °C and pH 8.0-9.5, and 40-50 °C and pH 7.0, respectively (Aluko, 2018). Regarding Endocut-02, no optimum temperature and pH were found other than a pH range of 6.0-10.0 informed by the vendor, Tailorzyme ApS. To be able to work under controlled conditions, a weak buffer solution was used. The utilized buffer was the same main sodium phosphate buffer

as used in the proteolytic activity measurements, diluted into a 0.01 M solution. The utilized buffer had a pH at 7.3, which decreased to pH 6.4 when mixed in chicken meat. The use of buffer with pH 7.0 in the hydrolysis was conducted due to the use of the same buffer when measuring the proteases' activities. However, the pH had increased before it was used for hydrolysis, possibly due to the dilution to 0.01 M solution, and the pH should therefore have been decreased before utilization. During hydrolysis the pH can be controlled by adding NaOH to maintain the desired level for the protease, and the consumption of NaOH could be used to calculate the degree of hydrolysis (Nchienzia, Morawicki and Gadang, 2010). Nevertheless, the pH would have been very difficult to adjust and control in a small-scale hydrolysis. However, it is potentially cheaper and more relevant for the industry to not use buffer solutions and pH adjustments (Lapeña *et al.*, 2018). If another pH had been used or the pH had been controlled during hydrolysis, other results would most likely have occurred.

Working with higher temperatures could also have led to better utilization of the protease, both regarding closer to optimum temperature and easier access to connective tissue, since a tight configuration of the triple helix can protect the collagen molecule from the protease. A increased temperature up to 50-60 °C could have led to an initial breakdown of the triple helix and a loss of the three-dimensional structure (Powell, Hunt and Dikeman, 2000). However, the occurrence of gel formation is more likely when using higher temperatures. Cliche *et al.* (2003) found that chicken skin heated to 40 °C allowed recovery of all the collagen in the solid phase, while heated to 60 °C made both the liquid and solid phases to gel. No gel formation was observed in the phases after heating to 40 °C. Thus, the clue of gel formation could be by monitoring the time and temperature of the hydrolysis. However, the use of heat inactivation at 95 °C is the main reason for gel formation in the present study, which is highlighted by the gel formation of the background sample. Heating above 70 °C is reported to affect the proteins' secondary structure, which can be detected by FTIR (Murayama and Tomida, 2004). However, this inactivation method was chosen due to being an easy and available method for inactivation of proteases. The vendors' advice of inactivation for 15 minutes over 90 °C should be sufficient, but due to some proteases ability to function at high temperatures, the products' protease activity should be tested. On the contrary, the use of another inactivation method than heat could lose a considerable part of the background reaction, leading to a reduction of the total yield. In addition, the problem with microorganisms can occur if there is no heat-treatment of the residual raw materials. An alternative to heat inactivation could be immobilization of the proteases with physical or chemical methods, which leads to a reusing of the proteases

(Dwevedi and Kayastha, 2011). Another alternative could be inactivation with the use of dense phase CO_2. This could cause inactivation due to pH lowering, conformational changes of the protease or be a inhibitory effect on the protease's activity (Damar and Balaban, 2006). Regardless of inactivation method, the microbial quality of the hydrolysate should be tested to make sure that the product is safe for human consumption.

5. Conclusion

The search for a protease with high selectivity towards either collagen or myofibrillar proteins appeared to be challenging. None of the studied proteases showed a clear selectivity when using the applied process conditions. Nevertheless, the proteases with the highest and lowest ratio of the yield of Achilles tendons and chicken meat, Endocut-02 and Bromelain, respectively, were chosen for closer evaluation. After trials in both small-scale and upscaled hydrolyses, Bromelain appeared to have the highest digestion of Achilles tendons and chicken meat, while Endocut-02 had a greater digestion of the more complex residual raw materials, such as MDCR and artificial MDCR. The results showed that the molecular weight distributions were quite similar in hydrolysates obtained from the same raw material in both small-scale and upscale, where an increased yield was observed in the larger scale. A screening of proteases' selectivity towards residual raw materials of poultry was possible in a volume of 2 g substrate, however the disadvantage of variation in yield was a great uncertainty. Thus, a larger scale is required to obtain more reliable results. In addition, the proteases produced hydrolysates with different molecular weight distributions which affect the properties of the product. The obtained knowledge could be of importance for further development of the future multistep processing of residual raw materials of poultry, possibly leading to complete utilization of the raw material and value creation for the industry.

6. Future perspectives

This master thesis was a part of a larger research project and conducted for initial experiments in the startup phase of the project. Thus, these results will be an experience for further work, where obtained knowledge can be useful for later experiments. Nevertheless, a recommendation for future trials is to measure the collagen content in the produced hydrolysates. Here, the Sircol soluble and insoluble collagen assays can be conducted (Biocolor, 2011, n.d.), or an assay for determination of hydroxyproline (Edwards and O'Brien, 1980). In addition, other inactivation methods for the proteases without heat should be investigated due to the formation of gelatin in collagen rich residual raw materials. Optimization of the process condition should also be conducted to allow the proteases to work at their optimum temperature and pH.

7. References

Ahmad, T., Ismail, A., Ahmad, S. A., Khalil, K. A., Kumar, Y., Adeyemi, K. D. and Sazili, A. Q. (2017) Recent advances on the role of process variables affecting gelatin yield and characteristics with special reference to enzymatic extraction: A review, *Food Hydrocolloids*, 63, pp. 85-96. doi: https://doi.org/10.1016/j.foodhyd.2016.08.007.

Ahmed, F. and Modrek, B. (1992) Biosep-SEC-S high-performance size-exclusion chromatographic columns for proteins and peptides, *Journal of Chromatography A*, 599(1-2), pp. 25-33.

Aitken, A. and Learmonth, M. P. (2009) Protein determination by UV absorption *The protein protocols handbook.* Springer, pp. 3-6.

Aluko, R. E. (2018) 15 - Food protein-derived peptides: Production, isolation, and purification, in Yada, R. Y. (ed.) *Proteins in Food Processing (Second Edition).* Woodhead Publishing, pp. 389-412.

Alvarado, C. Z. and Owens, C. M. (2005) Chapter 31 Poultry: Chemistry and Biochemistry, in Hui, Y. H. (ed.) *Handbook of Food Science, Technology and Engineering.* Taylor & Francis.

Aryee, A. N. A., Agyei, D. and Udenigwe, C. C. (2018) 2 - Impact of processing on the chemistry and functionality of food proteins, in Yada, R. Y. (ed.) *Proteins in Food Processing (Second Edition).* Woodhead Publishing, pp. 27-45.

Aspevik, T., Oterhals, Å., Rønning, S. B., Altintzoglou, T., Wubshet, S. G., Gildberg, A., Afseth, N. K., Whitaker, R. D. and Lindberg, D. (2018) Valorization of Proteins from Co- and By-Products from the Fish and Meat Industry, in Lin, C. S. K. (ed.) *Chemistry and Chemical Technologies in Waste Valorization.* Cham: Springer International Publishing, pp. 123-150.

Barbut, S. (2015a) Structure and muscle physiology in Barbut, S. (ed.) *The Science of Poultry and Meat Processing.*

Barbut, S. (2015b) Portioning, deboning and fresh meat composition, in Barbut, S. (ed.) *The Science of Poultry and Meat Processing.*

Barth, A. (2007) Infrared spectroscopy of proteins, *Biochimica et Biophysica Acta (BBA) - Bioenergetics*, 1767(9), pp. 1073-1101. doi: https://doi.org/10.1016/j.bbabio.2007.06.004.

Bateman, J. F., Lamande, S. R. and Ramshaw, J. A. (1996) Collagen superfamily, in Comper, W. D. (ed.) *Extracellular Matrix: Molecular Components and Interactions* Melbourne, Australia: Harwood academic publishers, pp. 22-67.

Benjakul, S., Klomklao, S. and Simpson, B. K. (2009) Enzymes in fish processing, in Whitehurst, R. J. and Oort, M. v. (ed.) *Enzymes in Food Technology.* 2nd edn. Wiley-Blackwell, pp. 211-235.

Biocolor (2011) Sircol Soluble Collagen Assay (S1000): Biocolor Ltd.

Biocolor (n.d.) Sircol Insoluble Collagen Assay (S2000): Biocolor Ltd.

Boland, M. J., Rae, A. N., Vereijken, J. M., Meuwissen, M. P. M., Fischer, A. R. H., van Boekel, M. A. J. S., Rutherfurd, S. M., Gruppen, H., Moughan, P. J. and Hendriks, W. H. (2013) The future supply of animal-derived protein for human consumption, *Trends in Food Science & Technology*, 29(1), pp. 62-73. doi: https://doi.org/10.1016/j.tifs.2012.07.002.

Bosman, F. T. and Stamenkovic, I. (2003) Functional structure and composition of the extracellular matrix, *J Pathol*, 200(4), pp. 423-428. doi: 10.1002/path.1437.

Brandelli, A., Sala, L. and Kalil, S. J. (2015) Microbial enzymes for bioconversion of poultry waste into added-value products, *Food Research International*, 73, pp. 3-12. doi: https://doi.org/10.1016/j.foodres.2015.01.015.

Bruno, S. F., Ekorong, F. J. A. A., Karkal, S. S., Cathrine, M. S. B. and Kudre, T. G. (2019) Green and innovative techniques for recovery of valuable compounds from seafood by-products and discards: A review, *Trends in Food Science & Technology*, 85, pp. 10-22. doi: https://doi.org/10.1016/j.tifs.2018.12.004.

Böcker, U. (2007) *Fourier-transform infrared microspectroscopy of muscle food - process-related changes in secondary structure of myofibrillar proteins and their relationships to meat functional properties* Philosophiae Doctor Thesis, Norwegian University of Life Science.

Böcker, U., Wubshet, S. G., Lindberg, D. and Afseth, N. K. (2017) Fourier-transform infrared spectroscopy for characterization of protein chain reductions in enzymatic reactions, *Analyst*, 142(15), pp. 2812-2818. doi: 10.1039/C7AN00488E.

Cao, H. and Xu, S.-Y. (2008) Purification and characterization of type II collagen from chick sternal cartilage, *Food Chemistry*, 108(2), pp. 439-445. doi: https://doi.org/10.1016/j.foodchem.2007.09.022.

Chan, J. T. Y., Omana, D. A. and Betti, M. (2011) Functional and rheological properties of proteins in frozen turkey breast meat with different ultimate pH, *Poultry Science*, 90(5), pp. 1112-1123. doi: 10.3382/ps.2010-01185.

Charney, J. and Tomarelli, R. M. (1947) A colorimetric method for the determination of the proteolytic activity of duodenal juice, *Journal of Biological Chemistry*, 171, pp. 501-505.

Charvolin, J. and Sadoc, J. F. (2012) About collagen, a tribute to Yves Bouligand, *Interface Focus*, 2(5), pp. 567-574. doi: 10.1098/rsfs.2012.0014.
Cheng, F.-Y., Liu, Y.-T., Wan, T.-C., Lin, L.-C. and Sakata, R. (2008) The development of angiotensin I-converting enzyme inhibitor derived from chicken bone protein, *Animal Science Journal*, 79(1), pp. 122-128. doi: doi:10.1111/j.1740-0929.2007.00507.x.
Choe, J. and Kim, H. Y. (2017) Effects of chicken feet gelatin extracted at different temperatures and wheat fiber with different particle sizes on the physicochemical properties of gels, *Poultry Science*, 97(3), pp. 1082-1088. doi: 10.3382/ps/pex381.
Chung, L., Dinakarpandian, D., Yoshida, N., Lauer-Fields, J. L., Fields, G. B., Visse, R. and Nagase, H. (2004) Collagenase unwinds triple-helical collagen prior to peptide bond hydrolysis, *The EMBO journal*, 23(15), pp. 3020-3030. doi: 10.1038/sj.emboj.7600318.
Clemente, A. (2000) Enzymatic protein hydrolysates in human nutrition, *Trends in Food Science & Technology*, 11(7), pp. 254-262. doi: https://doi.org/10.1016/S0924-2244(01)00007-3.
Cliche, S., Amiot, J., Avezard, C. and Gariepy, C. (2003) Extraction and characterization of collagen with or without telopeptides from chicken skin, *Poultry Science*, 82(3), pp. 503-509. doi: 10.1093/ps/82.3.503.
Coelho, D. F., Saturnino, T. P., Fernandes, F. F., Mazzola, P. G., Silveira, E. and Tambourgi, E. B. (2016) Azocasein Substrate for Determination of Proteolytic Activity: Reexamining a Traditional Method Using Bromelain Samples, *Biomed Res Int*, 2016. doi: 10.1155/2016/8409183.
Coultate, T. (2009) Proteins, in Coultate, T. (ed.) *Food: The Chemistry of its Components* 5th edn. Cambridge, UK: RSC Publishing, pp. 160-213.
Czech, I. (2016) *Collagen Peptides – Source, Properties and Benefits*. Seagarden AS(Accessed: 11.09.2018).
Damar, S. and Balaban, M. O. (2006) Review of Dense Phase CO2 Technology: Microbial and Enzyme Inactivation, and Effects on Food Quality, *Journal of Food Science*, 71(1), pp. R1-R11. doi: 10.1111/j.1365-2621.2006.tb12397.x.
Deeslie, W. D. and Cheryan, M. (1992) Fractionation of Soy Protein Hydrolysates using Ultrafiltration Membranes, *Journal of Food Science*, 57(2), pp. 411-413. doi: 10.1111/j.1365-2621.1992.tb05505.x.
Depalle, B., Qin, Z., Shefelbine, S. J. and Buehler, M. J. (2015) Influence of cross-link structure, density and mechanical properties in the mesoscale deformation mechanisms of collagen fibrils, *J Mech Behav Biomed Mater*, 52, pp. 1-13. doi: 10.1016/j.jmbbm.2014.07.008.
Di Cera, E. (2009) Serine proteases, *IUBMB life*, 61(5), pp. 510-515. doi: 10.1002/iub.186.
Dwevedi, A. and Kayastha, A. M. (2011) Enzyme Immobilization: A Breakthrough in Enzyme Technology and Boon to Enzyme Based Industries in Haggerty, L. M. (ed.) *Protein Structure.* Nova Science Publishers, Incorporated, pp. 31-50. Available at: http://ebookcentral.proquest.com/lib/ntnu/detail.action?docID=3017834.
Eason, J. R., Ryan, D., Page, B., Watson, L. and Coupe, S. A. (2007) Harvested broccoli (Brassica oleracea) responds to high carbon dioxide and low oxygen atmosphere by inducing stress-response genes, *Postharvest Biology and Technology*, 43(3), pp. 358-365. doi: https://doi.org/10.1016/j.postharvbio.2006.10.001.
Edwards, C. A. and O'Brien, W. D. (1980) Modified assay for determination of hydroxyproline in a tissue hydrolyzate, *Clinica Chimica Acta*, 104(2), pp. 161-167. doi: https://doi.org/10.1016/0009-8981(80)90192-8.
Esbensen, K., Schönkopf, S. and Midtgaard, T. (1994) *Multivariate Analysis in Practice*. Trondheim: Camo AS.
European Union (2009) *Regulation (EC) No. 1096/2009 of the European Parliament and of the Council of 21 October 2009 laying down health rules as regards animal by-products and derived products not intended for human consumption and repealing Regulation (EC) No 1774/2002 (Animal by-products Regulation)*.
FAO (2009) *How to Feed the World in 2050*. Rome: Food and Agriculture Organization of the United Nations. Available at: http://www.fao.org/fileadmin/templates/wsfs/docs/expert_paper/How_to_Feed_the_World_in_2050.pdf (Accessed: 22.01.19).
Ferreira, A. M., Gentile, P., Chiono, V. and Ciardelli, G. (2012) Collagen for bone tissue regeneration, *Acta Biomaterialia*, 8(9), pp. 3191-3200. doi: https://doi.org/10.1016/j.actbio.2012.06.014.
Fonkwe, L. G. and Singh, R. K. (1996) Protein recovery from mechanically deboned turkey residue by enzymic hydrolysis, *Process Biochemistry*, 31(6), pp. 605-616. doi: https://doi.org/10.1016/S0032-9592(95)00101-8.
Franco, D. G., Spalanzani, R. N., Lima, E. E., Marchetti, C. R., Silva, P. O., Masui, D. C., Giannesi, G. C. and Zanoelo, F. F. (2017) Biochemical properties of a serine protease from Aspergillus flavus and application in dehairing, *Biocatalysis and Biotransformation*, 35(4), pp. 249-259. doi: 10.1080/10242422.2017.1322584.

Freedman, B. R., Gordon, J. A. and Soslowsky, L. J. (2014) The Achilles tendon: fundamental properties and mechanisms governing healing, *Muscles, ligaments and tendons journal*, 4(2), pp. 245-255. Available at: https://www.ncbi.nlm.nih.gov/pubmed/25332943.

Garnero, P., Borel, O., Byrjalsen, I., Ferreras, M., Drake, F. H., McQueney, M. S., Foged, N. T., Delmas, P. D. and Delaissé, J.-M. (1998) The collagenolytic activity of cathepsin K is unique among mammalian proteinases, *Journal of Biological Chemistry*, 273(48), pp. 32347-32352.

Gbogouri, G. A., Linder, M., Fanni, J. and Parmentier, M. (2004) Influence of Hydrolysis Degree on the Functional Properties of Salmon Byproducts Hydrolysates, *Journal of Food Science*, 69(8), pp. C615-C622. doi: 10.1111/j.1365-2621.2004.tb09909.x.

Gelse, K., Pöschl, E. and Aigner, T. (2003) Collagens—structure, function, and biosynthesis, *Advanced Drug Delivery Reviews*, 55(12), pp. 1531-1546. doi: https://doi.org/10.1016/j.addr.2003.08.002.

Gómez-Guillén, M. C., Turnay, J., Fernández-Díaz, M. D., Ulmo, N., Lizarbe, M. A. and Montero, P. (2002) Structural and physical properties of gelatin extracted from different marine species: a comparative study, *Food Hydrocolloids*, 16(1), pp. 25-34. doi: https://doi.org/10.1016/S0268-005X(01)00035-2.

Gómez-Guillén, M. C., Giménez, B., López-Caballero, M. E. and Montero, M. P. (2011) Functional and bioactive properties of collagen and gelatin from alternative sources: A review, *Food Hydrocolloids*, 25(8), pp. 1813-1827. doi: https://doi.org/10.1016/j.foodhyd.2011.02.007.

Gross, J. (1961) COLLAGEN, *Scientific American*, 204(5), pp. 120-134. Available at: http://www.jstor.org/stable/24937463.

Harrington, D. J. (1996) Bacterial collagenases and collagen-degrading enzymes and their potential role in human disease, *Infection and immunity*, 64(6), pp. 1885-1891. Available at: https://www.ncbi.nlm.nih.gov/pubmed/8675283.

Hart, D. J., Hadad, C. M., Craine, L. E. and Hart, H. (2012) Amino Acids, Peptides, and Proteins, in Hart, D. J., *et al.* (ed.) *Organic Chemistry: A Brief Course* 13th edn. Brooks/Cole, Cengage Learning, pp. 492-526.

Hashim, D. M., Man, Y. B. C., Norakasha, R., Shuhaimi, M., Salmah, Y. and Syahariza, Z. A. (2010) Potential use of Fourier transform infrared spectroscopy for differentiation of bovine and porcine gelatins, *Food Chemistry*, 118(3), pp. 856-860. doi: https://doi.org/10.1016/j.foodchem.2009.05.049.

Hong, H., Chaplot, S., Chalamaiah, M., Roy, B. C., Bruce, H. L. and Wu, J. (2017) Removing Cross-Linked Telopeptides Enhances the Production of Low-Molecular-Weight Collagen Peptides from Spent Hens, *Journal of Agricultural and Food Chemistry*, 65(34), pp. 7491-7499. doi: 10.1021/acs.jafc.7b02319.

Hong, P., Koza, S. and Bouvier, E. S. (2012) Size-Exclusion Chromatography for the Analysis of Protein Biotherapeutics and their Aggregates, *J Liq Chromatogr Relat Technol*, 35(20), pp. 2923-2950. doi: 10.1080/10826076.2012.743724.

Kang, C. K. and Rice, E. E. (1970) Degradation of various meat fractions by tenderizing enzymes, *Journal of Food Science*, 35(5), pp. 563-565. doi: 10.1111/j.1365-2621.1970.tb04809.x.

Khiari, Z., Ndagijimana, M. and Betti, M. (2014) Low molecular weight bioactive peptides derived from the enzymatic hydrolysis of collagen after isoelectric solubilization/precipitation process of turkey by-products, *Poultry Science*, 93(9), pp. 2347-2362. doi: 10.3382/ps.2014-03953.

Kijowski, J. and Niewiarowicz, A. (1985) A method of protein extraction from chicken bone residue and the chemical and electrophoretic characteristics of the extract, *International Journal of Food Science & Technology*, 20(1), pp. 43-49. doi: doi:10.1111/j.1365-2621.1985.tb01901.x.

Kim, H. W., Song, D. H., Choi, Y. S., Kim, H. Y., Hwang, K. E., Park, J. H., Kim, Y. J., Choi, J. H. and Kim, C. J. (2012) Effects of soaking pH and extracting temperature on the physicochemical properties of chicken skin gelatin, *Korean Journal for Food Science of Animal Resources*, 32(3), pp. 316-322. doi: 10.5851/kosfa.2012.32.3.316.

Kim, S.-K. and Mendis, E. (2006) Bioactive compounds from marine processing byproducts – A review, *Food Research International*, 39(4), pp. 383-393. doi: https://doi.org/10.1016/j.foodres.2005.10.010.

Kuipers, B. J. H. and Gruppen, H. (2007) Prediction of Molar Extinction Coefficients of Proteins and Peptides Using UV Absorption of the Constituent Amino Acids at 214 nm To Enable Quantitative Reverse Phase High-Performance Liquid Chromatography−Mass Spectrometry Analysis, *Journal of Agricultural and Food Chemistry*, 55(14), pp. 5445-5451. doi: 10.1021/jf070337l.

Lantto, R., Kruus, K., Puolanna, E., Honkapää, K., Roininen, K. and Bruchert, J. (2009) Enzymes in meat processing, in Whitehurst, R. J. and Oort, M. v. (ed.) *Enzymes in Food Technology.* 2nd edn. Wiley-Blackwell, pp. 264-291.

Lapeña, D., Vuoristo, K. S., Kosa, G., Horn, S. J. and Eijsink, V. G. H. (2018) Comparative Assessment of Enzymatic Hydrolysis for Valorization of Different Protein-Rich Industrial Byproducts, *Journal of Agricultural and Food Chemistry*, 66(37), pp. 9738-9749. doi: 10.1021/acs.jafc.8b02444.

Lasekan, A., Abu Bakar, F. and Hashim, D. (2013) Potential of chicken by-products as sources of useful biological resources, *Waste Management*, 33(3), pp. 552-565. doi: https://doi.org/10.1016/j.wasman.2012.08.001.

Li-Chan, E. C. Y. and Lacroix, I. M. E. (2018) 1 - Properties of proteins in food systems: An introduction, in Yada, R. Y. (ed.) *Proteins in Food Processing (Second Edition).* Woodhead Publishing, pp. 1-25.
Lin, L. and Li, B.-f. (2006) Radical scavenging properties of protein hydrolysates from Jumbo flying squid (Dosidicus eschrichitii Steenstrup) skin gelatin, *Journal of the Science of Food and Agriculture*, 86(14), pp. 2290-2295. doi: doi:10.1002/jsfa.2600.
Lindberg, D., Aaby, K., Borge, G. I. A., Haugen, J.-E., Nilsson, A., Rødbotten, R. and Sahlstrøm, S. (2016) *Kartlegging av restråstoff fra jordbruket*. (67/2016): Nofima.
Malawer, E. G. (1995) Introduction to Size Exclusion Chromatography, in Wu, C.-S. (ed.) *Handbook of Size Exclusion Chromatography* MARCEL DEKKER, INC.
Maleki, M. R., Mouazen, A. M., Ramon, H. and De Baerdemaeker, J. (2007) Multiplicative Scatter Correction during On-line Measurement with Near Infrared Spectroscopy, *Biosystems Engineering*, 96(3), pp. 427-433. doi: https://doi.org/10.1016/j.biosystemseng.2006.11.014.
Manninen, A. H. (2009) Protein hydrolysates in sports nutrition, *Nutrition & metabolism*, 6, pp. 38-38. doi: 10.1186/1743-7075-6-38.
Margot, A., Flaschel, E. and Renken, A. (1997) Empirical kinetic models for tryptic whey-protein hydrolysis, *Process Biochemistry*, 32(3), pp. 217-223. doi: https://doi.org/10.1016/S0032-9592(96)00060-X.
Megazyme (2007) Assay of endo-protease using azo-casein. Wicklow, Ireland: Megazyme International Ireland
Moreno, M. M. C. and Cuadrado, F. V. (1993) Enzymic hydrolysis of vegetable proteins: mechanism and kinetics, *Process Biochemistry*, 28(7), pp. 481-490. doi: https://doi.org/10.1016/0032-9592(93)85032-B.
Mori, S. and Barth, H. G. (1999) *Size exclusion chromatography*. Springer-Verlag Berlin Heidelberg.
Murayama, K. and Tomida, M. (2004) Heat-Induced Secondary Structure and Conformation Change of Bovine Serum Albumin Investigated by Fourier Transform Infrared Spectroscopy, *Biochemistry*, 43(36), pp. 11526-11532. doi: 10.1021/bi0489154.
Mutilangi, W. A. M., Panyam, D. and Kilara, A. (1996) Functional Properties of Hydrolysates from Proteolysis of Heat-denatured Whey Protein Isolate, *Journal of Food Science*, 61(2), pp. 270-275. doi: 10.1111/j.1365-2621.1996.tb14174.x.
Nchienzia, H. A., Morawicki, R. O. and Gadang, V. P. (2010) Enzymatic hydrolysis of poultry meal with endo- and exopeptidases, *Poultry Science*, 89(10), pp. 2273-2280. doi: 10.3382/ps.2008-00558.
Næs, T., Isaksson, T., Fearn, T. and Davies, T. (2002) Scatter correction of spectroscopic data *A user-friendly guide to Multivariate Calibration and Classification.* Chichester, UK: NIR Publications.
Olafsen, T., Richardsen, R., Nystøyl, R., Strandheim, G. and Kosmo, J. P. (2014) *Analyse marint restråstoff, 2013*. SINTEF Fiskeri og havbruk AS.
Pasupuleti, V. K. and Braun, S. (2010) State of the Art Manufacturing of Protein Hydrolysates, in Pasupuleti, V. K. and Demain, A. L. (ed.) *Protein Hydrolysates in Biotechnology.* Dordrecht: Springer Netherlands, pp. 11-32.
Pasupuleti, V. K., Holmes, C. and Demain, A. L. (2010) Applications of Protein Hydrolysates in Biotechnology, in Pasupuleti, V. K. and Demain, A. L. (ed.) *Protein Hydrolysates in Biotechnology.* Dordrecht: Springer Netherlands, pp. 1-10.
Perisic, N., Afseth, N. K., Ofstad, R. and Kohler, A. (2011) Monitoring Protein Structural Changes and Hydration in Bovine Meat Tissue Due to Salt Substitutes by Fourier Transform Infrared (FTIR) Microspectroscopy, *Journal of Agricultural and Food Chemistry*, 59(18), pp. 10052-10061. doi: 10.1021/jf201578b.
Perumal, S., Antipova, O. and Orgel, J. P. (2008) Collagen fibril architecture, domain organization, and triple-helical conformation govern its proteolysis, *Proc Natl Acad Sci U S A*, 105(8), pp. 2824-2829. doi: 10.1073/pnas.0710588105.
Phenomenex (n.d.) *BioSep-SEC-S: Aqueous Size Exclusion/Gel Filtration for Protein and Peptide Analysis*. Available at: http://www.bvr.by/kscms/uploads/editor/file/phenomenex/biosep.pdf (Accessed: 13.05.19).
Podzimek, S. (2011) Size Exclusion Chromatography, in Podzimek, S. (ed.) *Light Scattering, Size Exclusion Chromatography and Asymmetric Flow Field Flow Fractionation.*
Powell, T. H., Hunt, M. C. and Dikeman, M. E. (2000) Enzymatic assay to determine collagen thermal denaturation and solubilization, *Meat Science*, 54(4), pp. 307-311. doi: https://doi.org/10.1016/S0309-1740(99)00092-3.
Provost, J. J., Bodwin, J., Kelly, B. S., Colabroy, K. L. and Wallert, M. A. (2016) *The science of cooking: Understanding the biology and chemistry behind food and cooking*. John Wiley & Sons.
Prystupa, D. A. and Donald, A. M. (1996) Infrared study of gelatin conformations in the gel and sol states, *Polymer Gels and Networks*, 4(2), pp. 87-110. doi: https://doi.org/10.1016/0966-7822(96)00003-2.
Ricard-Blum, S. (2011) The collagen family, *Cold Spring Harbor perspectives in biology*, 3(1), pp. a004978.

Rossi, D. M., Flôres, S. H., Heck, J. X. and Ayub, M. A. Z. (2009) Production of High-protein Hydrolysate from Poultry Industry Residue and their Molecular Profiles, *Food Biotechnology*, 23(3), pp. 229-242. doi: 10.1080/08905430903102828.

Roupas, P., De Silva, K., Smithers, G. and Ferguson, A. (2007) Waste management and co-product recovery in red and white meat processing, in Waldron, K. (ed.) *Handbook of waste management and co-product recovery in food processing.* Woodhead Publishing Limited pp. 305-331.

Scanlon, M. G., Henrich, A. W. and Whitaker, J. R. (2018) 13 - Factors affecting enzyme activity in food processing, in Yada, R. Y. (ed.) *Proteins in Food Processing (Second Edition).* Woodhead Publishing, pp. 337-365.

Shoulders, M. D. and Raines, R. T. (2009) Collagen Structure and Stability *Annual review of biochemistry*, 78, pp. 929-958. doi: 10.1146/annurev.biochem.77.032207.120833.

Shyu, D. J. H., Tzen, J. T. C. and Jeang, C. L. (2006) Enzyme Activities, in Hui, Y. H. (ed.) *Food Biochemistry and Food Processing.* First edn. Iowa, USA: Blackwell Publishing, pp. 155-174

Sibilla, S., Godfrey, M., Brewer, S., Budh-Raja, A. and Genovese, L. (2015) An overview of the beneficial effects of hydrolysed collagen as a nutraceutical on skin properties: Scientific background and clinical studies, *The Open Nutraceuticals Journal*, 8(1).

SSB (2019) *Kjøttproduksjon*. Available at: https://www.ssb.no/jord-skog-jakt-og-fiskeri/statistikker/slakt/aar (Accessed: 17.04 2019).

Stevens, J. R., Newton, R. W., Tlusty, M. and Little, D. C. (2018) The rise of aquaculture by-products: Increasing food production, value, and sustainability through strategic utilisation, *Marine Policy*, 90, pp. 115-124. doi: https://doi.org/10.1016/j.marpol.2017.12.027.

Striegel, A., Yau, W. W., Kirkland, J. J. and Bly, D. D. (2009) *Modern size-exclusion liquid chromatography: practice of gel permeation and gel filtration chromatography*. John Wiley & Sons.

Stuart, B. (1997) *Biological Applications of Infrared Spectroscopy* England: John Wiley & Sons.

Tang, J. and Wong, R. N. S. (1987) Evolution in the structure and function of aspartic proteases, *Journal of Cellular Biochemistry*, 33(1), pp. 53-63. doi: 10.1002/jcb.240330106.

Tarté, R. (2009) Chapter 7: Meat-Derived Protein Ingredients in Tarté, R. (ed.) *Ingredients in Meat Products: Properties, Functionality and Applications.* Springer, New York, NY.

Tavano, O. L. (2013) Protein hydrolysis using proteases: An important tool for food biotechnology, *Journal of Molecular Catalysis B: Enzymatic*, 90, pp. 1-11. doi: https://doi.org/10.1016/j.molcatb.2013.01.011.

Toldrá, F. and Reig, M. (2006) Biochemistry of Raw Meat and Poultry in Hui, Y. H. (ed.) *Food Biochemistry and Food Processing.* Iowa, USA: Blackwell Publishing, pp. 293-314.

Vasileva-Tonkova, E., Nustorova, M. and Gushterova, A. (2007) New Protein Hydrolysates from Collagen Wastes Used as Peptone for Bacterial Growth, *Current Microbiology*, 54(1), pp. 54-57. doi: 10.1007/s00284-006-0308-y.

Walsh, G. (2014) *Proteins : Biochemistry and Biotechnology*. Hoboken, UNITED KINGDOM: John Wiley & Sons, Incorporated.

Watanabe, K. (2004) Collagenolytic proteases from bacteria, *Applied Microbiology and Biotechnology*, 63(5), pp. 520-526. doi: 10.1007/s00253-003-1442-0.

Wubshet, S. G., Måge, I., Böcker, U., Lindberg, D., Knutsen, S. H., Rieder, A., Rodriguez, D. A. and Afseth, N. K. (2017) FTIR as a rapid tool for monitoring molecular weight distribution during enzymatic protein hydrolysis of food processing by-products, *Analytical Methods*, 9(29), pp. 4247-4254. doi: 10.1039/C7AY00865A.

Wubshet, S. G., Wold, J. P., Afseth, N. K., Böcker, U., Lindberg, D., Ihunegbo, F. N. and Måge, I. (2018) Feed-Forward Prediction of Product Qualities in Enzymatic Protein Hydrolysis of Poultry By-products: a Spectroscopic Approach, *Food and Bioprocess Technology*. doi: 10.1007/s11947-018-2161-y.

Wubshet, S. G., Lindberg, D., Veiseth-Kent, E., Kristoffersen, K. A., Böcker, U., Washburn, K. E. and Afseth, N. K. (2019a) Bio-analystical Aspects in Enzymatic Protein Hydrolysis of By-products.

Wubshet, S. G., Wold, J. P., Böcker, U., Sanden, K. W. and Afseth, N. K. (2019b) Raman spectroscopy for quantification of residual calcium and total ash in mechanically deboned chicken meat, *Food Control*, 95, pp. 267-273. doi: https://doi.org/10.1016/j.foodcont.2018.08.017.

Xiong, Y. L. (2018) Muscle proteins, in Yada, R. Y. (ed.) *Proteins in Food Processing (Second Edition).* Woodhead Publishing, pp. 127-148.

Zhang, Y.-Z., Ran, L.-Y., Li, C.-Y. and Chen, X.-L. (2015) Diversity, Structures, and Collagen-Degrading Mechanisms of Bacterial Collagenolytic Proteases, *Applied and Environmental Microbiology*, 81(18), pp. 6098-6107. doi: 10.1128/aem.00883-15.

APPENDIX A
Protocol
Small-scaled Enzymatic Protein Hydrolysis

This protocol has been performed on poultry residual raw materials; Achilles tendons from turkey, leg bone and meat from chicken, and mechanically deboned chicken residue (MDCR). The reaction time for the enzymes were 1 and 3 hours.

Preparation of raw material

All raw materials are prepared before starting the experiment. Weigh up 2 g (between 2.000 – 2.050 g) of raw material into a 10 ml tube (79x16mm, Sarstedt). Mark the tube with the weight of the sample and type of raw material, in addition to the weight of the empty tube. Store the prepared samples in a -40 °C freezer.

Start of experiment

The hydrolysis will take place in heating cabinet (TS8136, Termaks) where the tubes are fastened on an end-over-end mixer (Cell culture roller drum, Bellco Biotechology). The tubes are fastened on the side and front of the wheel using rubber bands and paper clips.

1. Defrost the required number of tubes of each raw material if several are used. Mark the tubes with type of enzyme and reaction time, if necessary. Remember to include 0-samples of the raw materials without addition of enzyme.
2. Using a serological pipette, add 7.5 ml of 0.01 M sodium phosphate buffer in each tube.
3. Prepare an enzyme solution of 1 % w/w or individually calculated concentrations. If using 1 % w/w, 1 ml of solution should contain 0.02 g of enzyme. Dilute the enzyme with X ml of buffer, according to how many tubes that are being used. Make 2 ml more than this number. *Example: If you have 8 tubes, multiply 0.02 g of enzyme and 1 ml of buffer with 10. Your solution should then contain 0.2 g enzyme and 10 ml buffer.*
4. Pre-heat the samples in a water bath at 45 °C to achieve a sample temperature of 40 °C. If many tubes and time points are used, split the number of tubes and pre-heat the tubes that are going to have the longest reaction time first and fasten them on the outside of the wheel.
5. When a sample temperature of 40 °C is reached, add 1 ml of the enzyme solution into the tube.
6. Fasten the tubes in the end-over-end mixer and place it in the heating cabinet for incubation at 42 °C.
7. When hydrolysis is finished, put the samples in a water bath at 95 °C for inactivation of the enzymes. On a sample without enzyme, measure how long it takes for the temperature to reach 90 °C. Let the samples inactivate for 15 minutes after reaching this temperature. **NB: Remember to open the lids to avoid excess pressure in the tubes.**

Filtration

1. Prepare and weigh filter papers (Ø 125 mm, 597, Whatman) for filtration.
2. Right after the inactivation, filter the samples using vacuum and a Büchner flask with a glass funnel and folded filter paper. Pre-heat the funnel with hot water and soak the filter paper. Place a 50 ml falcon tube in the flask to collect the filtrated water phase. If using a raw material that could create gelatin, prioritize these samples.
3. Dry the filter papers with residuals in a heating cabinet at 50 °C until completely dry, in addition to the empty tubes after filtration in case some sample is left in the tube.
4. Weigh the dried filters and tubes for calculation of remaining weight. Transfer the residual into tubes for storage in a -20 °C freezer.

Samples for analysis

Samples for FTIR and SEC analyses are prepared using a 5 ml syringe and needle (0.8x55 mm) to extract the water phase. Replace the needle with a 0.45 µl Millipore filter to filtrate it into Eppendorf tubes and vials, leaving at least 0.5 ml in each tube.

APPENDIX B
Protocol
Upscaled Enzymatic Protein Hydrolysis

This protocol has been performed on poultry residual raw materials; Achilles tendons from turkey, leg bone and meat from chicken, and mechanically deboned chicken residue (MDCR), in addition to an artificial MDCR composed of 1/3 of the first three raw materials. Two enzymes, ENDOCUT-02 and Bromelain, were used based on a previous small-scale screening on the same raw materials. The following protocol is upscaled 20x compared to the small-scale screening.

1. Weigh up 40 g of raw material and transfer it into a 500 ml screw cap bottle together with 150 ml of 0.01 M sodium phosphate buffer.
2. Prepare enzyme solutions in a 50 ml falcon tube dissolving X mg or µl of enzyme in 20 ml buffer.
    a. ENDOCUT-02: 6.9 µl * 20 = 138 µl
    b. Bromelain: 6,9 mg * 20 = 138 mg
3. Place the bottle in a 42 °C water bath.
4. When the sample has reached a temperature of 40 °C, take it out from the water bath and wrap the bottle in aluminum foil and place it on a magnetic stirrer. Make sure that the temperature is over 40 °C since addition of enzyme will lower the temperature. Add enzyme solution (20 ml). An alternative is to preheat the enzyme solution.
5. Extract 2 ml of sample after 2.5, 5, 10, 15, 20 and 40 minutes using a serological pipette, and transfer it into a 15 ml tube.
6. Screw on a special lid with a drilled hole to relieve pressure, and microwave the sample for 4 seconds to start the boiling, before placing the sample in a water bath at 95 °C for 15 minutes.
7. After 60 minutes, transfer the final sample into a beaker covered with cling film and microwave for 30 + 20 seconds followed by 15 minutes in a 95 °C water bath. **Remember to open the screw cap to avoid excess pressure in the bottle.**

Extraction of water phase and filtration

1. Transfer the water phase from the tubes in a 2 ml Eppendorf tube and centrifuge at 40 °C and 13 300 rpm in a microcentrifuge (VWR Microstar 17R).
2. Using a Büchner flask and funnel, filtrate the 60 minutes sample through a pre-weighed filter paper (Ø 125 mm, 597, Whatman).
3. Extract the water phase from the tubes and flask using a 5 ml syringe and needle (0.8x55 mm). Replace the needle with a 0.45 µl Millipore filter to filtrate it into Eppendorf tubes and vials, leaving at least 0.5 ml in each tube.

APPENDIX C
Calculation of protease activity

The proteolytic activity of all proteases was calculated by using the linear regression function in GraphPad Prism 8.

Table C.1. Linear regression of the liquid enzyme TAIL-10.

Best-fit values	
Slope	9260
Y-intercept	0,1241
X-intercept	-0,0000134
1/slope	0,000108
Std. Error	
Slope	305
Y-intercept	0,03991
95% Confidence Intervals	
Slope	8290 to 10231
Y-intercept	-0,002959 to 0,2511
X-intercept	-2,972e-005 to 2,947e-007
Goodness of Fit	
R square	0,9968
Sy.x	0,05327
Is slope significantly non-zero?	
F	921,8
DFn, DFd	1, 3
P value	<0,0001
Deviation from zero?	Significant
Equation	Y = 9260*X + 0,1241
Data	
Number of X values	5
Maximum number of Y replicates	1
Total number of values	5
Number of missing values	0

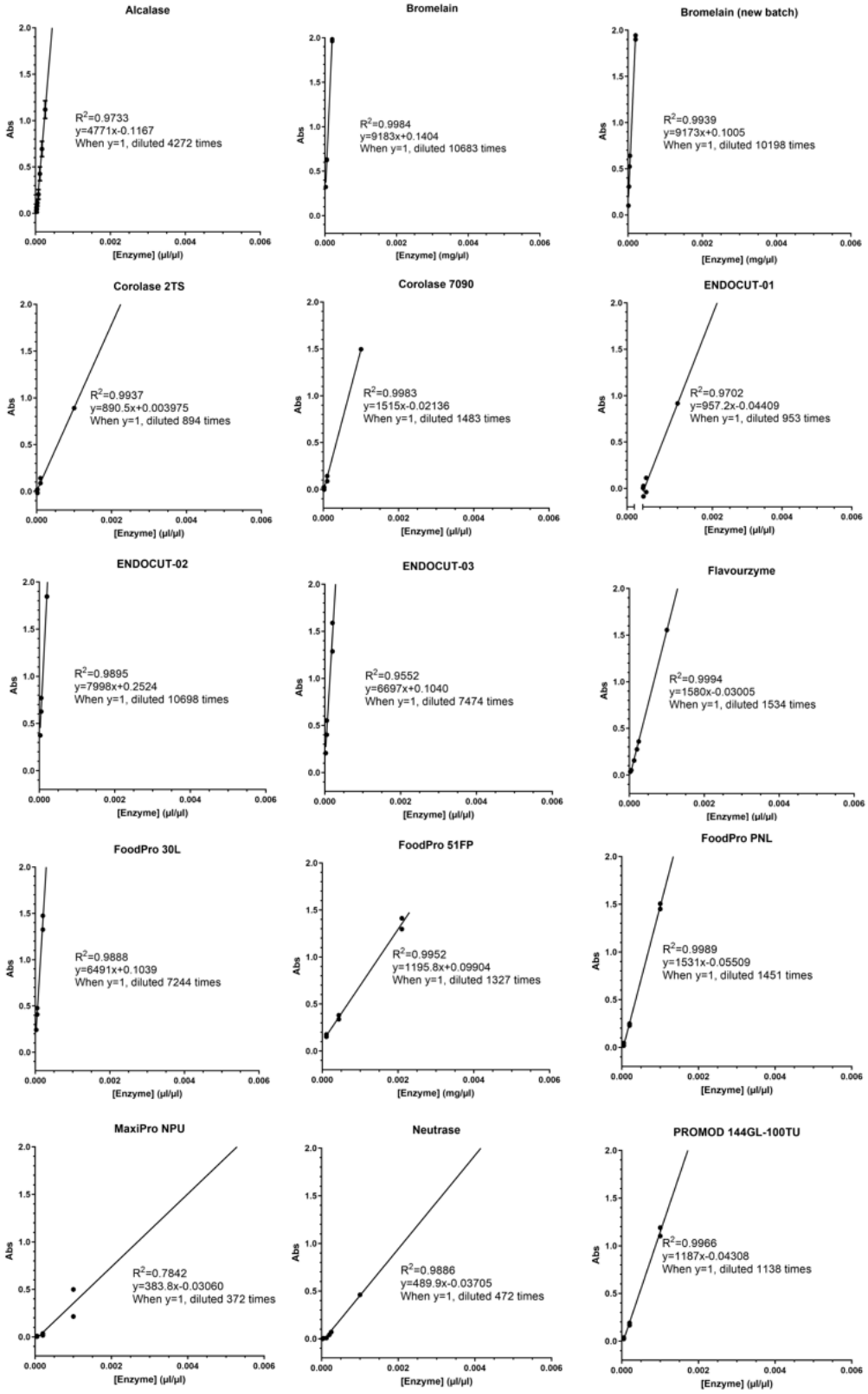

Figure C.1. Showing the proteolytic activity of all proteases, including R^2, the linear function and how many times the proteases had to be diluted to achieve an absorbance y=1 (the figure continues on the next page).

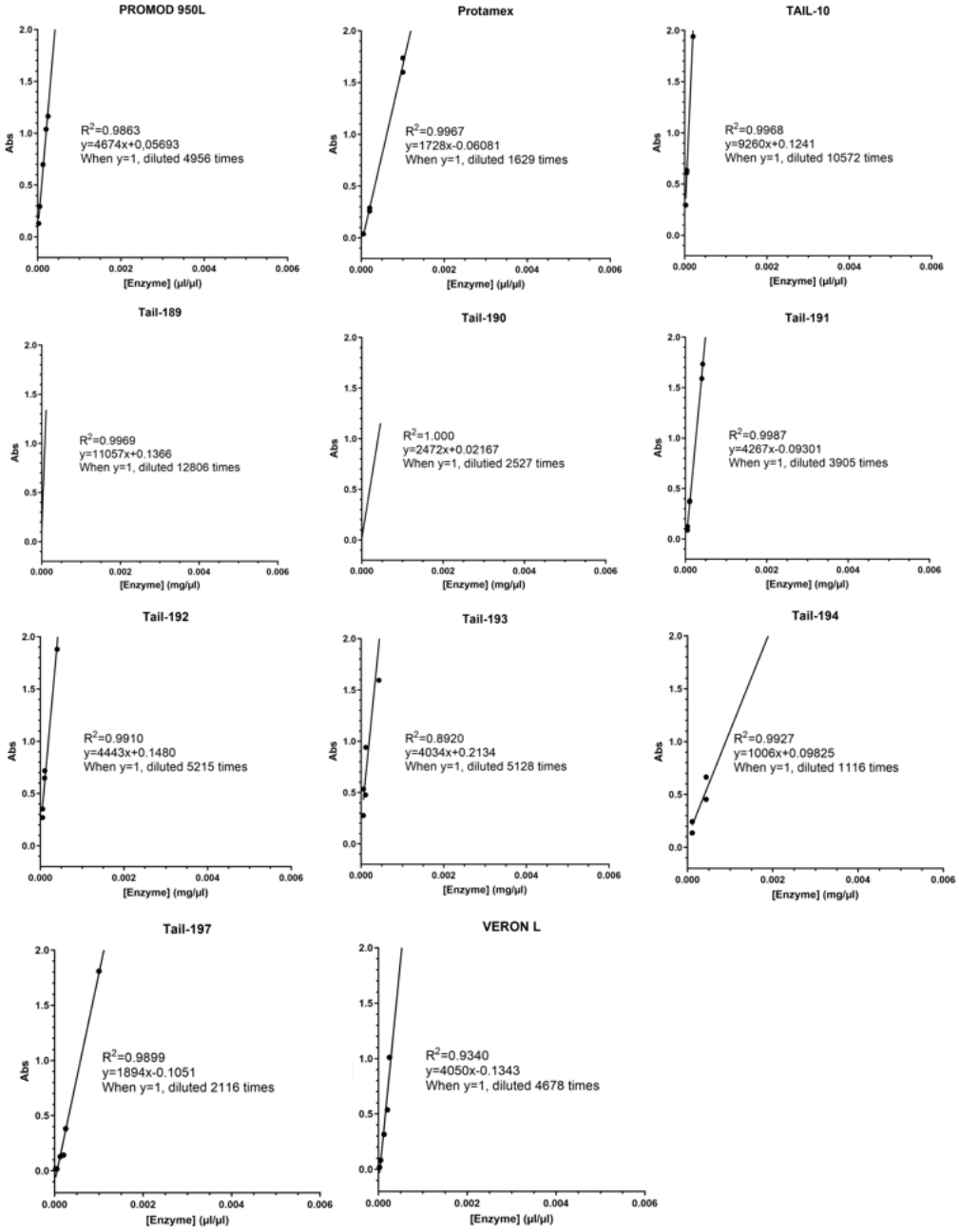

Figure C.1.The previous figure continued.

APPENDIX D – Calculations of yield

Formulas for calculation of yield

$$Sample\ weight\ (dry)(mg) = Sample\ weight\ (wet)(mg) * \left(1 - \frac{Water\ content\ (\%)}{100\ \%}\right)$$

$$Background\ rx\ (\%) = \left(1 - \frac{Zero\ sample\ (dry)(mg)}{Sample\ weight\ (dry)(mg)}\right) * 100\ \%$$

$$Total\ yield\ (\%) = \left(1 - \frac{Weight\ after\ hydrolysis\ (dry)(mg)}{Sample\ weight\ (dry)(mg)}\right) * 100\ \%$$

$$Yield/Enzymatic\ rx\ (ER)(\%) = Total\ yield\ (\%) - Background\ rx\ (\%)$$

Table D.1. Calculations of total yield (%) and enzymatic yield (%) for all proteases on Achilles tendons (A) from the small-scaled EPH.

Enzyme	Sample name	Sample weight (wet) (mg)	Sample weight (dry) (mg)	Background rx (%)	Weight after hydrolysis (dry) (mg)	Total yield (%)	Enzymatic yield (%)
Alcalase	5A1	2026,8	813,1	21,4	465	42,8	21,4
	5A3	2025,7	812,7	22,4	345	57,5	35,1
Bromelain	14A1	2004,8	804,3	20,6	438	45,6	25,0
	14A3	2030,6	814,7	22,6	349	57,1	34,5
Corolase 2TS	2A1	2015,0	808,4	21,0	300	62,9	41,9
	2A3	2042,8	819,6	23,1	246	69,9	46,9
Corolase 7090	13A1	2029,9	814,4	21,5	331	59,4	37,8
	13A3	2027,4	813,4	22,5	260	68,1	45,6
ENDOCUT-01	9A1	2015,7	808,7	21,0	402	50,3	29,3
	9A3	2022,4	811,4	22,3	366	55,0	32,6
ENDOCUT-02	18A1	2027,8	813,5	21,5	449	44,8	23,4
	18A3	2000,5	802,6	21,5	373	53,6	32,1
ENDOCUT-03	1A1	2018,4	809,8	21,1	395	51,3	30,2
	1A3	2025,4	812,6	22,4	441	45,8	23,3
Flavourzyme	6A1	2048,4	821,8	22,3	529	35,6	13,4
	6A3	2013,2	807,7	22,0	543	32,7	10,8
FoodPro 30L	23A1	2020,1	810,4	21,2	448	44,7	23,5
	23A3	2012,4	807,4	21,9	422	47,8	25,9
FoodPro 51 FP	4A1	2033,6	815,9	21,7	426	47,8	26,1
	4A3	2003,1	803,6	21,6	362	54,9	33,3
FoodPro PNL	16A1	2034,6	816,3	21,7	410	49,7	28,0
	16A3	2047,8	821,6	23,3	331	59,7	36,4
Protamex	10A1	2011,3	806,9	20,8	297	63,3	42,4
	10A3	2035,4	816,6	22,8	193	76,4	53,6
PROMOD 144GL-100TU	19A1	2033,2	815,7	21,7	424	48,0	26,3
	19A3	2025,4	812,6	22,4	271	66,7	44,3
PROMOD P950L	22A1	2033,2	815,7	21,7	515	36,8	15,1
	22A3	2037,8	817,5	22,9	446	45,5	22,6
TAIL-10	12A1	2035,4	816,6	21,8	452	44,7	22,9
	12A3	2005,0	804,4	21,6	437	45,6	24,0
Tail-189	3A1	2031,4	815,0	21,6	462	43,3	21,7
	3A3	2041,9	819,2	23,1	432	47,2	24,2
Tail-190	20A1	2047,7	821,5	22,2	401	51,2	29,0
	20A3	2018,0	809,6	22,1	236	70,9	48,7
Tail-191	11A1	2048,6	821,9	22,3	285	65,4	43,1
	11A3	2013,7	807,9	22,0	279	65,5	43,5
Tail-192	7A1	2045,9	820,8	22,2	434	47,1	24,9
	7A3	2040,0	818,4	23,0	437	46,6	23,6
Tail-193	17A1	2028,4	813,8	21,5	332	59,2	37,7
	17A3	2028,1	813,7	22,5	232	71,5	49,0
Tail-194	8A1	2000,8	802,7	20,4	283	64,8	44,4
	8A3	2028,8	813,9	22,6	166	79,7	57,1
Tail-197	21A1	2027,5	813,4	21,5	297	63,5	42,1
	21A3	2030,8	814,7	22,6	291	64,3	41,7
VERON L	15A1	2029,8	814,3	21,5	422	48,2	26,6
	15A3	2007,7	805,5	21,7	369	54,2	32,5

Table D.2. Calculations of total yield (%) and enzymatic yield (%) for all proteases on bones (B) from the small-scaled EPH.

Enzyme	Sample name	Sample weight (wet) (mg)	Sample weight (dry) (mg)	Background rx (%)	Weight after hydrolysis (dry) (mg)	Total yield (%)	Enzymatic yield (%)
Alcalase	5B1	2017,7	935,5	13,6	703	24,8	11,2
	5B3	2024,9	938,8	24,3	840	10,5	-13,8
Bromelain	14B1	2014,1	933,8	13,5	796	14,8	1,3
	14B3	2016,2	934,8	24,0	672	28,1	4,1
Corolase 2TS	2B1	2048,4	949,7	14,9	637	32,9	17,9
	2B3	2014,9	934,2	24,0	676	27,6	3,7
Corolase 7090	13B1	2046,7	948,9	14,9	737	22,4	7,5
	13B3	2045,4	948,3	25,1	801	15,6	-9,5
ENDOCUT-01	9B1	2030,6	941,5	14,2	644	31,6	17,4
	9B3	2025,1	938,9	24,3	673	28,4	4,0
ENDOCUT-02	18B1	2002,8	928,6	13,0	602	35,2	22,2
	18B3	2022,2	937,6	24,2	704	25,0	0,7
ENDOCUT-03	1B1	2043,5	947,4	14,7	755	20,3	5,5
	1B3	2027,2	939,9	24,4	874	7,0	-17,4
Flavourzyme	6B1	2039,5	945,6	14,6	822	13,1	-1,5
	6B3	2012,9	933,3	23,9	750	19,6	-4,3
FoodPro 30L	23B1	2029,1	940,8	14,1	724	23,0	8,9
	23B3	2031,5	941,9	24,6	732	22,3	-2,3
FoodPro 51 FP	4B1	2019,9	936,5	13,7	775	17,3	3,6
	4B3	2027,2	939,9	24,4	746	20,6	-3,8
FoodPro PNL	16B1	2015,1	934,3	13,5	789	15,6	2,0
	16B3	2020,9	937,0	24,2	806	14,0	-10,2
Protamex	10B1	2005,8	930,0	13,1	866	6,9	-6,2
	10B3	2019,3	936,2	24,1	825	11,9	-12,3
PROMOD 144GL-100TU	19B1	2043,0	947,2	14,7	785	17,1	2,4
	19B3	2042,9	947,2	25,0	671	29,2	4,2
PROMOD P950L	22B1	2050,0	950,5	15,0	793	16,6	1,6
	22B3	2038,6	945,2	24,8	707	25,2	0,4
TAIL-10	12B1	2005,3	929,7	13,1	640	31,2	18,1
	12B3	2002,7	928,5	23,5	615	33,8	10,3
Tail-189	3B1	2048,8	949,9	15,0	730	23,2	8,2
	3B3	2049,8	950,4	25,3	694	27,0	1,7
Tail-190	20B1	2010,6	932,2	13,3	636	31,8	18,4
	20B3	2026,5	939,6	24,4	846	10,0	-14,4
Tail-191	11B1	2004,1	929,2	13,1	896	3,6	-9,5
	11B3	2024,4	938,6	24,3	606	35,4	11,1
Tail-192	7B1	2038,5	945,1	14,5	760	19,6	5,1
	7B3	2045,3	948,3	25,1	689	27,3	2,2
Tail-193	17B1	2008,2	931,1	13,2	721	22,6	9,4
	17B3	2024,6	938,7	24,3	866	7,8	-16,6
Tail-194	8B1	2029,0	940,7	14,1	633	32,8	18,6
	8B3	2047,0	949,1	25,1	593	37,5	12,4
Tail-197	21B1	2004,7	929,5	13,1	827	11,0	-2,1
	21B3	2037,4	944,6	24,8	579	38,7	14,0
VERON L	15B1	2049,2	950,1	15,0	736	22,5	7,5
	15B3	2029,9	941,1	24,5	703	25,3	0,8

Table D.3. Calculations of total yield (%) and enzymatic yield (%) for all proteases on meat (C) from the small-scaled EPH. The ER ratio between Achilles tendons and meat (A/C) is also included were the ratios of the selected proteases Bromelain and Endocut-02 are highlighted.

Enzyme	Sample name	Sample weight (wet) (mg)	Sample weight (dry) (mg)	Background rx (%)	Weight after hydrolysis (dry) (mg)	Total yield (%)	Enzymatic yield %	A/C Ratio EY
Alcalase	5C1	2047,9	512,2	19,0	258,7	49,5	30,5	0,7
	5C3	2022,2	505,7	18,1	199,5	60,6	42,5	0,8
Bromelain	14C1	2036,8	509,4	18,6	228,0	55,2	36,7	0,7
	14C3	2007,9	502,2	17,5	165,3	67,1	49,6	0,7
Corolase 2TS	2C1	2043,1	511,0	18,8	292,6	42,7	23,9	1,8
	2C3	2048,0	512,2	19,1	204,3	60,1	41,0	1,1
	2C1 Rep	2004,8	501,4	17,3	132,6	73,6	56,2	0,7
	2C3 Rep	2043,4	511,0	18,9	125,6	75,4	56,5	0,8
Corolase 7090	13C1	2030,8	507,9	18,3	243,9	52,0	33,6	1,1
	13C3	2040,2	510,2	18,8	252,7	50,5	31,7	1,4
ENDOCUT-01	9C1	2048,8	512,4	19,0	263,1	48,7	29,6	1,0
	9C3	2036,0	509,2	18,6	187,3	63,2	44,6	0,7
ENDOCUT-02	18C1	2036,5	509,3	18,6	341,2	33,0	14,5	1,6
	18C3	2029,8	507,6	18,4	403,2	20,6	2,2	14,6
ENDOCUT-03	1C1	2039,2	510,0	18,7	379,7	25,5	6,9	4,4
	1C3	2035,0	508,9	18,6	287,5	43,5	24,9	0,9
	1C1 Rep	2049,5	512,6	19,2	300,4	41,4	22,2	1,4
	1C3 Rep	2025,6	506,6	18,2	253,1	50,0	31,8	0,7
Flavourzyme	6C1	2037,0	509,4	18,6	317,1	37,8	19,2	0,7
	6C3	2048,9	512,4	19,1	280,8	45,2	26,1	0,4
FoodPro 30L	23C1	2030,9	507,9	18,3	286,1	43,7	25,3	0,9
	23C3	2023,1	506,0	18,1	241,6	52,2	34,2	0,8
FoodPro 51 FP	4C1	2043,1	511,0	18,8	312,6	38,8	20,0	1,3
	4C3	2034,6	508,8	18,6	245,5	51,8	33,2	1,0
	4C1 Rep	2009,5	502,6	17,5	179,5	64,3	46,7	0,6
	4C3 Rep	2041,3	510,5	18,8	138,5	72,9	54,0	0,6
FoodPro PNL	16C1	2037,8	509,6	18,6	278,1	45,4	26,8	1,0
	16C3	2046,9	511,9	19,0	243,2	52,5	33,4	1,1
Protamex	10C1	2042,2	510,7	18,8	226,0	55,7	37,0	1,1
	10C3	2042,9	510,9	18,9	172,9	66,2	47,3	1,1
PROMOD 144GL-100TU	19C1	2025,8	506,6	18,1	253,8	49,9	31,8	0,8
	19C3	2011,6	503,1	17,6	172,8	65,7	48,0	0,9
PROMOD P950L	22C1	2031,8	508,1	18,4	296,3	41,7	23,3	0,6
	22C3	2038,2	509,7	18,7	268,0	47,4	28,7	0,8
TAIL-10	12C1	2013,8	503,6	17,6	265,2	47,3	29,7	0,8
	12C3	2025,5	506,6	18,2	218,7	56,8	38,6	0,6
Tail-189	3C1	2041,3	510,5	18,7	353,2	30,8	12,1	1,8
	3C3	2039,7	510,1	18,8	375,1	26,5	7,7	3,1
	3C1 Rep	2045,4	511,5	19,0	275,2	46,2	27,2	0,8
	3C3 Rep	2009,1	502,5	17,5	139,8	72,2	54,7	0,4
Tail-190	20C1	2027,7	507,1	18,2	229,4	54,8	36,6	0,8
	20C3	2039,4	510,0	18,7	170,1	66,6	47,9	1,0
Tail-191	11C1	2020,6	505,3	17,9	131,3	74,0	56,1	0,8
	11C3	2003,7	501,1	17,3	96,9	80,7	63,4	0,7
Tail-192	7C1	2006,0	501,7	17,3	241,3	51,9	34,6	0,7
	7C3	2041,0	510,4	18,8	194,6	61,9	43,1	0,5
Tail-193	17C1	2016,5	504,3	17,7	244,4	51,5	33,8	1,1
	17C3	2031,5	508,1	18,4	195,5	61,5	43,1	1,1
Tail-194	8C1	2003,4	501,0	17,2	89,6	82,1	64,9	0,7
	8C3	2035,2	509,0	18,6	89,4	82,4	63,9	0,9
Tail-197	21C1	2033,0	508,4	18,4	239,5	52,9	34,5	1,2
	21C3	2046,5	511,8	19,0	214,2	58,1	39,1	1,1
VERON L	15C1	2030,5	507,8	18,3	248,8	51,0	32,7	0,8
	15C3	2025,1	506,5	18,2	202,8	60,0	41,8	0,8

Table D.4. Calculations of total yield (%) and enzymatic yield (%) for all proteases on MDCR (D) from the small-scaled EPH.

Enzyme	Sample name	Sample weight (wet) (mg)	Sample weight (dry) (mg)	Background rx (%)	Weight after hydrolysis (dry) (mg)	Total yield (%)	Enzymatic yield (%)
Alcalase	5D1	2030,7	812,7	4,0	478,4	41,1	37,1
	5D3	2003,8	801,9	18,0	464,7	42,0	24,1
Bromelain	14D1	2012,3	805,3	3,2	504,2	37,4	34,2
	14D3	2037,9	815,5	19,3	470,7	42,3	23,0
Corolase 2TS	2D1	2040,0	816,4	4,5	471,4	42,3	37,8
	2D3	2040,4	816,5	19,4	378,6	53,6	34,2
Corolase 7090	13D1	2039,6	816,2	4,5	579,2	29,0	24,6
	13D3	2047,9	819,5	19,7	421,4	48,6	28,9
ENDOCUT-01	9D1	2032,1	813,2	4,1	518,0	36,3	32,2
	9D3	2012,4	805,3	18,3	470,1	41,6	23,3
ENDOCUT-02	18D1	2035,3	814,5	4,3	512,8	37,0	32,8
	18D3	2051,6	821,0	19,9	446,0	45,7	25,8
ENDOCUT-03	1D1	2043,6	817,8	4,6	580,5	29,0	24,4
	1D3	2022,1	809,2	18,7	493,1	39,1	20,4
Flavourzyme	6D1	2000,7	800,7	2,6	604,8	24,5	21,9
	6D3	2032,3	813,3	19,1	573,3	29,5	10,4
FoodPro 30L	23D1	2010,5	804,6	3,1	519,4	35,4	32,4
	23D3	2003,2	801,7	17,9	558,6	30,3	12,4
FoodPro 51 FP	4D1	2047,1	819,2	4,8	565,0	31,0	26,2
	4D3	2023,9	809,9	18,8	535,0	33,9	15,2
FoodPro PNL	16D1	2048,7	819,9	4,9	513,8	37,3	32,4
	16D3	2003,2	801,7	17,9	531,1	33,7	15,8
Protamex	10D1	2030,1	812,4	4,0	533,4	34,3	30,3
	10D3	2031,6	813,0	19,1	484,3	40,4	21,4
PROMOD 144GL-100TU	19D1	2050,0	820,4	4,9	460,5	43,9	38,9
	19D3	2023,4	809,7	18,8	476,1	41,2	22,5
PROMOD P950L	22D1	2027,0	811,2	3,9	557,2	31,3	27,4
	22D3	2006,0	802,8	18,0	539,7	32,8	14,7
TAIL-10	12D1	2000,0	800,4	2,6	475,0	40,7	38,1
	12D3	2041,1	816,8	19,5	498,6	39,0	19,5
Tail-189	3D1	2013,7	805,9	3,2	528,7	34,4	31,2
	3D3	2038,0	815,6	19,3	498,9	38,8	19,5
Tail-190	20D1	2007,9	803,5	3,0	387,6	51,8	48,8
	20D3	2001,2	800,9	17,9	459,7	42,6	24,7
Tail-191	11D1	2037,6	815,4	4,4	433,5	46,8	42,5
	11D3	2034,7	814,3	19,2	472,2	42,0	22,8
Tail-192	7D1	2027,7	811,5	3,9	522,4	35,6	31,7
	7D3	2031,5	813,0	19,1	433,9	46,6	27,6
Tail-193	17D1	2021,1	808,8	3,6	353,6	56,3	52,7
	17D3	2015,3	806,5	18,4	375,1	53,5	35,1
Tail-194	8D1	2027,1	811,2	3,9	401,2	50,5	46,7
	8D3	2034,2	814,1	19,2	417,4	48,7	29,5
Tail-197	21D1	2034,1	814,0	4,2	513,0	37,0	32,8
	21D3	2004,8	802,3	18,0	582,4	27,4	9,4
VERON L	15D1	2007,4	803,3	2,9	527,7	34,3	31,4
	15D3	2021,2	808,9	18,7	478,0	40,9	22,2

Table D.5. Calculations of total yield (%) and enzymatic yield (%) of the small-scale hydrolysis with duplicates and time points (15, 30, and 60 minutes) on Achilles tendons (A), MDCR (D), and artificial (MDCR) with the selected proteases Bromelain (Br) and Endocut-02 (En).

Sample name	Sample weight (wet) (mg)	Sample weight (dry) (mg)	Background reaction (%)	Weight after hydrolysis (dry) (mg)	Total yield (%)	Enzymatic yield (%)
1BrA15	2084,6	835,9	21,5	564,7	32,4	11,0
2BrA15	2048,5	821,4	21,5	590,0	28,2	6,7
1BrD15	2014,0	805,6	3,9	630,8	21,7	17,8
2BrD15	2028,6	811,4	3,9	678,2	16,4	12,6
1BrDX15	2089,7	776,7	17,9	631,9	18,6	0,7
2BrDX15	2075,9	771,5	17,9	571,3	26,0	8,0
1EnA15	2083,6	835,5	21,5	615,4	26,3	4,9
2EnA15	2088,9	837,6	21,5	571,9	31,7	10,2
1EnD15	2044,1	817,6	3,9	617,9	24,4	20,6
2EnD15	2046,1	818,4	3,9	632,6	22,7	18,8
1EnDX15	2086,8	775,6	17,9	556,0	28,3	10,4
2EnDX15	2050,6	762,1	17,9	529,9	30,5	12,5
1BrA30	2007,8	805,1	21,5	484,6	39,8	18,3
2BrA30	2007,7	805,1	21,5	471,3	41,5	20,0
1BrD30	2036,5	814,6	3,9	642,4	21,1	17,3
2BrD30	2046,1	818,4	3,9	603,9	26,2	22,3
1BrDX30	2005,4	745,3	17,9	546,9	26,6	8,7
2BrDX30	2063,4	766,9	17,9	581,4	24,2	6,2
1EnA30	2017,5	809,0	21,5	572,8	29,2	7,7
2EnA30	2017,6	809,1	21,5	529,8	34,5	13,0
1EnD30	2056,3	822,5	3,9	582,8	29,1	25,3
2EnD30	2021,3	808,5	3,9	600,4	25,7	21,9
1EnDX30	2018,9	750,4	17,9	633,0	15,6	-2,3
2EnDX30	2037,4	757,2	17,9	626,0	17,3	-0,6
1BrA60	2026,6	812,7	21,5	484,6	40,4	18,9
2BrA60	2024,2	811,7	21,5	394,0	51,5	30,0
1BrD60	2025,0	810,0	3,9	705,2	12,9	9,1
2BrD60	2029,2	811,7	3,9	607,2	25,2	21,3
1BrDX60	2075,1	771,2	17,9	606,4	21,4	3,4
2BrDX60	2003,3	744,6	17,9	619,5	16,8	-1,2
1EnA60	2036,9	816,8	21,5	489,8	40,0	18,6
2EnA60	2062,8	827,2	21,5	484,7	41,4	19,9
1EnD60	2037,5	815,0	3,9	604,1	25,9	22,0
2EnD60	2046,6	818,6	3,9	560,7	31,5	27,6
1EnDX60	2071,5	769,9	17,9	550,5	28,5	10,6
2EnDX60	2064,4	767,3	17,9	553,6	27,8	9,9

Table D.6. Calculations of total yield (%) and enzymatic yield (%) of the 60-minutes sample from the upscaled hydrolysis of Achilles tendons (A), chicken bones (B), chicken meat (C), MDCR (D), and artificial MDCR (DX) by Bromelain (Br) and Endocut-02 (En).

Sample name	Sample weight (wet) (g)	Sample weight (dry) (g)	Background rx (%)	Weight after hydrolysis (dry) (g)	Total yield (%)	Enzymatic yield (%)
1EnA	40,06	16,06	21,5	7,37	54,1	32,7
2EnA	40,10	16,08	21,5	7,78	51,6	30,1
1BrA	40,27	16,15	21,5	6,49	59,8	38,3
2BrA	40,35	16,18	21,5	6,01	62,9	41,4
1EnB	40,11	18,61	14,0	15,82	15,0	1,0
2EnB	40,04	18,58	14,0	15,71	15,4	1,4
1BrB	40,20	18,65	14,0	16,88	9,5	-4,5
2BrB	40,13	18,62	14,0	15,85	14,9	0,9
1EnC	40,18	10,05	18,4	5,70	43,3	25,0
2EnC	40,11	10,03	18,4	5,06	49,5	31,2
1BrC	40,05	10,01	18,4	3,78	62,3	43,9
2BrC	40,18	10,05	18,4	4,01	60,1	41,8
1EnD	40,29	16,12	3,9	8,56	46,9	43,0
2EnD	40,03	16,01	3,9	8,01	50,0	46,1
1BrD	40,21	16,08	3,9	9,41	41,5	37,6
2BrD	40,08	16,03	3,9	8,04	49,9	46,0
1EnDX	39,87	14,82	17,9	9,32	37,1	19,2
2EnDX	39,53	14,69	17,9	9,02	38,6	20,7
1BrDX	39,87	14,82	17,9	7,51	49,3	31,4
2BrDX	40,01	14,87	17,9	7,78	47,7	29,8

APPENDIX E – Molecular weight distributions

*Table E.1. Average molecular weight (g/mol), area below the chromatogram (ml*V), fractions based on peptide size (A %), and the enzymatic yield (%) of hydrolysates from chicken bones run for 1 hour in the small-scale hydrolysis.*

Enzyme	Mw (g/mol)	A (ml*V)	F1 >15 aa (A%)	F2 7-15 aa (A%)	F3 2-7 aa (A%)	F4 free aa (A%)	EY (%)
Alcalase	3258	42,8	34,2	18,1	37,9	9,9	11,2
Bromelain	**3735**	**33,8**	**39,2**	**19,9**	**31,1**	**9,9**	**1,3**
Corolase 2TS	2397	53,7	31,2	22,8	38,7	7,3	17,9
Corolase 7090	6122	51,3	50,1	13,1	28,0	8,8	7,5
ENDOCUT-01	7009	47,2	53,8	12,0	24,4	9,9	17,4
ENDOCUT-02	**6672**	**50,1**	**52,6**	**14,1**	**25,4**	**7,8**	**22,2**
ENDOCUT-03	4015	24,9	35,4	16,7	34,0	14,0	5,5
Flavourzyme	3506	18,4	30,1	9,7	38,0	22,2	-1,5
FoodPro 30L	7416	43,9	53,5	13,3	25,0	8,2	8,9
FoodPro 51 FP	5480	39,2	39,1	10,4	35,5	15,0	3,6
FoodPro PNL	6197	50,9	51,9	12,8	27,2	8,2	2
Protamex	5799	41,2	48,3	12,5	28,5	10,7	-6,2
PROMOD 144GL-100TU	5184	43,9	52,3	17,4	21,7	8,5	2,4
PROMOD P950L	6493	41,1	49,0	14,0	28,0	9,1	1,6
TAIL-10	6182	42,3	48,1	13,8	28,6	9,4	18,1
Tail-189	5744	36,4	43,6	11,4	32,2	12,9	8,2
Tail-190	3404	45,8	35,0	17,9	38,0	9,1	18,4
Tail-191	2836	46,2	30,6	18,4	40,3	10,8	-9,5
Tail-192	4662	31,9	37,7	10,4	35,3	16,7	5,1
Tail-193	6135	46,3	45,5	11,2	30,9	12,5	9,4
Tail-194	2111	56,0	23,8	18,6	48,0	9,7	18,6
Tail-197	4869	39,9	47,6	14,5	28,4	9,5	-2,1
VERON L	4263	39,9	45,8	20,2	25,3	8,7	7,5

*Table E.2. Average molecular weight (g/mol), area below the chromatogram (ml*V), fractions based on peptide size (A %), and the enzymatic yield (%) of hydrolysates from chicken meat run for 1 hour in the small-scale hydrolysis.*

Enzyme	Mw (g/mol)	A (ml*V)	F1 >15 aa (A%)	F2 7-15 aa (A%)	F3 2-7 aa (A%)	F4 free aa (A%)	EY (%)
Alcalase	1924	71,1	19,8	20,7	51,2	8,4	30,5
Bromelain	**1684**	**83,0**	**18,1**	**25,3**	**49,5**	**7,1**	**36,7**
Corolase 2TS	1324	87,0	9,0	24,7	58,9	7,4	56,2
Corolase 7090	1778	73,5	16,1	21,0	54,2	8,8	33,6
ENDOCUT-01	1987	66,8	18,9	20,1	51,4	9,7	29,6
ENDOCUT-02	**2953**	**47,0**	**31,9**	**16,9**	**42,2**	**9,1**	**14,5**
ENDOCUT-03	3172	47,8	34,3	14,6	40,3	10,8	22,2
Flavourzyme	2105	48,6	18,9	12,5	53,4	15,2	19,2
FoodPro 30L	2211	72,9	24,5	20,4	45,8	9,4	25,3
FoodPro 51 FP	1273	85,4	8,5	13,6	65,1	12,8	46,7
FoodPro PNL	1676	69,7	15,0	21,1	55,4	8,6	26,8
Protamex	1767	71,7	17,2	20,9	52,0	9,9	37,0
PROMOD 144GL-100TU	1617	74,0	17,5	25,7	48,3	8,5	31,8
PROMOD P950L	2185	72,7	23,6	19,1	47,7	9,7	23,3
TAIL-10	2489	52,1	26,4	18,2	46,3	9,2	29,7
Tail-189	1701	82,7	13,1	16,5	58,7	11,6	27,2
Tail-190	1815	73,2	18,3	20,7	52,5	8,6	36,6
Tail-191	1275	96,0	8,1	18,8	64,2	8,8	56,1
Tail-192	1384	61,5	9,8	15,8	62,4	12,1	34,6
Tail-193	1488	79,5	11,3	16,8	60,4	11,6	33,8
Tail-194	963	108,0	3,9	15,3	71,4	9,4	64,9
Tail-197	1652	94,7	15,3	21,5	54,7	8,5	34,5
VERON L	1934	36,6	23,6	24,0	44,7	7,7	32,7

*Table E.3. Average molecular weight (g/mol), area below the chromatogram (ml*V), fractions based on peptide size (A %), and the enzymatic yield (%) of hydrolysates from MDCR run for 1 hour in the small-scale hydrolysis.*

Enzyme	Mw (g/mol)	A (ml*V)	F1 >15 aa (A%)	F2 7-15 aa (A%)	F3 2-7 aa (A%)	F4 free aa (A%)	EY (%)
Alcalase	3331	61,6	31,1	17,4	42,9	8,7	37,1
Bromelain	**2900**	**75,6**	**36,0**	**24,6**	**32,7**	**6,7**	**34,2**
Corolase 2TS	2179	101,2	25,5	23,5	44,5	6,5	37,8
Corolase 7090	3517	56,9	33,2	16,4	41,1	9,4	24,6
ENDOCUT-01	5063	64,7	23,4	14,8	35,9	9,8	32,2
ENDOCUT-02	**7141**	**62,6**	**48,4**	**14,2**	**29,9**	**7,5**	**32,8**
ENDOCUT-03	5850	52,6	42,3	16,3	32,8	8,6	24,4
Flavourzyme	2759	26,2	22,8	10,9	45,9	19,5	21,9
FoodPro 30L	4236	44,1	34,9	17,9	38,2	9,1	32,4
FoodPro 51 FP	2961	49,2	25,6	11,8	47,4	15,2	26,2
FoodPro PNL	4234	63,0	37,7	15,3	38,4	8,7	32,4
Protamex	4894	61,1	41,4	15,2	34,1	9,3	30,3
PROMOD 144GL-100TU	2874	62,5	34,4	23,2	34,1	8,3	38,9
PROMOD P950L	4273	49,3	35,3	17,3	28,3	9,0	27,4
TAIL-10	7110	61,5	48,3	13,6	31,0	7,2	38,1
Tail-189	3275	51,2	27,6	13,1	46,5	12,9	31,2
Tail-190	3049	65,0	28,7	17,4	44,5	9,4	48,8
Tail-191	2545	83,6	27,3	17,8	45,9	9,0	42,5
Tail-192	3330	42,7	26,8	10,9	46,5	15,9	31,7
Tail-193	4827	53,9	35,5	10,6	41,1	12,8	52,7
Tail-194	1605	87,5	17,1	19,2	54,4	9,4	46,7
Tail-197	4022	60,2	38,4	17,4	36,1	8,2	32,8
VERON L	3446	63,4	40,4	22,6	30,0	7,1	31,4

*Table E.4. Average molecular weight (g/mol), area below the chromatogram (ml*V), fractions based on peptide size (A %), and the enzymatic yield (%) of the background samples of chicken bones, chicken meat, and MDCR run for 1 hour in the small-scale hydrolysis.*

Raw material	Mw (g/mol)	A (ml*V)	F1 >15 aa (A%)	F2 7-15 aa (A%)	F3 2-7 aa (A%)	F4 free aa (A%)
Chicken bones	2084	1,5	18,95	5,22	39,0	36,81
Chicken meat	2541	15,6	12,8	1,7	62,3	23,3
MDCR	5108	6,8	27,7	2,1	42,8	27,4

*Table E.5. Average molecular weight (g/mol), area below the chromatogram (ml*V), fractions based on peptide size (A %), and the enzymatic yield (%) of hydrolysates from MDCR (D) and artificial MDCR (DX) using Bromelain (Br) and ENDOCUT-02 (En), run in the small-scale hydrolysis with duplicates and time points (15, 30 and 60 min). * One of the duplicates of ENDOCUT-02 on artificial MDCR for 15 minutes were not analyzed due to being very viscous.*

Sample name	Mw (g/mol)	A (ml*V)	F1 >15 aa (A%)	F2 7-15 aa (A%)	F3 2-7 aa (A%)	F4 free aa (A%)	EY (%)
1BrD15	5241	35,6	47,4	18,1	26,9	7,6	17,8
2BrD15	4703	37,7	43,5	19,9	28,9	7,6	12,6
1BrD30	5002	45,0	44,1	19,9	28,8	7,2	17,3
2BrD30	3719	61,6	40,6	23,9	29,3	6,2	22,3
1BrD60	3270	48,3	35,5	22,0	34,4	8,1	9,1
2BrD60	4584	48,7	40,1	19,0	32,8	8,2	21,3
1EnD15	6849	32,0	47,7	14,6	29,0	8,7	20,6
2EnD15	6265	30,9	46,4	15,3	29,6	8,6	18,8
1EnD30	6362	46,0	47,7	16,0	29,0	7,3	25,3
2EnD30	5534	42,5	43,9	17,4	31,1	7,6	21,9
1EnD60	5317	48,7	41,6	17,0	33,2	8,2	22,0
2EnD60	5153	46,4	42,3	16,8	32,8	8,1	27,6
1BrDX15	9305	71,0	60,2	13,7	21,5	4,6	0,7
2BrDX15	8238	61,4	55,4	15,0	24,5	5,2	8,0
1BrDX30	9021	69,4	57,9	13,9	23,3	5,0	8,7
2BrDX30	9766	78,2	63,6	12,6	19,5	4,3	6,2
1BrDX60	7604	82,5	55,1	15,0	24,8	5,1	3,4
2BrDX60	9489	69,4	56,2	12,9	25,4	5,5	-1,2
2EnDX15*	6017	48,4	42,0	17,2	33,6	7,2	12,5
1EnDX30	8968	55,9	54,7	13,4	26,0	5,8	-2,3
2EnDX30	10812	68,2	59,2	12,0	23,7	5,1	-0,6
1EnDX60	9448	73,3	57,4	11,9	25,1	5,6	10,6
2EnDX60	8899	69,0	53,4	13,0	27,5	6,1	9,9

*Table E.6. Average molecular weight (g/mol), area below the chromatogram (ml*V), fractions based on peptide size (A %), and the enzymatic yield (%) of hydrolysates from chicken bones (B), chicken meat (C), MDCR (D) and artificial MDCR (DX) using Bromelain (Br) and ENDOCUT-02 (En), run in the upscaled hydrolysis with duplicates. Only the 60 minutes samples are analyzed.*

Sample name	Mw (g/mol)	A (ml*V)	F1 >15 aa (A%)	F2 7-15 aa (A%)	F3 2-7 aa (A%)	F4 free aa (A%)	EY (%)
1BrB60	3791	32,1	43,4	18,2	29,7	8,8	-4,5
2BrB60	4454	31,8	46,3	16,6	28,3	8,8	0,9
1EnB60	8220	35,0	52,3	12,6	26,3	8,8	1,0
2EnB60	7912	31,4	49,7	12,7	28,1	9,5	1,4
1BrC60	1882	82,9	20,1	21,9	49,5	8,5	43,9
2BrC60	1850	87,9	19,4	22,3	50,0	8,3	41,8
1EnC60	3146	56,4	31,3	15,8	42,7	10,2	25,0
2EnC60	3162	52,2	30,6	15,8	43,3	10,3	31,2
1BrD60	4045	57,6	42,2	18,7	31,5	7,6	37,6
2BrD60	3865	64,6	41,5	19,5	31,4	7,6	46,0
1EnD60	7011	47,9	42,2	14,2	34,3	9,3	43,0
2EnD60	6270	45,9	39,1	15,1	36,5	9,4	46,1
1BrDX60	6103	88,8	52,8	16,0	26,3	5,0	31,4
2BrDX60	6255	93,3	54,4	15,0	25,6	5,0	29,8